FUZZY-DRIVEN ENERGY STORAGE SYSTEM FOR IMPROVING RELIABILITY OF ELECTRICITY SUPPLY DURING ISLANDING OF PHOTOVOLTAIC SYSTEM

ACE KHAW LIN YI

MASTER OF ENGINEERING SCIENCE

LEE KONG CHIAN FACULTY OF ENGINEERING SCIENCE
UNIVERSITI TUNKU ABDUL RAHMAN
APRIL 2018

FUZZY-DRIVEN ENERGY STORAGE SYSTEM FOR IMPROVING RELIABILITY OF ELECTRICITY SUPPLY DURING ISLANDING OF PHOTOVOLTAIC SYSTEM

By

ACE KHAW LIN YI

A dissertation submitted to
the Department of Electrical and Electronics Engineering,
Lee Kong Chian Faculty of Engineering and Science,
Universiti Tunku Abdul Rahman,
in partial fulfillment of the requirements for the degree of
Master of Engineering Science
April 2018

ABSTRACT

FUZZY-DRIVEN ENERGY STORAGE SYSTEM FOR IMPROVING RELIABILITY OF ELECTRICITY SUPPLY DURING ISLANDING OF PHOTOVOLTAIC SYSTEM

Ace Khaw Lin Yi

The increasing use of renewable energy has helped in reducing CO_2 and fossil fuel dependency. Geographical location of Malaysia has a high level of solar irradiation throughout the year which is ideal for Photovoltaic (PV) systems installation. PV systems are expected to grow on the low voltage distribution networks in the future. Under the current regulatory frameworks, islanding operation of PV systems is not permissible due to safety concern of the working personnel working on the line. Consequently, PV systems must be disconnected immediately in the event of the grid outage as per Malaysian Standards, MS 1873. However, it is proven that islanding operation of PV systems would enable the owners to consume the available solar energy and help the utility company improve the reliability of electricity supply. To enable the islanding operation of PV systems, a fuzzy-based control strategy is developed to drive the operation of the energy storage system to maintain the frequency and voltage within the statutory limit during the transition from grid-connected to islanding operation. A low voltage experimental network is setup. Several experimental case studies are performed to investigate the strength of the proposed fuzzy controlled strategy and described in detail. The experimental results showed that

the fuzzy-based control strategy is able to maintain the frequency and voltage within the statutory limits before the islanded network is reconnected to the grid. It is also shown that the fuzzy controller has better performance than the proportional-integrator controller.

ACKNOWLEDGEMENTS

I would like to express my sincere appreciation to my supervisor, Dr. Wong Jianhui, and co-supervisor, Prof. Ir. Dr. Lim Yun Seng, for their constant guidance and encouragement throughout the research and thesis preparation. I am truly grateful to my project partner, Hau Lee Cheun for his support and guidance towards developing the experimental laboratory.

Without the financial support from Collaborative Research in Engineering, Science & Technology (CREST), this work would not have been possible. I would like to thank CREST for granting me this rare opportunity. I also would like to thank industrial partner, ERS Energy Sdn Bhd and contractor for the development of PV panel and construction of the experimental low voltage distribution network.

I would like to thank my colleagues, Tang Zhi Xuan, and Chok Eu-Tjin for their guidance throughout my studies. Besides, I would also like to thank Ipeknaz Özden from Sabancı University for her moral support throughout my thesis preparation.

APPROVAL SHEET

This dissertation entitled "**FUZZY-DRIVEN ENERGY STORAGE SYSTEM FOR IMPROVING RELIABILITY OF ELECTRICITY SUPPLY DURING ISLANDING OF PHOTOVOLTAIC SYSTEM"** was prepared by ACE KHAW LIN YI and submitted as partial fulfillment of the requirements for the degree of Master of Engineering Science at Universiti Tunku Abdul Rahman.

Approved by:

_____

(Dr. Wong Jianhui) Date: ……..
Supervisor
Department of Electrical and Electronics Engineering
Lee Kong Chian Faculty of Engineering and Science
Universiti Tunku Abdul Rahman

_____

(Prof. Ir. Dr. Lim Yun Seng) Date: ……..
Co-supervisor
Department of Electrical and Electronics Engineering
Lee Kong Chian Faculty of Engineering and Science
Universiti Tunku Abdul Rahman

LEE KONG CHIAN FACULTY OF ENGINEERING SCIENCE

UNIVERSITI TUNKU ABDUL RAHMAN

Date: _____

SUBMISSION OF DISSERTATION

It is hereby certified that **ACE KHAW LIN YI** (ID No: **15UEM08254**) has completed this dissertation entitled "**Fuzzy-driven Energy Storage System for Improving Reliability of Electricity Supply During Islanding of Photovoltaic System**" under the supervision of Dr. Wong Jianhui (Supervisor) from the Department of Electrical and Electronics Engineering, Lee Kong Chian Faculty of Engineering and Science, and Prof. Ir. Dr. Lim Yun Seng (Co-Supervisor) from the Department of Electrical and Electronics Engineering, Lee Kong Chian Faculty of Engineering and Science.

I understand that University will upload softcopy of my dissertation in pdf format into UTAR Institutional Repository, which may be made accessible to UTAR community and public.

Yours truly,

_____
(ACE KHAW LIN YI)

DECLARATION

I (ACE KHAW LIN YI) hereby declare that the dissertation is based on my original work except for quotations and citations which have been duly acknowledged. I also declare that it has not been previously or concurrently submitted for any other degree at UTAR or other institutions.

Name: _____

Date: _____

TABLE OF CONTENTS

LIST OF TABLES

LIST OF FIGURES

LIST OF ABBREVIATIONS / NOTATIONS

AC	Alternate Current
a-Si	Amorphous Silicon
BESS	Battery-based Energy Storage System
BMS	Battery Management System
CIGS	Copper Indium Gallium Selenide
CO2	Carbon Dioxide
CT	Current Transformer
DC	Direct Current
DG	Distributed Generator
EC	Energy Commission
ESS	Energy Storage System
FiT	Fit-in-Tariff
FLC	Fuzzy Logic Controller
GaAs	Gallium Arsenide
GBI	Green Building Index
GHG	Greenhouse Gas
IEC	International Electrotechnical Commission
IEEE	institute of Electrical and Electronic Engineers
LV	Low Voltage

MPPT	Maximum Power Point Tracking
MS	Malaysian Standard
NaS	Sodium Sulphur
NDZ	Non-Detection Zone
NEM	Net Energy Metering
NI	National Instrument
NiCd	Nickel Cadmium
NiMH	Nickel-Metal Hydride
NREL	National Renewable Energy Laboratory
OUF	Over/Under Frequency
OUV	Over/Under Voltage
P_{BESS}	Active power of BESS, W
P_{BESS}^{*}	Active power of BESS during islanded operation, W
P_{EXCESS}	Active power mismatch between PV system and load, W
P_{FUZZY}	Active power fuzzy output, W
P_{GRID}	Active power of export/import from grid, W
P_{LOAD}	Active power consumption of load emulator, W
P_{PV}	Active power output of PV system, W
Pb	Lead
PCC	Point of Common Coupling
PI	Proportional-Integral

PID	Proportional-Integral-Differential
PV	Photovoltaic
Q_{BESS}	Reactive power of BESS, Var
Q^*_{BESS}	Reactive power of BESS during islanded operation, Var
Q_{GRID}	Reactive power of export/import from grid, Var
Q_{LOAD}	Reactive power consumption of load emulator, Var
Q_{PV}	Reactive power output of PV system, Var
RE	Renewable Energy
RES	Renewable Energy Resources
RM	Ringgit Malaysia
SAIDI	System Average Interruption Duration Index
SAIFI	System Average Interruption Frequency Index
SEB	Sarawak Energy Berhad
SEDA	Sustainable Energy Development Authority
SESB	Sabah Electricity Sdn. Bhd.
SOC	State-of-Charge
TNB	Tenaga Nasional Berhad
USD	United State Dollar
VI	Virtual Instrument
VRLA	Valve-regulated Lead Acid
ΔP	Active power mismatch between PV system and load, W
ΔP_{BESS}	Change in BESS active power output, W

ΔQ	Reactive power mismatch between PV system and load, Var
ΔQ_{BESS}	Change in BESS reactive power output, Var

CHAPTER 1

INTRODUCTION

1.1. Research Background

Greenhouse Gas (GHG) emission which is the gaseous compound that trapped heat in the atmosphere has caused global warming. Carbon Dioxide (CO_2), one of the main contributor of GHG is mainly emitted from the combustion of fossil fuel for electricity generation (US EPA, 2015). The increase in fossil fuel price and adverse effect on the environment has caused the emergence of renewable energy sources such as wind, solar and hydro. In the effort to promote the use of renewable energy sources, the Malaysian government has introduced various incentive and tax reduction program under the Renewable Energy Act 2011 (SEDA, 2011c). It can be seen that in the recent year, the share for electricity generation using Photovoltaic (PV) systems has increased exponentially due to the advancement of technology (Cengiz et al., 2015).

Electricity generation from solar energy is abundant and available throughout the world. The geographic location of Malaysia situated closed the equator received tremendous sunlight throughout the year. With this benefit, Malaysia has great potential to utilise PV system for electricity generation. Figure 1.1 shows the global map of solar energy where Malaysia receives an average of 1400 to 1800 kWh/m^2 of sunlight per annum. Thus, the installation of PV systems in Malaysia is promising and expected to increase in the future. However, the installation of PV system without proper coordination poses power quality issues such as voltage rise to the conventional electrical distribution network.

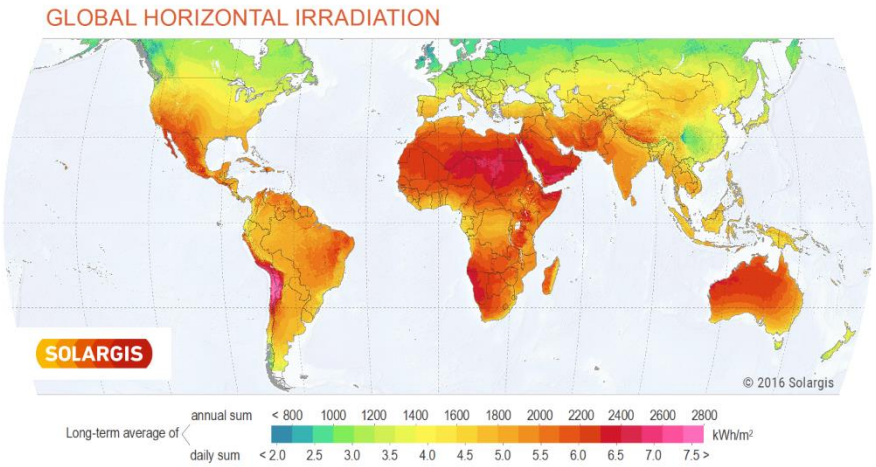

Figure 1.1: Global map showing amount of solar energy hits the earth

(Source: http://i.imgur.com/9EPpKod.png)

The utility companies in Malaysia has continuously improved the reliability to ensure electricity flows to power up billions of homes. However, power supply from generating station to the remote area is often subjected to various kinds of faults on the interconnection lines; consequently, the consumers

from the remote end may experience power interruption. It has been a challenging task and concern for the utility company to improve the reliability of the power supply in the remote area.

The implementation of Eleventh Malaysia Plan (2016 -2020) has announced the target setting to reduce the Greenhouse Gas (GHG) emission by 40% by 2020, and the Malaysian government has to play an important role to promote the use of Renewable Energy (RE) generation (Prime Minister's Department, 2017). At present, the cumulative total installed capacity for PV systems in Malaysia has increased from 31.56 MW to 339.14 MW from the Year 2012 to the Year 2017 respectively (SEDA, 2017a). Under the current regulatory framework, PV system is required to shut down in the event of grid outage to prevent the formation of an energised islanded network. Such a practice is established to protect the working personnel that working on the line which might expose to an unintentional energised islanded network. Islanding operation refers to a sectional of the electrical power system being energised by one or more PV systems while being isolated from the main utility grid (Mohamad et al., 2011). However, if the PV systems are forced to shut down in the event of grid outage, the available clean energy from PV system is not utilised.

Voltage and frequency in the distribution network have to be maintained within the allowable limit to ensure safe operation of electrical equipment. At present, there are two methods of providing voltage and frequency regulation in the islanded network. Rotating type generator such as synchronous generator is

common used to regulate the voltage and frequency in the islanded network (Zhao, Yang, et al., 2017). However, the use of diesel fuel to drive the generator for producing electricity in the islanded network can emits GHG which is non-environmental friendly (Usman et al., 2017).

Besides, the recent development in Energy Storage System (ESS) technology, such as Battery-based Energy Storage System (BESS), is able to provide ancillary service such as frequency regulation to support islanding operation (Xu et al., 2016; Moradi et al., 2016). This ensures continuity supply of power in the islanded network in the event of grid outage. However, there are no relevant studies which focus on the frequency variation during the transition period from grid connected to islanded mode under various level of generation and demand.

1.2. Research Objectives

The objectives of this research thus are as listed:

I. To study the performance of islanded network with energy storage system under various levels of generation and demand.

II. To design a control algorithm for energy storage system in conducting islanding operation of PV systems.

III. To evaluate the performance of the proposed control in improving reliability and quality of electricity supply throughout islanding operation.

1.3. Research Methodology

The objectives are achieved by carrying out the research work plan in four stages as follows: -

Stage I: Consists of the background study on the research topic. This includes the investigation of challenges associated with islanding operation with renewable energy sources. A thorough literature review is conducted on the existing methods for islanding operation with renewable energy sources. The rules and regulations, and standards for interconnection of renewable energy are studied as well. The feasibility of using BESS for islanding operation is explored.

Stage II: Design and develop a Low Voltage (LV) experimental network consists of BESS, PV system, and load emulator for islanding operation. A monitoring system consists of multiple measuring devices is designed to measure and record the data in the experimental network. A communication link between the BESS and a supervisory computer is developed to control the power flow of the BESS.

Stage III: The correlation between voltage and frequency during grid outage is studied. A fuzzy controlled BESS is developed to ensure PV system remain connected whilst voltage and frequency for the network are within statutory limit.

Stage IV: Investigate the performance of the proposed fuzzy control in improving reliability and quality of electricity supply during islanding of PV system. The proposed control is tested under various weather condition and load demand. Besides, the performance of the proposed fuzzy controller is compared to a conventional Proportional-Integral (PI) controller.

1.4. Dissertation Overview

This dissertation consisted of five chapters is lay out as follows:

CHAPTER 2 covered a thorough literature review on the research topic. In this chapter, the challenges of conducting islanding operation are reviewed and the benefits of conducting islanding are explored. Besides, the standards and guidelines for interconnection PV systems on the electrical grid are studied as well. Followed by, a review on the existing methods for ESS in conducting islanding operation of PV system.

CHAPTER 3 illustrates the detail setup of the LV experimental network consists of PV system, BESS, and load emulator. In this chapter, the design and development of each hardware components are being outlined to provide an overview of the experimental network. The communication between the BESS and supervisory computer is established and elaborated as well. The working principle and feature of the BESS are explained in detail.

CHAPTER 4 discussed the feasibility studies on continuous operation of PV systems with BESS during grid outages. This chapter can be divided into two major studies as follows:

Part I: Feasibility study: Several experiments were set up to conduct a preliminary study to investigate the problems and challenges associated with the islanding operation of PV system. Next, the feasibility study of using BESS to allow continuous operation of PV systems during grid outage in an islanded network.

Part II: Fuzzy controlled BESS to maintain the voltage and frequency within the islanded network to allow PV systems to remain connected. In this section, a simple fuzzy logic controller and an improved version of the fuzzy logic controller will be discussed in detail including the input and output membership functions. Several case studies have been conducted to evaluate the effectiveness of the proposed control strategy in improving the reliability of electricity supply during islanding of PV systems. In the last section of the chapter, a simple PI controller is developed to compare with the fuzzy logic controller.

CHAPTER 5 draws a conclusion of the project. The limitation and hence the proposed future work are discussed as well.

1.5. Publication and Patent

Based on the outcome of the research findings, a patent is undergoing the filling process where the draft document is under proof reading (As of June 2018), one journal and one international conference papers have been published as follows: -

Table 1.1: List of publications

No.	Title	Patent/journal/conference
1.	Fuzzy-based control algorithm for the bi-directional inverter with batteries for conducting islanded operation of photovoltaic systems	Patent No: PI2018700169
2.	Review of droop-controlled bi-directional inverter in conducting islanded operation of photovoltaic systems https://doi.org/10.1063/1.4979399 **(Published)**	Conference: American Institute of Physics Conference Proceedings
3.	Feasibility of Continues Operation of Photovoltaic Systems with Energy Storage during Grid Outages http://www.ijeetc.com/index.php?m=content&c=index&a=show&catid=179&id=1132 **(Published)**	International Journal of Electrical and Electronic Engineering & Telecommunications (IJEETC): Scopus
4.	Fuzzy Controlled Energy Storage System for Improving Reliability of Electricity Supply During Islanding of Photovoltaic Systems DOI: http://dx.doi.org/10.1002/etep.2604 **(Published)**	International Transactions on Electrical Energy Systems (ITEES) (Impact Factor: 1.087)

CHAPTER 2

LITERATURE REVIEW

2.1. Introduction

The electricity generation in Malaysia primarily depends on fossil fuel as it is reliable over a long period of time, and has the price advantage, especially for coal. Figure 2.1 shows the primary energy supply for electricity generation highly dependent on coal (39.3%) and natural gas (48.1%) (Suruhanjaya Tenaga, 2017). Due to the limited resources of carbon-based fuel for electricity generation, Malaysian government has increased the amount for coal import from neighbourhood country to meet the increasing demand of electricity (Energy Commission, 2015c). Figure 2.2 shows the projection of the capacity mix in Malaysia from the Year 2016 to the Year 2026 (Suruhanjaya Tenaga, 2017). It is foreseen that the use of coal power plants is expected to increase in the near future. However, burning fossil fuels releases Carbon Dioxide (CO_2), which contributes to climate change. The emergence of Renewable Energy Sources (RES) has become a promising solution to reduce the dependency on fossil fuels for electricity generation. In the effort of promoting RES, the

Malaysian government has introduced a series cash incentives and tax reduction scheme to reduce the use of fossil fuels for electricity generation (Wong et al., 2014).

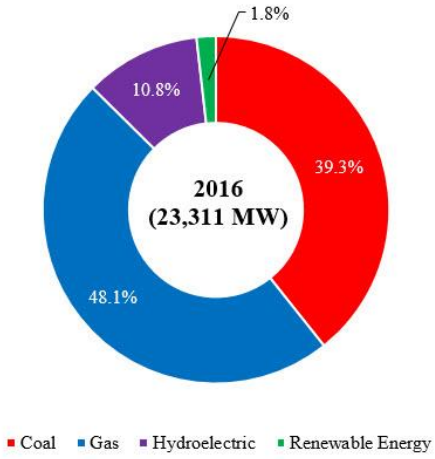

Figure 2.1: Primary energy supply at Malaysia in the year 2016

Note: Combined Cycle Gas Turbine (CCGT), Open Cycle Gas Turbine (OCGT) and Conventional Thermal (Gas) are categorised under natural gas. Renewable energy consisted of solar PV, biogas, mini hydro and biomass

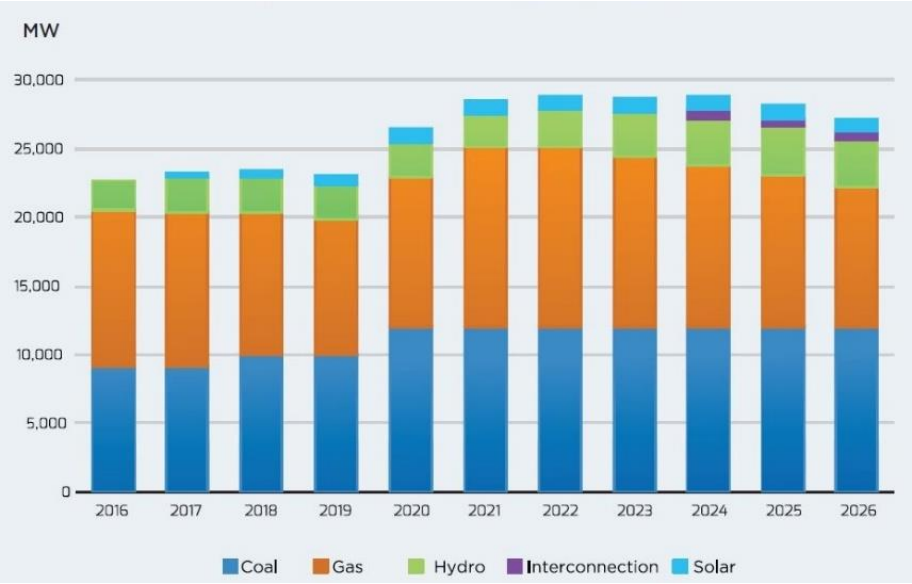

Figure 2.2: Projection of generation mix in Malaysia from Year 2016 – Year 2026 (Suruhanjaya Tenaga, 2017)

2.2. National Grid in Malaysia

The electricity supply in Malaysia is supplied and distributed by three companies, namely Tenaga Nasional Berhad (TNB), Sabah Electricity Sdn. Bhd. (SESB) and Sarawak Energy Berhad (SEB) as the sole distributor in Peninsular Malaysia, Sabah and Sarawak respectively. Figure 2.3 illustrated the area of service for these utility companies in Malaysia where SESB and SEB are the main distributors for East Malaysia.

Figure 2.3: Distributor licensee in Malaysia

The electrical network between generation side and consumer side consists of generation, transmission and distribution subsystems. Electricity is generated from power plants and deliver to the consumer over a long transmission line and distributed across the network in a unidirectional power flow manner (Yusof R, 2015). Most of the power plants are located far from the consumer areas, thus high voltage transmission system is used to transmit the electricity over a long distance in order to ensure its efficiency by reducing transmission and distribution line (I_2R_{line}) losses. A step-up transformer is used to increase the voltage levels at the transmission subsystem and a step-down

transformer is used to reduce the voltage levels for suitable utilisation as shown in Figure 2.4.

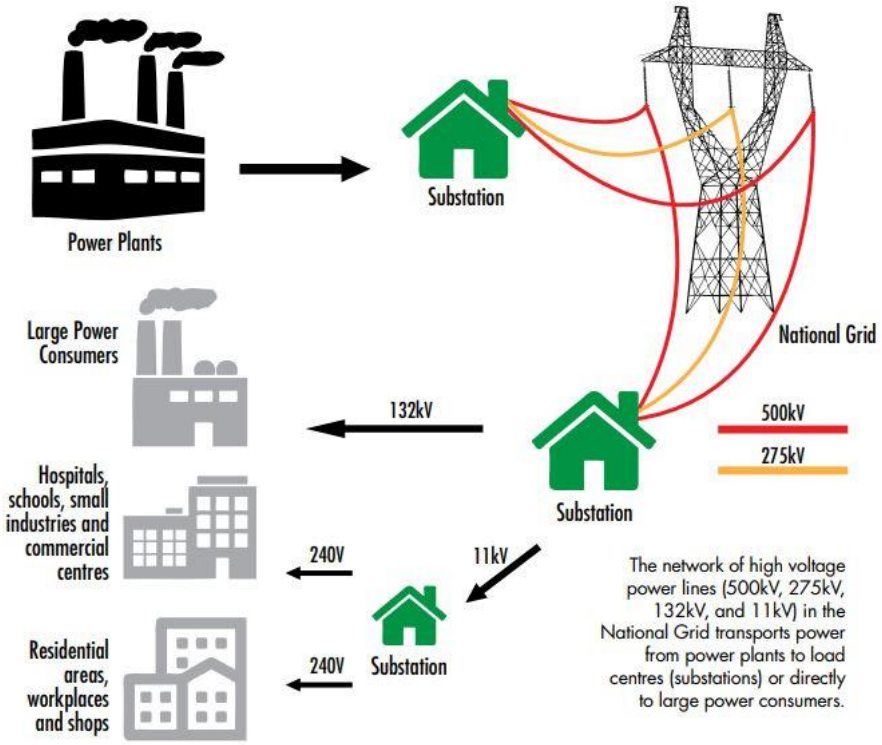

Figure 2.4: Grid network for Malaysia power system (Suruhanjaya Tenaga, 2015)

The Malaysian distribution network is categorise under medium voltage (1000 V to 33000 V) and low voltage (<1000V). The low voltage distribution network adopted a three-phase four wire. For a single-phase system, it is rated at 230 V while three-phase is rated at 400 V (Annuar A, 2010). Throughout the entire electrical network, the frequency is regulated at 50Hz ±1%. The TT earthing system is grounded at the substation, on the neutral point of transformer secondary side. This grounding method provides safety protection against electrical shock and earth fault. (Yusof R, 2015).

2.3. Renewable Energy Sources in Malaysia

In the effort of reducing Greenhouse Gas (GHG) emission, the Malaysian government has taken the initiative in promoting and utilising Renewable Energy Sources (RES) such as biomass, biogas, solar and mini-hydro. In this regard, the government has undertaken a project on the development of a strategy for RES as the fifth fuel in the 8th Malaysia Plan (Prime Minister's Department, 2001). The planning for implementing RES is further emphasised in the 9th Malaysia plan (Prime Minister's Department, 2006). In the 10th Malaysia plan, Feed-in-Tariff (FiT) programme under Renewable Energy Act 2011 is introduced and implemented to establish and catalyse the generation of RES (Prime Minister's Department, 2016). Under the FiT programme, consumers are allowed to sell the total electricity generated by the RES to the distribution licensee. In the 11th Malaysia plan, Net Energy Metering (NEM) scheme is introduced to complement the current FiT programme. NEM programme allows the customer to export and sell excess electricity generated from the PV system ($P_{EXCESS} = P_{PV} - P_{LOAD}$) to the distribution licensee (TNB, 2016). Besides introducing the FiT and NEM programme, the Malaysian government also take extra effort to promote RES and reduce GHG emissions by using Green Building Index (GBI). It is used as a green rating tool to benchmark the energy consumption of a buildings to raise awareness about the environmental issues among the developers (Green Building Index, 2013).

In the recent years, generation capacity for RES has been increasing tremendously to achieve the objective of 11th Malaysia plan in order to reduce

the dependency of generating electricity using fossil fuel, that ultimately reduces the GHG emissions. Figure 2.5 depicts the accumulated capacity from the Year 2012 to the Year 2017 for various installed RES such as solar, wind, mini-hydro, biomass and biogas (SEDA, 2017b). It is shown that FiT programme has effectively increased the penetration of PV from 4720 MWh to 848262 MWh between the Year 2012 to Year 2017 respectively.

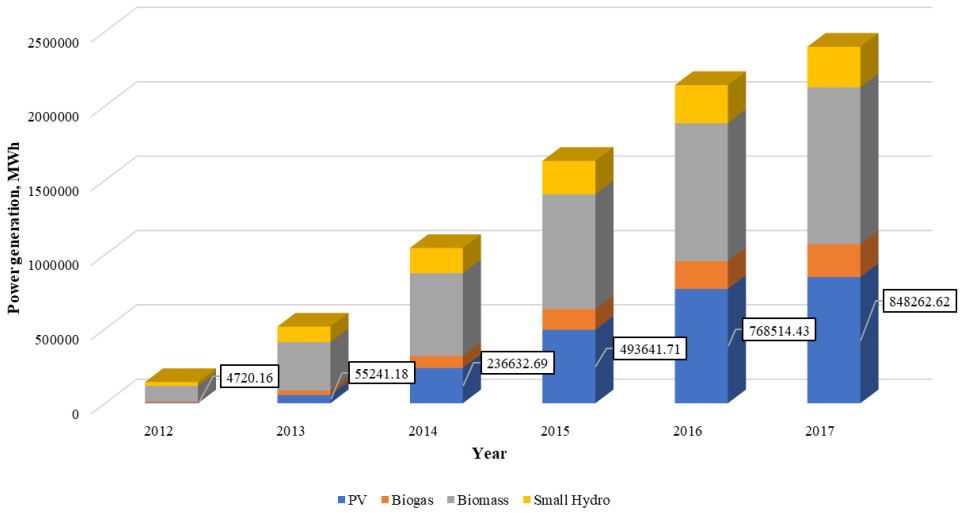

Figure 2.5: Increment in PV installation has increased tremendously from the Year 2012 to Year 2017

PV system is widely used due to the advantages of minimising GHG emission, minimal maintenance requirements such as dust cleaning for solar panel, silent operation, environment-friendly and reliable (Solarvis, 2017). At present, three types of commercially available solar cell which are commonly used are made of monocrystalline, polycrystalline, and amorphous silicon. Table 2.1 shows the highest efficiency of various types of PV module as of July 2017. Gallium Arsenide (GaAs) type of thin film solar module has the highest

efficiency as compared with Monocrystalline, Multicrystalline, Copper Indium Gallium Selenide (CIGS) and Amorphous Silicon (a-Si). The high cost of GaAs solar cell manufacturing presents a drawback of using it due to the complicated fabrication process (Hayes and Clemens, 2015). It is learnt that 8 inches in diameter of the gallium arsenide wafer can cost approximately USD5000 as compared to the silicon wafer that only cost USD5 (Abate-Stanford, 2015). With the progressive advancement of fabrication technology, mass production of the solar cell is achievable and the cost for the solar cell will be declining as indicated by Swanson's effect (Greenpowerco, 2016).

Table 2.1: Types of solar cell technology and efficiency (Green et al., 2017)

Solar Cell Technology	Monocrystalline	Multicrystalline	Thin film (GaAs)	Thin film (CIGS)	Thin film (a-Si)
Efficiency, %	24.4 ± 0.5 [a]	19.9 ± 0.4	24.8 ± 0.5	19.2 ± 0.5 [b]	12.3 ± 0.3

[a] Highest efficiency of crystalline silicon solar cell in the world achieved by Kaneka, Japan (Yoshikawa et al., 2017)

[b] Solar Frontier's CIGS thin film has achieved an efficiency world record of 19.2 % (Solar Frontier, 2017)

Recently, the largest single-site solar power plant (Amcorp Gemas) with a capacity of 10.25 MW, located in Gemas, Negeri Sembilan, Malaysia has been commissioned (Amcorp, 2013). The plant currently running at its full capacity and generates up to 1.2 million kWh of electricity per month. Besides, another pilot large-scale solar plant with a generation capacity of 50 MW will be commissioned by the early year 2018 whereby this project is expected to reduce 36,000 tonnes of carbon emissions per annum (Ryan, 2017).

2.4. Renewable Energy Incentives and Framework in Malaysia

In the effort of reducing GHG emission, legitimate regulatory framework is established in order to promote the utilisation of Renewable Energy (RE) in Malaysia. Therefore, a policy is established in National Renewable Energy Policy and Action Plan (2009) to enhance the utilisation of RE generation. The Malaysia parliament enacts Renewable Energy (RE) Act 2011 to provide establishment and implementation of a special tariff system to catalyse the generation of RE (Malaysian Government, 2011). Besides, Sustainable Energy Development Authority Act 2011 is also enacted under the 10th Malaysia Plan to provide the establishment of the Sustainable Energy Development Authority Malaysia (SEDA, 2011d). Under the RE Act 2011, Feed-in Tariff (FiT) scheme is introduced to promote the utilisation of RE. Under the FiT scheme, the owner of the RE can opt to sell the electricity produced from the Renewable Energy Sources (RES) to the distribution licensees under a special FiT rate regulated by SEDA as shown in Table 2.2 (SEDA, 2011b). There are four eligible RES under FiT scheme, namely, PV, hydro, biomass, and biogas.

Sustainable Energy Development Authority of Malaysia (SEDA Malaysia) is formed to administrate and manage the implementation of the FiT mechanism which is mandated under the RE Act 2011 (SEDA, 2011a). According to the RE Act 2011, a customer who utilises more than 300 kWh of electricity is subjected to an additional surcharge of 1% to the RE fund for the implementation of the FiT mechanism (SEDA, 2013a). The additional surcharge is then revised from 1.0% to 1.6% effectively from 1st January 2014

(SEDA, 2013b). The RE fund is created under RE Act 2011 allow electricity generated from the RES to be paid off with a premium tariff. As of 2016, the cumulative installed capacity of the renewable energy contributes at 1.7% of the total electricity generation in Malaysia (Suruhanjaya Tenaga, 2017). In the Malaysia Eleventh Plan, Net Energy Metering (NEM) scheme is introduced to further intensify the growth of RE. NEM is implemented to promote and encourage utilisation of RE, by prioritising internal consumption before any excess electricity generated is fed to the grid (Suruhanjaya Tenaga, 2017). With the implementation of various policies to promote RE generation, electricity generation from RE is forecasted to increase gradually in the future.

Table 2.2: FiT rates for solar PV (Community) as of 1st January 2017

No.	Description of Qualifying Renewable Energy Installation	FiT Rates (RM per kWh)
(a)	Basic FiT rates having installed capacity of:	1st January 2017
(i)	Up to and including 4 kW	0.7424
(ii)	Above 4 kW and up to and including 24 kW	0.7243
(iii)	Above 24 kW and up to including 72 kW	0.5218
(b)	Bonus FiT rates having the following criteria (one or more)	
(i)	Use as installation in buildings or building structure	+0.1395
(ii)	Use as building materials	+0.1060
(iii)	Use of locally manufactured or assembled solar PV modules	+0.0500
(iv)	Use of locally manufactured or assembled solar inverters	+0.0500

2.5. International Regulations for Integration of Renewable Energy Sources

Institute of Electrical and Electronic Engineers (IEEE) and International Electrotechnical Commission (IEC) has developed a guideline for integrating Renewable Energy Sources (RES) in the electrical power systems. These standards are developed to ensure operation safety of the electric power system with the integration of RES such as photovoltaic, wind, and microturbines. Therefore, the design and operation of grid-connected RES must comply with the regulation standards. The details of the technical requirements for the voltage, frequency, power quality in the standards will be elaborated.

2.5.1. IEEE 1547 Standard for Interconnecting Renewable Energy Sources

As the energy market is slowly modernised, the tremendous increase in Renewable Energy (RE) integration has given a sense of urgency to the standards development process (NREL, 2014). IEEE 1547 (2014) Standard for Interconnecting Distributed Resources with Electric Power Systems was published to facilitate the requirements for the integration of RE into the electrical power system. The IEEE 1547 standard has specified the criteria and technical requirement for RE integration, which includes the response for abnormal condition and islanding specifications. All the inverter is required to shut down and disconnect from the grid in the event of the grid outage. The disconnection time is subjected to abnormal voltage and frequency deviation.

Table 2.3 and Table 2.4 depicts the default response time for an interconnection system when abnormal voltage and frequencies occurred (IEC, 2004; IEEE Std, 2014). The grid-connected RE sources shall cease to energise and disconnect from the grid within the clearing time as long as the system voltage and frequency are out of the stipulated range. The clearing time indicates the period from the start of an abnormal condition to the RE source cease to energise.

Table 2.3: Responses of the interconnection system to abnormal voltages (by default)

IEC 61727		IEEE 1547	
Voltage range	Disc. Time (Seconds)	Voltage range (% of base voltage)	Disc. Time (Seconds)
		<45%	0.16
<50%	0.10	45% to 60%	1.00
50% to 85%	2.00	60% to 88%	2.00
85% to 110%	Remain Operation	88% to 110%	Remain Operation
110% to 135%	2.00	110% to 120%	1.00
>135%	0.05	>120%	0.16

Table 2.4: Responses of interconnection system to frequency deviation

IEC 61727		IEEE 1547	
Frequency (Hz)	Disc. Time (Seconds)	Frequency (Hz)	Disc. Time (Seconds)
		< 57	0.16
< 49	0.2	< 59.5	2.00
49 to 51	Continue Operation	59.5 to 60.5	Continue Operation
> 51	0.2	> 60.5	2.00
		> 62	0.16

2.5.2. MS 1837:2010 Installation of Grid-connected Photovoltaic (PV) System

In anticipating the integration of grid-connected PV system, the Malaysian regulatory body has published an installation guideline for the technical requirement of a grid-connected PV system (Malaysia Standard, 2013). With the effect of NEM scheme for PV integration in Malaysia, the utility company (TNB) has published a Technical Guideline for Connection of Indirect Solar PV Power Generation for Net Energy Metering (NEM) where the system response requirement for voltage and frequency abnormality is tabled in Table 2.5 (TNB, 2016)

Table 2.5: PV disconnection time during voltage and frequency abnormality

MS 1837		
	Conditions	Disconnection Time (Seconds)
Voltage Range	<50%	0.10
	50% to 90%	2.00
	90% to 110%	Continue Operation
	110% to 135%	2.00
Frequency Range	-1%	0.20
	50 Hz	Continue Operation
	+1%	0.20

Many existing international standards are published for the interconnection of distributed energy sources. At present, the experts from

working committees are still developing the regulations and the researchers are researching for a better approach to allow PV systems to operate safely within the islanded network (IEEE Std, 2003).

2.6. Islanding Operation of Renewable Energy Sources

Islanding is a condition where Renewable Energy Sources (RES) continues to power a location while the location is being isolated from the utility grid (Heidari et al., 2016). At present, many policies and incentives are introduced by the government in the effort of promoting the use of RES to reduce GHG emission. Prior to grid outage, RES connected in the islanded network is possible to remain energised. At present, international standards required all RES to shut down in the event of grid outage (IEEE Std, 2014). This is because working personnel working on the line might expose to an unintentional energised islanded network (Tedde and Smedley, 2014). Besides, it can potentially damage the electrical appliances and switchgear when the voltage and frequency of the islanded network fall out of statutory limits. Islanding operation can be classified into intentional islanding and unintentional islanding which will further discuss in the following sections.

2.6.1. Intentional Islanding

Intentional islanding is also known as planned islanding operation which refers to a scheduled maintenance where working personnel on the utility line intentionally islanded a portion of the network for maintenance and upgrading

work. Before isolating one section of the network from the utility grid, the power generation and demand is matched to avoid large transient of voltage and frequency when the network is transit into islanding operation. To ensure safe operation of planned islanding, numerous study has been conducted to investigate the feasibility of intentional islanding. A proposed clustering scheme method ensures each islanded network comprised of generators has proven that the voltage and frequency are regulated to prevent blackout during intentional islanding operation on an IEEE 9-bus system (Esmaeilian and Kezunovic, 2017). Another simulation study has proposed a power management method could maintain the voltage and currents in the intentional islanding mode as required by the international standard, IEEE-1547 (Balaguer et al., 2011; Lee et al., 2013). A dynamic impact study of intentional islanding is conducted to analyse the performance of distributed generator under islanding operation. The findings show that the protection setting limit for voltage and frequency is required to be changed during islanding operation (Fuangfoo et al., 2007). Besides, a simulation study has proven to have minimal power disruption when islanding network consists of generators (Quirós-Tortós et al., 2015).

2.6.2. Unintentional Islanding

Unlike intentional islanding, unintentional islanding happens unintendedly and randomly at any time. Unintentional islanding occurred when there is a fault present in the electrical network which triggers the protection system and isolate the fault from the rest of the network, hence grid outage. In the event of the grid outage, Renewable Energy Sources (RES) in the islanded network is

conceivable to form. According to IEEE 1547 standard, RES are required to disconnect from the grid in the event of grid outage (IEEE Std, 2014). Therefore, all electronic based inverter is embedded with anti-islanding protection system to detect islanding event and cease to energise from the formation of an island. Besides, available methods for islanding detection are discussed in section 2.10.

2.7. Benefits of Islanding Operation with Renewable Energy Sources

The benefits of allowing islanding operation of RES is the continuity supply from RES in the event of the grid outage. The reliability of the electricity supply is often linked to the duration and number of interruption in the distribution network. To measure system reliability, System Average Interruption Duration Index (SAIDI) and System Average Interruption Frequency Index (SAIFI) is often used as an index to measure the power interruption (IEEE Std, 2012). The indices serve as a tool for comparing utility performance reliability. Figure 2.6 shows an index of 52.58 numbers of electricity supply interruption per 1000 consumers in Malaysia for the year of 2015 (Energy Commission, 2015a). The data from Energy Commission (EC) Malaysia stated that power interruption in Sabah is the highest, recorded at an index of 35.15 number of electricity supply interruption per 1000 customers as compared to the index for Peninsular Malaysia and Sarawak state that recorded 7.42 and 10.03 respectively (Energy Commission, 2015b). Therefore, the idea to allow the continuous supply of RES to energise the load within the islanded network can reduce power interruption in the rural area when the grid is out of service, if the voltage and frequency are regulated within the statutory limit. Thus, improving the reliability of electricity

supply, especially in the area that suffers from frequent interruption.

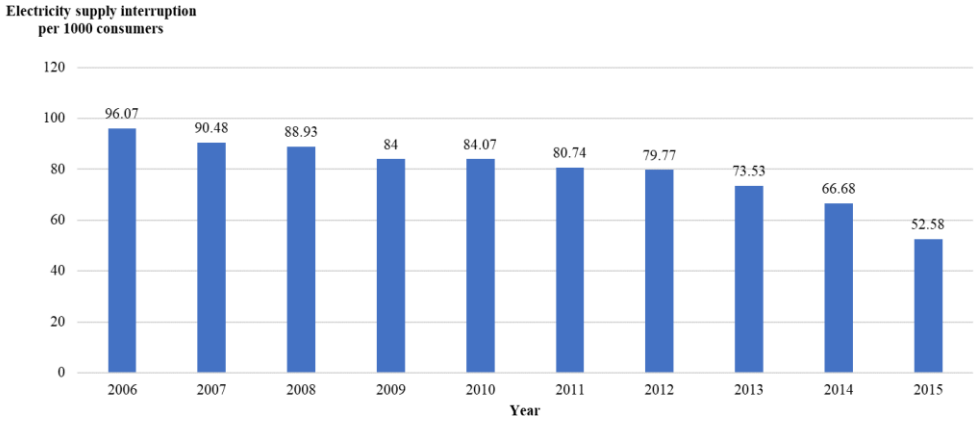

Figure 2.6: Electricity supply interruption per 1000 consumers in Malaysia from Year 2006 to Year 2015

SAIDI is an index that indicates the average duration of interruption in the power supply indicated in minutes per customer while SAIFI indicates the average frequency of interruptions in power supply. Equation (2.1) and (2.2) explains the formulation of SAIDI and SAIFI respectively,

$$SAIDI = \frac{Total\ duration\ of\ the\ interruption}{Number\ of\ customers\ served} = \frac{\sum U_i N_i}{N_T} \tag{2.1}$$

$$SAIFI = \frac{Total\ number\ of\ the\ interruption}{Number\ of\ customers\ served} = \frac{\sum \lambda_i N_i}{N_T} \tag{2.2}$$

Where, U_i is the annual outage time for location i

N_i is the number of customers

N_T is the total number of customers served

λ_i is the failure rate

With these indices implemented to measure the electricity supply reliability, Malaysia is having SAIDI of 61 minutes of interruption per customer per year (Agüero, 2015; Azman, 2013). Figure 2.7 shows the SAIDI indices for selected countries. Figure 2.8 and Figure 2.9 shows that although Malaysia is having a relatively low SAIDI as compared to other countries, Sabah state remains as the highest SAIDI and SAIFI respectively. The high interruption in Sabah creates discomfort among the consumers. Therefore, islanding operation of RES to energise the load in the event of grid outage could potentially improve SAIDI and SAIFI (Barker and Mello, 2000; Fuangfoo et al., 2007; Mahat et al., 2011).

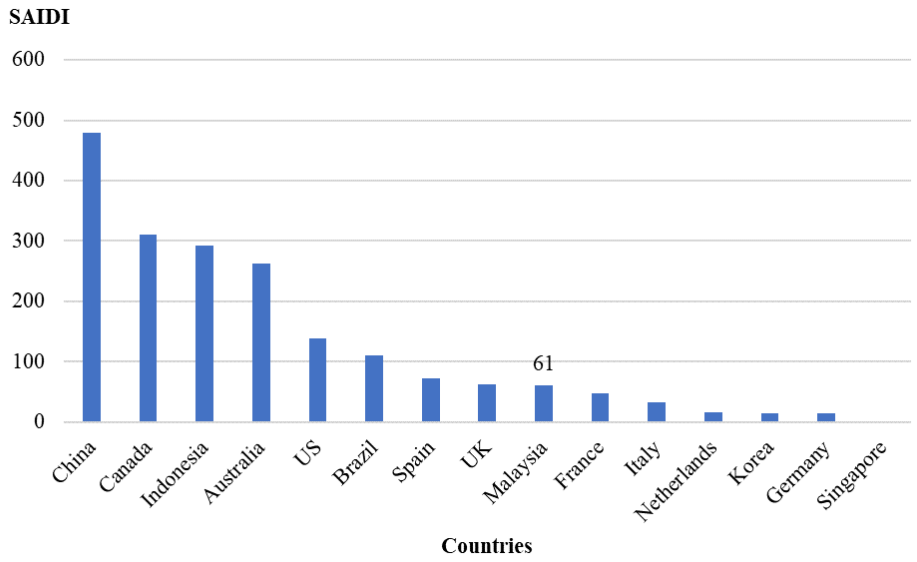

Figure 2.7: SAIDI of several developed and developing countries in the Year 2013

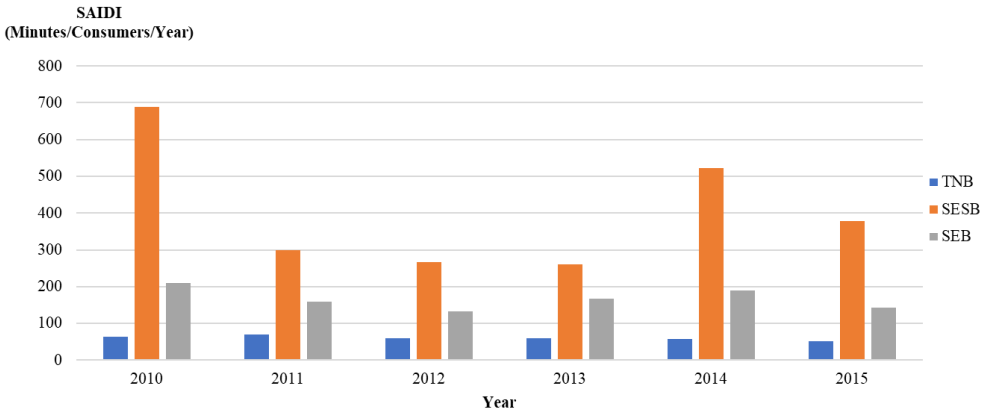

Figure 2.8: SAIDI indices for grid operators in Peninsular Malaysia (TNB), Sabah (SESB) and Sarawak (SEB) respectively

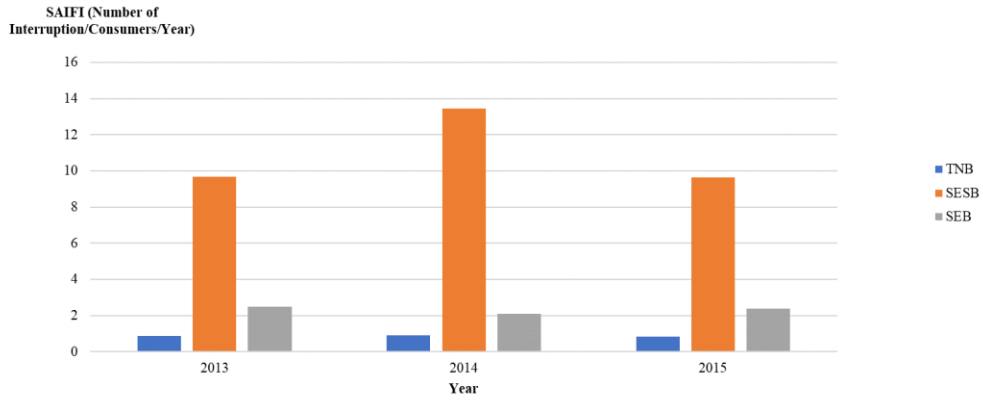

Figure 2.9: SAIFI indices for grid operators in Peninsular Malaysia, Sabah, and Sarawak for Year 2013, 2014 and 2015 respectively

Power restoration after the grid is out of service can be time-consuming as the restoration work might subject to weather condition. This causes unsatisfactory among consumers that experiences frequent grid outage. When a fault present in the distribution network, protection system will be triggered which causes grid outage. In the event of grid outage, RES is required to shut down as required by various international standards. Therefore, available clean

energy from RES are not utilised, even in a good weather condition. Simulation studies have shown that islanding operation of RES is able to improve the reliability and quality of the electricity supply (Chowdhury et al., 2008; Manaffam et al., 2017). To ensure continuity operation of RES in the event of grid outage, the voltage and frequency within the islanded network have to be regulated within the allowable limits. Hence, allowing islanding operation of RES provides consumers with an opportunity to utilise the available clean energy during in the event of grid outages.

In addition, utilisation of RES can reduce GHG emission such as Carbon Dioxide (CO_2). CO_2 avoidance from PV system installation from the Year 2012 to Year 2017 has increased from 5003 tonnes to 589651 tonnes as shown in Figure 2.10. It is shown that implementation of RE Act 2011 has increased the growth of PV system and increase CO_2 avoidance dramatically throughout the past years. Thus, with the increasing growth of PV system in the electrical network, a feasibility study on the islanding operation with PV system should be considered.

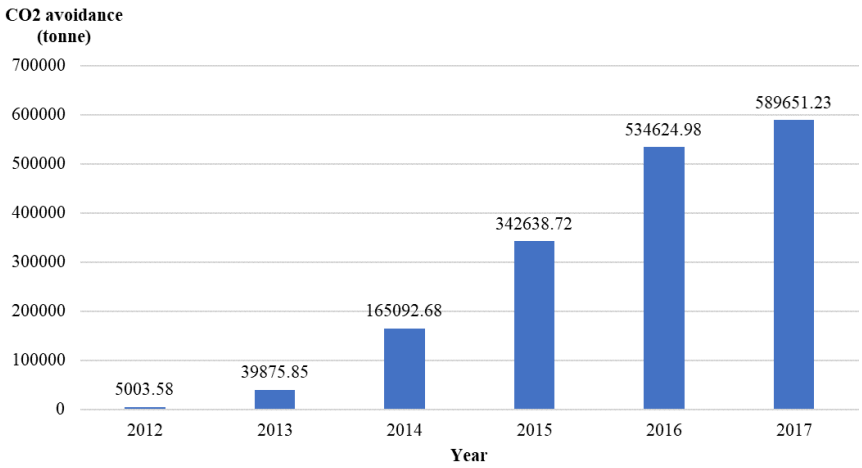

Figure 2.10: CO_2 avoidance from Year 2012 to Year 2017 with PV system installation

2.8. Technical Aspect for Allowing Islanding Operation of PV Systems

In the 21st-century energy market for consumers, the growth of RES has transformed the traditional grid from unidirectional to bi-directional power flow whereby several technical aspects must be considered to ensure safety and reliability of renewable energy operating in islanding operation.

2.8.1. Voltage and Frequency Regulation

In the distribution network, the voltage and frequency must be regulated within the statutory limit to ensure safe operation of the electrical equipment. When the network is connected to the grid, the voltage and frequency of the network is regulated by the power plant that ramp up or down the generation to support the change in supply and demand. According to Malaysia's Grid Code and Distribution Code, the voltage at the distribution network has to be maintained

within +10% and -6% of the rated voltage of 400 V and 230 V for three phase and single phase system respectively, while the network frequency has to be maintained at ±1% of 50Hz (Yusof R, 2015). This is to ensure issue such as voltage rise and voltage sag can be prevented which would otherwise potentially damage electrical equipment. When the grid is out of service, the voltage and frequency are no longer governed by the grid. Therefore, regulating unit in the islanded network is responsible to ensure the voltage and frequency within the islanded network operate within the allowable limit (Cha et al., 2014).

2.8.2. Grounding Protection of Islanded Network

One of the challenges to allow RES to continue for operation during islanding is the absence of neutral point. In Malaysia, Low Voltage (LV) distribution network practises a TT grounding system where the neutral point is grounded on the transformer side of the LV network. In the event of the grid outage, the neutral point of the islanded network might not be properly grounded. The absence of neutral point will cause protection device failed to operate in the event of fault occurrence. Therefore, several methods are proposed to earth the neutral point to ensure safe operation of an islanded network (Dempsey, 2017). The first approach uses a zig-zag transformer with no secondary winding to obtain system neutral for the grounding of a three-phase system. The internal connection of the zig-zag transformer as shown in Figure 2.11 (IEEE Std, 1992).

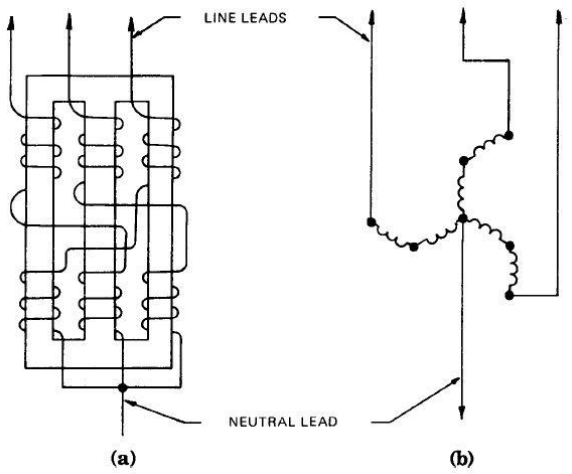

Figure 2.11: (a) core windings and (b) connections of three-phase zigzag grounding transformer (IEEE Std, 1992)

A project under Clemson University has demonstrated the use of zigzag grounding transformer in normal operation and islanding operation as shown in Figure 2.12. In the event of the grid outage, the system transit into islanding operation and the breaker for zigzag grounding transformer is closed to provide grounding for the islanded network. This ensures safe operation of all protection devices in the islanded network.

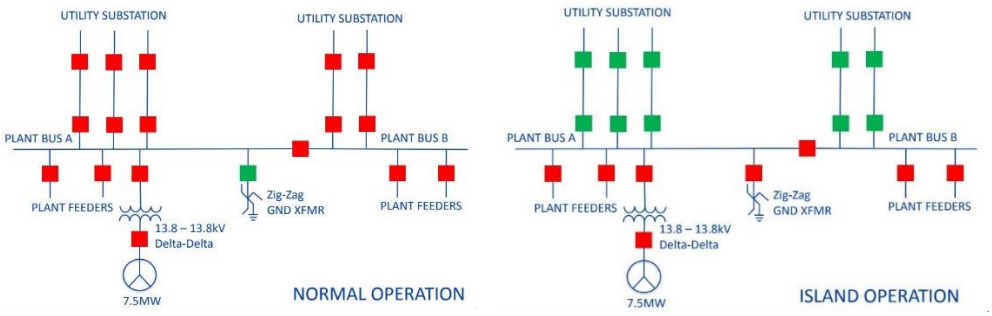

(a) (b)

Figure 2.12: Deactivation and activation of the zigzag grounding transformer during (a)normal operation and (b) islanding operation respectively (Dempsey, 2017)

2.8.3. Synchronisation of the Islanded Network

Another important aspect of operating islanding network is the synchronisation mechanism. When the grid is disconnected, islanded network operates independently. Synchronisation is needed before the active islanded network is reconnected to the main grid after grid outage. Before reconnection back to the grid, it is mandatory to ensure the phase angle and magnitude of the voltage and frequency in the islanded network and the grid are closely matched. Reclosing into an active islanded network without synchronisation would cause high inrush current which can potentially damage electrical equipment. IEEE1547-2003 provides recommendations on the requirement for synchronisation before the active island is reconnected with the grid. With the latest technology available, modern inverter is equipped with synchronising equipment to sync the voltage and frequency in order to operate in grid connected and islanded operation (Thompson, 2016; William et al., 2017).

2.9. Methods for Voltage and Frequency Regulation for Islanding Operation

In a small scaled electrical network such as microgrid, inertia present in the system is low whereby a slight difference in power generation and demand can result in frequency excursion. If the voltage and frequency are not properly maintained, it will potentially damage the electrical equipment connected to it. Therefore, two methods have been employed to regulate the voltage and frequency within the islanded network. The first method utilises diesel generator to regulate the power mismatch within the islanded network. The second methods utilise energy storage system to regulate the power mismatches within the islanded network, hence restoring the voltage and frequency. At present, several studies have been conducted to investigate the feasibility of these two methods in conducting islanding operation.

2.9.1. Rotational Type Generator

Rotational type of generator, such as synchronous and diesel generator is widely used in islanding operation to provide voltage and frequency regulation and to provide uninterruptible power supply to the islanded network in the event of grid outage. Besides, generator can provide a voltage reference to the working of other RES. The operating principle of a generator used in islanded network is similar to the generators used in power plant. A diesel generator is equipped with Automatic Voltage Regulator (AVR) and governor droop control to regulate the voltage in the islanded network (Arulampalam et al., 2010). The frequency of the islanded network varies with the rotational speed of generator.

A proposed control is developed by utilising diesel generator in the islanded network to maintain synchronism between islanded network with the main grid (Best et al., 2007). The control algorithm was also performed under load disturbance condition. In Thailand, a study is performed to investigate the dynamic and steady-state performance of islanding operation with mini-hydro power station located at Namman and Namsan. It is found that mini-hydro generating unit connected to distribution network can operate in islanding operation which presents a great opportunity to provide continuity supply (Tantimaporn et al., 2010). The use of generator has been long developed for islanding application to regulate and voltage and frequency. Hence, it allowed integration of RES into the islanded network. However, the use of fossil fuel to drive the generator for islanding operation is not environmental friendly as it emits GHG during its operation. Rotating type of machine has inertia which gives them a relatively slow response as compared to other inverter-based devices (Best et al., 2007). Therefore, new technology in the power electronic converter is used to develop an energy storage system to provide fast response for voltage and frequency regulation during islanding operation.

2.9.2. Energy Storage System for Islanding Application

Energy Storage System (ESS) has been used in the power system especially as an uninterruptible power supply in the past decades. The types of ESS technology is discussed in section 2.12. ESS technology has proven to be reliable in providing voltage and frequency regulation especially in microgrid (Zhao, Hong, et al., 2017). Microgrid is a future distribution network which

enables RES integration. In a microgrid, several Distributed Generator (DG) such as ESS, PV, and wind are connected to the grid through power inverters. During islanding operation of a microgrid, the voltage and frequency should be maintained within statutory limit, while the load in the microgrid has to be shared proportionally among all DG by adopting power sharing control strategy. Power sharing control strategy is required to ensure the power generation and demand are balanced to stabilise the voltage and frequency.

DG in the microgrid can be classified into grid-forming DG and grid-following DG (Brabandere et al., 2007). The grid-forming DG (i.e. ESS) act as a voltage source inverter to provide a voltage reference to other current source inverters in the microgrid. The grid-following DG (i.e. PV systems, and wind turbine) act as a current source inverter. In the event of islanding operation, ESS is responsible for power sharing according to their rating and availability (Lidula and Rajapakse, 2011). Several control strategies categorised into with communication and without communication, to achieve power sharing among DG's are discussed in the following section.

2.9.2.1. Power Sharing Strategy with Communication

Power sharing strategy with communication-based can provide excellent voltage and frequency regulation. A central controller is responsible for data collection and analyse the data to make necessary action to be taken by other DG. The instruction to be taken by DG is then sent through low bandwidth communication to DG surrounding for execution (Andishgar et al., 2017).

Vandoorn et al. (2013) presented a Phase Lock Loop (PLL) module which can provide consistency in frequency and phase angle of the voltage. A central control unit consists of a current sharing bus is developed to detect the current of the load. A current sharing bus is then specified the reference value of current for each module. This current reference, i_{ref} is calculated based on $i_{ref} = i_{load}/N$ where N is the number of modules in the microgrid and i_{load} is the measured load current. Upon receiving the current reference from the current sharing bus, the inverter measures its output and adjust accordingly to achieve equal current distribution.

Tenti et al. (2013) utilised master and slave technique for power sharing strategy. In this method, each inverter is connected in parallel. In the islanded network, one inverter acts as a master module, while the rest of the inverters act as slave module. The master module is in-charge of parallel operation to control the remaining slave inverters, regulate the bus voltage and specifies reference current for the slave inverter. The slave inverter then tracks the current reference provided by the master module and adjust accordingly to achieve equal current distribution. However, the system tends to fail when the master unit fails. If the master module failed to operate, the system will not be working as well. This drawback can be overcome by using a control strategy developed by Shafiee, Guerrero, et al. (2014) which does not rely on the central unit. In the event of a single unit fault, the entire system will not be affected. The control strategy proposed a current control loop embedded into the inverter to track the reference current provided by current sharing bus. The current sharing bus is required to distribute the reference current for each inverter in the islanded network, and

hence restore the frequency and amplitude deviation during islanding operation, when a module failed, other inverters remain operated.

However, these techniques required communication link between each module in the microgrid, which increases the overall system cost. The long-distance communication link has a higher tendency of having interruption which reduces system reliability and expandability. Therefore, power sharing strategy without communication is considered.

2.9.2.2. Power Sharing Strategy without Communication

The power sharing control strategy that operates without communication is generally based on droop concept which is commonly used in the decentralised network. Strategy without communication is used to connect remote inverters. It can avoid complexity and high cost incurred in developing communication system. Such a system offers plug and play feature for each inverter and it is more flexible in terms of future system expansion. With the voltage and frequency droop characteristics curve, all sources in the islanded network can achieve power sharing without any investment on communication system (Huang et al., 2011). However, droop control method does not guarantee consistency of voltage and frequency amplitude, but the elimination of communication link makes this method looks attractive (Divshali et al., 2012).

The details for power sharing control strategy using droop control is presented by (Tayab et al., 2017). The droop control method in the power

electronic inverter is widely adopted (Lidula and Rajapakse, 2011). The working principle is based on the behaviour of a synchronous generator, which is to increase the active power when frequency decreases (Planas et al., 2013). Figure 2.13 depicts the conventional voltage and frequency droop characteristics curve where the active power and reactive power of the inverter output varies with the frequency and voltage of the network respectively. Many papers have demonstrated that the best way to control power electronic inverter in the microgrid is the use of droop control (Ustun et al., 2011; Zamora and Srivastava, 2010).

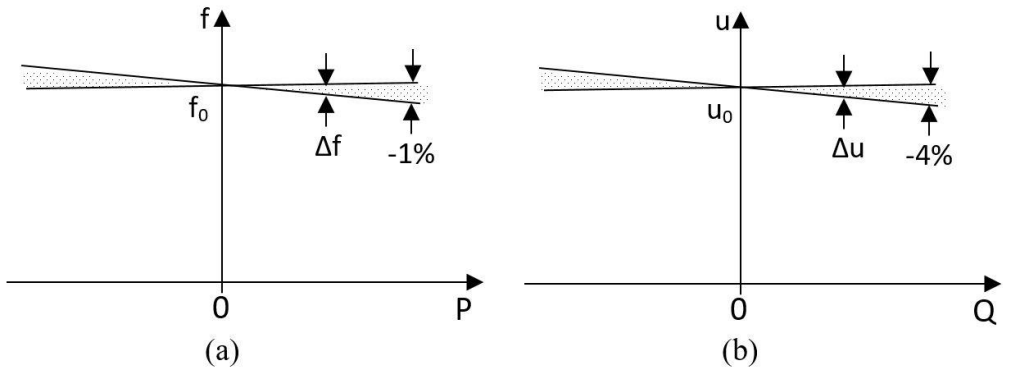

Figure 2.13: Droop characteristics curve of frequency and voltage (Engler, 2004)

Guerrero et al. (2009) has developed a conventional droop control scheme for voltage source inverter in a simulation model. It is shown that the proposed droop method can achieve accurate active and reactive power regulation, showing good steady-state and transient response during load switching in the islanded network. Besides, Vasquez et al. (2009) presented a voltage and frequency droop control to achieve power sharing among DG's in

the islanded network. However, conventional droop control presents several drawbacks such as slow transient response, poor harmonic load sharing among DG (Guerrero et al., 2011). Therefore, a virtual impedance loop-based is developed to overcome limitations of conventional droop control

Numerous studies have achieved actual power sharing by implementing virtual output impedance in droop control through a fast control loop which emulates the line impedance (Zhang et al., 2014). Since power sharing is affected by line impedance, Brabandere et al. (2007) has demonstrated the use of complex finite-output impedance to obtain voltage droop. The author managed to achieve efficient control in voltage and frequency of the islanded network. With the use of virtual impedance control loop, accurate power sharing can be achieved for an inductive and resistive line. In addition, virtual impedance control offers an additional feature to the inverter such as harmonic current sharing (Guerrero et al., 2013).

In the conventional droop techniques, issue such as line impedance dependency and slow response can be solved by using adaptive droop control. An adaptive droop control method is proposed to maintain the voltage amplitude and achieve accurate reactive power sharing in the islanded network (Yang et al., 2006). Shafiee, Nasirian, et al. (2014) has proposed an adaptive integral loop technique which can improve power sharing dynamic response among inverters in the islanded network. Besides, microgrid impedance is calculated to predetermine adaptive droop parameters which can ensure accurate power sharing and reduce line losses (Oureilidis and Demoulias, 2016).

2.10. Islanding Detection Methods

At present, there have been many methods being developed and deployed to detect the occurrence of islanding. These methods are embedded into the power electronic inverter to detect the occurrence of islanding and disconnect from the grid. Failed to detect islanding and disconnect immediately can potentially lead to equipment damages. Thus, Non-Detection Zone (NDZ) as illustrated in Figure 2.14 is used as a tool to evaluate the performance of the islanding detection (Isa et al., 2015; Ye et al., 2003; Zhu et al., 2009). NDZ is a region formed by power mismatch between generation and demand during the starts of an islanding operation. The boundary of the NDZ is the region where islanding event is not detectable during the occurrence of islanding. Thus, there are possibilities where renewable energy sources connected at the Point of Common Coupling (PCC) remain connected and energise the load when the voltage and frequency remained within NDZ.

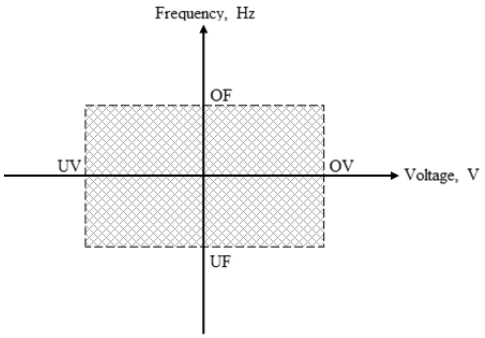

Figure 2.14: NDZ is the shaded region used to evaluate islanding performance

Islanding detection methods as shown in Figure 2.15 can be categorised into local and remote techniques. The local technique utilises parameters measured on the power line which comprises of active methods, passive methods, and hybrid methods (Li et al., 2014). The passive method monitors the voltage and frequency which is easy to implement and suitable for low-cost application as it just requires monitoring of line parameters. Active methods inject a small amount of disturbance to detect whether the voltage and frequency changes are affected. This method is great for improving islanding detection capability and helps in reducing NDZ. However, active methods utilise disturbance injection to distort the waveform which can potentially cause power quality issue. Hybrid methods utilise the advantages of active and passive methods to detect islanding. This method has a small NDZ, but the design and structure of the hybrid method are complicated as compared to others.

Remote methods incorporate communication devices installed to monitor the status of the breaker at the substation. This method has small NDZ and does not cause power quality degradation. However, the use of communication devices requires a high initial cost, which is not economical for a small system. Therefore, the cost of implementing remote methods is much more expensive as compared with local methods.

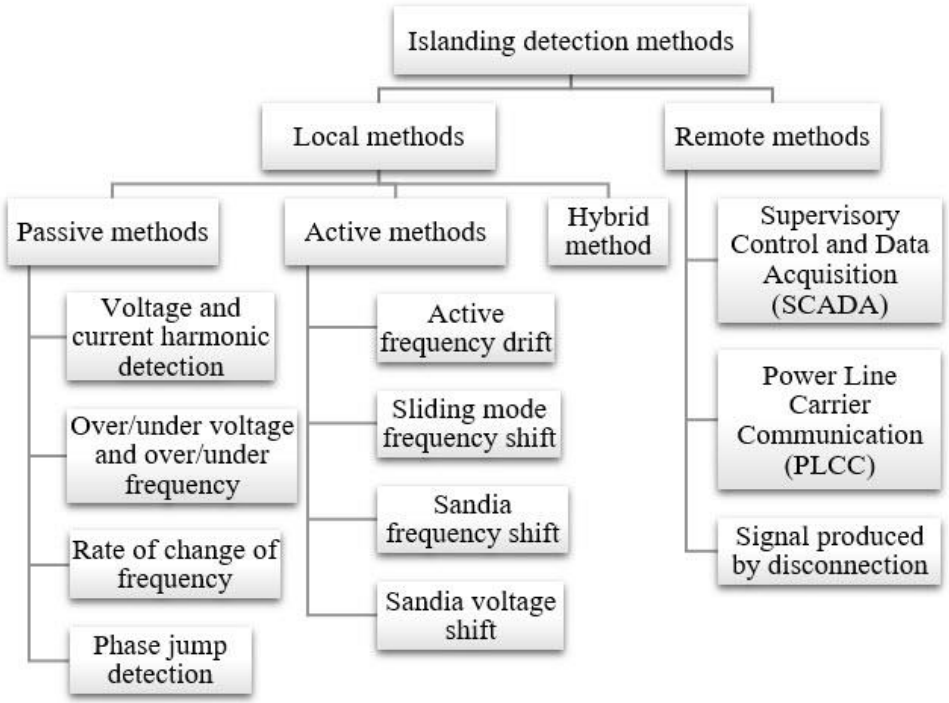

Figure 2.15: Classification of islanding detection methods

2.10.1. Passive Methods

2.10.1.1. Over/undervoltage and Over/underfrequency (OUV and OUF)

Over/undervoltage and Over/underfrequency (OUV and OUF) method monitor the voltage and frequency of the network. The detection method utilises threshold settings for voltage and frequency. The inverter monitors the voltage and frequency at the PCC and cease to energise and disconnect from the grid when the voltage and frequency exceeded the predefined threshold. The change in frequency and voltage after the system are islanded is mainly caused by the mismatches of active and reactive power respectively during the intercept of islanding occurrence as shown in equation (2.2) and (2.3) as follows:

$$\Delta P = P_{load} - P_{Generation} \quad (2.3)$$

$$\Delta Q = Q_{load} - Q_{Generation} \quad (2.4)$$

In grid-connected operation, the ΔP and ΔQ is supported by the grid to achieve a balance between generation and demand. Prior to islanding, voltage and frequency will drift until ΔP = 0 and ΔQ = 0 (Ku Ahmad et al., 2013; Velasco et al., 2010). Therefore, OUV and OUF can be utilised to detect islanding occurrence by monitoring parameter of voltage and frequency. The advantages of OUV and OUF is low-cost implementation and does not cause power quality issue. But, these methods present large NDZ as the primary disadvantages.

2.10.1.2. Rate of Change of Frequency (ROCOF)

In the event of islanding occurrence, power mismatch between generation and demand at the starts of islanding creates frequency change. The change in frequency is measured by df/dt over a few cycles. If the setting threshold for df/dt is exceeded, the inverter will disconnect from the grid and cease to energise (Hashemi et al., 2017; Mahat et al., 2008). ROCOF method is more sensitive as compared to OUV/OUF. Thus, the detection speed for ROCOF is faster. If the power mismatch is large at the start of islanding, ROCOF method can provide highly reliable detection. In fact, detection time for ROCOF is around 24 ms (Li et al., 2014). However, drawback of using ROCOF detection method is the high sensitivity to load switching. It may not detect occurrence of islanding accurately because it is unable to differentiate whether the voltage and

frequency change is affected by the load switching or islanding occurrence.

2.10.1.3. Phase Jump Detection

Phase Jump detection (PJD) method monitors the phase of voltage and current of the output inverter. This method is implemented using Phase Lock Loop (PLL) to detect zero crossing of voltage in each and every cycle (Giampaolo et al., 2014). During grid-connected operation, the output current of the inverter is synchronised with the voltage at PCC. In the event of islanding, the output of the inverter remains unchanged, the voltage will experience a sudden "jump" due to load phase angle. The phase angle differences are used to indicate the occurrence of islanding event. If the change is greater than setting threshold, it will be deemed as islanding event. PJD method of islanding detection is fast and usually detects islanding event up to 20 ms and it does not cause power quality issue (Singam and Hui, 2006). The drawback of using this method is the difficulty in choosing the threshold value. A load such as the motor type of load increase difficulty in setting the threshold. Therefore, appropriate threshold setting is required to ensure high accuracy of PJD detection and prevent nuisance trip (Hanif et al., 2011).

2.10.2. Active Methods

2.10.2.1. Active Frequency Drift

Active Frequency Drift (AFD) is a method that injects a small amount of disturbance to distort the current waveform. In the normal operation, the voltage

and frequency within the network is governed by the power plants and well maintain within statutory limits. Prior to grid outage, small amount of disturbance injected by inverter will shift the current frequency waveform. This disturbance injection causes a phase error between current and voltage. The output current frequency of inverter is drifted until the voltage frequency exceed the threshold of over/under frequency and islanding occurrence is detected (Wang et al., 2016; Wen et al., 2016). The advantages of AFD detection method is the simple implementation and has small NDZ. AFD is sensitive to load parameters and the detection time increases when the load is not resistive and the NDZ increases with high reactance load. Thus, AFD detection method is great for a system that made up of pure resistive load. The latest development of AFD with positive feedback or Sandia frequency shift is proposed which effectively reduces the detection time (Reis et al., 2015).

2.10.2.2. Sliding Mode Frequency Shift

Sliding Mode Frequency Shift (SMS) utilises positive feedback to shift the voltage phase at the PCC. The voltage-current phase angle of the inverter is indicated as followed,

$$\theta_{sms} = \theta_m \sin\left(\frac{\pi f^{k-1} - f_r}{2f_m - f_n}\right) \tag{2.5}$$

Where θ_m is the maximum phase angle at frequency f_m, f_r is the rated frequency, and f^{k-1} is the frequency of the previous cycle (Mohammadpour et al., 2016). In grid-connected mode, the phase angle between inverter current

and voltage at PCC is zero. When the grid is disconnected, phase lock loop (PLL) is not able to tune the frequency which causes the frequency to drift away (Jeong et al., 2013; Laour et al., 2014). Thus, islanding event is detected when the frequency drifted beyond the threshold of OUF. SMS detection method has smaller NDZ as compared with other active methods and easy to implement with software. However, method which utilise disturbance injection may present power quality issues. An improved SMS strategy with linearised frequency positive feedback is developed can effectively improve the reliability of the conventional SMS and provide shorter detection time with smaller NDZ (Liu et al., 2010).

2.10.3. Remote Methods

2.10.3.1. Power Line Carrier Communication

Power Line Carrier Communication (PLCC) method utilises communication link between the utility side and the receiver at the consumer side. A continuous signal is sent from transmitter to the receiver that is embedded into the inverter. Islanding operation is detected when the signal is interrupted (Xu et al., 2007).

The PLCC method measure four consecutive cycles of signal. When signal disappears in consecutive three cycles, islanding is detected (Wang et al., 2007). This method has no NDZ and does not cause power quality degradation. The use of communication has significantly improved islanding detection. However, installation cost for communication is expensive and uneconomical in low-density renewable energy sources network.

2.10.3.2. Supervisory Control and Data Acquisition

Supervisory Control and Data Acquisition (SCADA) is a system that monitors the grid parameters such as the status of the auxiliary contacts of circuit breaker. Prior to grid outage, SCADA system will send a signal of the status of the circuit breaker to other inverters. Upon receiving the signal from SCADA system, the inverter will disconnect and cease to energise. The advantage of using SCADA system is similar to Signal Produced by Disconnect (SPD) where SPD detect islanding using signal transmission between the inverter and external power grid (Bayrak and Kabalci, 2016). SCADA system is highly effective and does not cause power quality to deteriorate. With the proper installation and communication protocol available, NDZ can be eliminated and reliability of islanding detection is improved. However, SCADA system required high investment cost as the instrument and communication link is expensive (Khamis et al., 2013). Thus, this system is suitable for large-scale electrical network above medium voltage network as it has zero NDZ (Laghari et al., 2015). Table 2.6 illustrated the comparison of various islanding detection technique.

Table 2.6: Comparison of various islanding detection methods

Categories	IDM	Advantages	Disadvantages
Passive	OUV/OUF	• Low-cost • Easy to implement	• Large NDZ • High error detection rate
	ROCOF	• Small NDZ • Easy to implement	• High error detection rate
	PJD		
Active	AFD	• Small NDZ	• Power quality degradation
	SMS	• Small NDZ • Improved disconnection time	
Remote	PLCC	• Zero NDZ	• High implementation cost • Additional communication devices required
	SCADA	• Zero NDZ • Highly reliable	

2.11. Fuzzy Controller in Islanding Application

Fuzzy logic is one of the basic Artificial Intelligent (AI) which used to provide human-like reasoning technique. Instead of the conventional Boolean logic of "0" and "1", fuzzy logic can further classify the Boolean logic based on "degree of truth". At present, Fuzzy Logic Controller (FLC) has been developed and deployed in the power system to solve various kind of issue such as voltage rise (Qamar et al., 2017), peak demand reduction (Chua et al., 2017), and frequency regulation (Falahati et al., 2016). This subsection aims to review the use of FLC in the islanding application.

FLC has been widely used in the area of anti-islanding protection such as islanding detection. A fuzzy rules-based approach is developed and presented by Samantaray et al. (2010) to detect the occurrence of islanding by using

MATLAB. The approach has shown that the FLC can detect islanding accurately for wide variations in operating parameters of the electrical network. Aguiar et al. (2015) has make used of fuzzy logic to create positive feedback loop to accurately detect whether the network is islanded. The proposed idea has eliminated the disturbance injection and the results have proven this method to be effective as compared to conventional active detection approach. Besides, an Adaptive Neuro-Fuzzy Inference System (ANFIS) is developed to improve the effectiveness of islanding detection (Bitaraf et al., 2012). The results have shown that ANFIS is able to reduce the window of NDZ in passive islanding detection, hence improving the detection time and accuracy. An optimised version of ANFIS is developed by Shayeghi et al. (2016) has demonstrated that the optimisation algorithm is capable to reduce the NDZ to almost zero.

In addition, FLC was applied in microgrid as well. A Fuzzy Interference System (FIS) is developed in MATLAB Simulink, to improve energy storage lifecycle and reduce grid fluctuation caused by intermittent renewable energy sources in the microgrid (Teo et al., 2016). A Fuzzy Secondary Controller (FSC) is developed to regulate the voltage and frequency levels in the grid-connected and stand-alone mode. It is simulated using PSCAD and the results have shown that it can reduce the dependency on communication link method by using only local measurements and provide flexible strategy to connect microgrid with the utility grid. Similar method utilising diesel generator was developed which is less environmental friendly (Agnoletto et al., 2016; Neves et al., 2016).

Besides the abovementioned FLC in anti-islanding detection, there are researchers who utilise FLC to maintain the islanding operation in the event of the grid outage. A simulation study in MATLAB has proposed a control to maintain islanding operation for 8 days until the battery reaches the critical level (Lebrón and Andrade, 2016). A Fuzzy Gain Schedule Proportional-Integral-Derivative (FSDPID) is developed to provide frequency regulation in the islanded network under various load variation. The proposed control algorithm has integrated fuzzy and PI controller, and results were compared against PID controller in restoring frequency in the islanded network (Kumar et al., 2016). An adaptive FLC is simulated in MATLAB to regulate the voltage in the islanded network, and the results have proven that FLC provides better damping response, transient behaviour as compared to the conventional PI controller. Besides, a research paper has proven that FLC is capable to mitigate voltage fluctuation caused by load variation during islanded operation (Choudhury et al., 2016). A comparison is conducted to compare the response time between PID and fuzzy controller in regulating power mismatch under sudden load change condition. The results have proven that fuzzy performed better as compared to PID for voltage and frequency regulation in the event of disturbance (Kermani, 2016). Takagi-Sugeno (TS) Fuzzy based adaptive charging power control of plug-in electric vehicles is developed by Jamroen et al. (2016) has proven to stabilise network frequency islanded operation, which reduces the chances of power outages as well. Generally, many research works done has proven that fuzzy can be one of the effective solutions for islanding operation. However, most works have been studied using simulation approach and focused after islanding operation instead of the transition period between

grid-connected and islanded mode.

2.12. Energy Storage System Technology

In the application of islanding operation, Energy Storage System (ESS) is used to mimic the behaviour of a synchronous generator to provide voltage and frequency regulation in the islanded network. At present, numerous research and development have been conducted to improve the energy storage technologies. Figure 2.16 depicts the types of ESS technologies including mechanical energy storage, electrical energy storage and electrochemical energy storage.

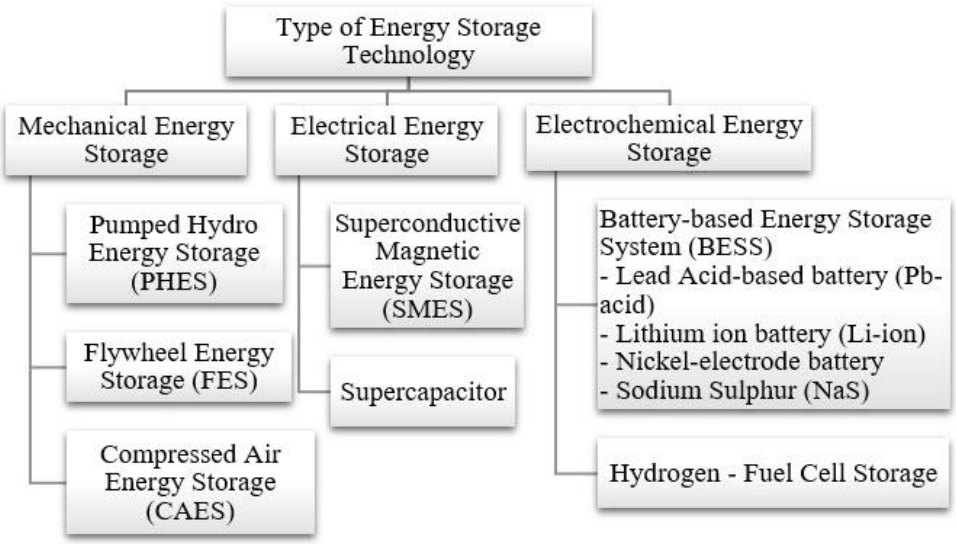

Figure 2.16: Types of energy storage technologies

Mechanical energy storage technologies can be classified into Pumped Hydro Energy Storage (PHES), Flywheel Energy Storage (FES) and Compressed Air Energy Storage (CAES). PHES technology stores energy in

the form of water in an elevated height reservoir. Electricity is generated when the stored water is released from the reservoir, flowing through a turbine located at a lower level to generate electricity. FES uses a high-speed rotor driven by an electrical machine to store rotational energy. Contrarily, CAES stored the energy in a form of compressed air using large tank buried underground. Electricity is generated when compressed air is heated and released to turn a turbine generator set.

Electrical energy storage can be classified into Superconductive Magnetic Energy Storage (SMES) and supercapacitor. SMES stores energy in the form of magnetic field generated by the current of superconducting coil cooled at a low temperature to achieve negligible resistance. Conversely, supercapacitor stores energy by applying voltage difference between positive and negative plate to build up static charges across these parallel plates in an insulating dielectric.

Electrochemical energy storage such as Battery-based Energy Storage System (BESS) and fuel cell stores energy in the form of chemical energy in the electrochemical cells. BESS stores energy when a DC voltage is applied to the battery and reverse its operation, restoring the battery charges. Fuel cell store energy in the form of hydrogen. When electricity is needed, electrochemical reaction of hydrogen reacts with fuel cells to produce electricity. At present, there are numerous types of batteries being used in BESS. The batteries vary with energy density, life cycle, efficiency, cost etc. Obtained from Alhamali et al. (2016), Table 2.7 summarises the characteristics of different battery

technology used in BESS such as Valve-regulated Lead Acid (VRLA), Lithium-ion (Li-ion), Nickel Cadmium (NiCd), Nickel-Metal Hydride (NiMH), and Sodium Sulfur (NaS).

Table 2.7: Types of battery technologies

	VRLA	Li-ion	NiCd	NiMH	NaS
Energy density (kWh/m^3)	≈ 75	250 ~ 620	< 200	< 350	< 400
Power density (kW/m^3)	90 ~ 700	1300 ~ 10000	75 ~ 700	500 ~ 3000	120 ~ 160
Life cycle (Cycles)	2000	4500	3000	300 ~ 500	4500
Lifetime (Years)	3 ~ 15	8 ~ 15	15 ~ 20	5 ~ 10	12 ~ 20
Self-discharge	Low	Low	Low	Medium	Medium
Cost[a] (RM/kW)	1000 ~ 3250	3500 ~ 15000	1750 ~ 5000	2100 ~ 6000	3500 ~ 10000
Cost[a] (RM/kWh)	250 ~ 1500	1000 ~ 9000	1000 ~ 5000	1200 ~ 6000	1000 ~ 4500
Efficiency (%)	80 ~ 90	90 ~ 98	90	70 ~ 75	85 ~ 90

[a] Conversion rate of 1 EURO to 5 MYR.

Each of the battery technologies as mentioned in Table 2.7 have its own advantages and disadvantages. There is no battery technology that fits all grid operation. However, after considering the energy density, life cycle, and cost, VRLA is selected for this project. Low-cost, setup simplicity and scalable advantages of VRLA provides a suitable solution for islanding application. Besides, technical characteristic of VRLA allows rapid charge and discharge feature which is beneficial for islanding operation.

2.13. Summary

In summary, several incentives provided by the government to promote the use of renewable energy has been presented. With the initiative by the government, the number of PV installation is expected to increase. Therefore, several international standards for interconnecting renewable energy with the grid is discussed. It is understood that the grid-connected PV system is required to disconnect in the event of grid outage to prevent islanding operation. However, disconnecting PV in the event of grid outage causes available energy to be wasted. Therefore, the benefits of allowing islanding operation of PV system is elaborated. Several technical aspects of allowing islanding operation have been reviewed. Types of power sharing strategy to regulate the voltage and frequency in the islanding network have been reviewed as well. Application of fuzzy logic control strategy in islanding application has been elaborated.

CHAPTER 3

SYSTEM ARCHITECTURE AND DEVELOPMENT OF LOW VOLTAGE EXPERIMENTAL NETWORK

3.1. Introduction

In this chapter, the design and development for the system architecture and the lab-scaled experimental Low Voltage (LV) distribution network will be discussed. The details of the key elements design will be described. Two major investigations are conducted on the experimental network as follows:

I. Feasibility study of the PV system in conducting islanding operation.
II. Feasibility study of the BESS in assisting islanding operation with PV system.

This experimental network served as a platform to conduct the feasibility study of PV system in conducting islanding operation with the aids of a battery-based energy storage system.

3.2. Experimental Low Voltage Distribution Network

A lab-scaled experimental Low Voltage (LV) distribution network consists of a three-phase LV distribution board rated at 400 V is powered by grid emulator or utility grid. Figure 3.1 shows the distribution board is designed in such a way to emulate typical Malaysian LV distribution network with a three phase four wire radial system that is highly resistive. The distribution board consists of seven nodes connected to grid supply, two PV systems, a three-phase load emulator, and a Battery-based Energy Storage System (BESS) consists of bi-directional inverter with batteries and two spares nodes.

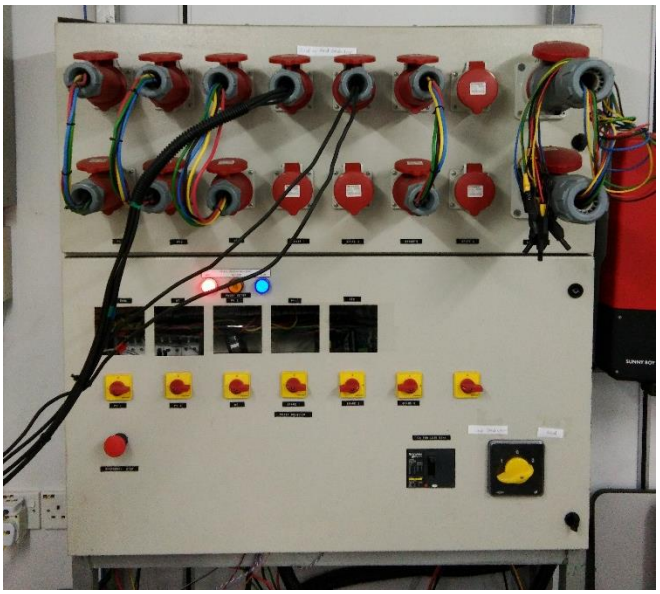

Figure 3.1: Experimental LV distribution network

3.3. Photovoltaic (PV) System

A commercial available single-phase Photovoltaic (PV) system compliance with international standard is used in the project to ensure proper operation during the study. Two single-phase PV systems rated at 3.6 kW_P are connected in one phase to form a total capacity of 7.2 kW_P. Each PV system is made up of 16 polycrystalline solar modules (Manufactured by Sanyo Electric) interconnected with each other to form a string and coupled with a DC-AC PV inverter. Table 3.1 shows the specification of the solar module with its power output rated at 230 W. In this project, a total number of 32 units of solar modules are installed on the rooftop of the university building. The solar modules are mounted to face east direction with a 5° tilting angle to allow rainwater to flow. Figure 3.2(a) and Figure 3.2(b) shows the top view of the solar modules mounted on the rooftop of the university and the PV inverter manufactured by SMA that is installed at the laboratory.

Table 3.1: PV module specification

Model No. VBMS230AE01	**Nominal values**
Maximum Power (Pmax)	230 W
Short Circuit current (Isc)	8.42 A
Open Circuit Voltage (Voc)	37.0 V
Maximum Power Current (Imp)	7.83 A
Maximum Power Voltage (Vmp)	29.4 V
Maximum System Voltage	1000 V
Minimum Pmax	218.5 W
Max. Over-current Protection Rating	15 A

*All technical data at standard test conditions: AM 1.5, 1000W/m^2 irradiance, 25℃ cell temperatures.

(a) (b)

Figure 3.2: (a) Location and top view of 32 units of solar modules installed at the rooftop of the university building (b) PV inverter rated at 3.6 kW$_P$ installed at the laboratory

3.4. Load Emulator

A three-phase 9.0 kW load emulator is made up of 18 power resistors rated at 500 W each and controllable with 15 solid state relay as shown in Figure 3.3(a) and Figure 3.3(b) respectively. The solid-state relay is activated via National Instrument (NI) digital input/output module, NI-9403 which houses in the CompactDAQ chassis. Figure 3.4 depicts the control system for load emulator where the LabVIEW is installed on the supervisory computer which uses graphical programming to control the NI-9403 signals. In this project, single phase is used whereby the total controllable load is 3.0 kW.

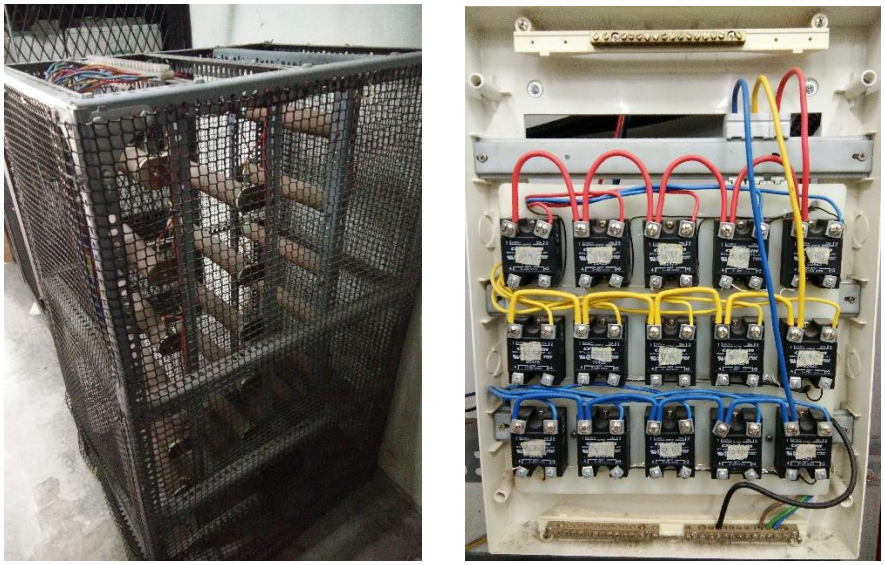

(a) (b)

Figure 3.3: Load bank located at the back of laboratory for proper air ventilation (b) Solid state relay for controlling each resistor

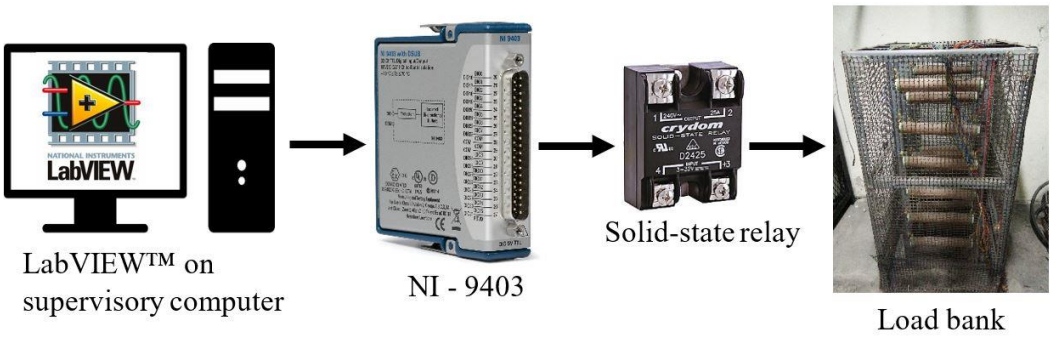

Figure 3.4: Control system for load emulator

3.5. Battery-based Energy Storage System (BESS)

3.5.1. Hardware Architecture

A battery-based energy storage system (BESS) consists of a 6.0 kW bi-directional inverter coupled with Valve-Regulated Lead Acid (VRLA) batteries is integrated into the LV experimental distribution network as shown in Figure 3.5(a) and Figure 3.5(b) respectively. The bi-directional inverter (Model number: SI8.0H), manufactured by SMA Solar Technology is capable to control bi-directional flow of active and reactive power where the charging and discharging is executed autonomously or user selection. The BESS is capable to act as a voltage source to provide a voltage reference to other current source inverters during islanding operation. The current source inverter in this project is PV system. Besides, the bi-directional inverter is equipped with features such as droop control, battery monitoring system which is further elaborated in section 3.6.

(a) (b)

Figure 3.5: (a) Three units of 6.0 kW bi-directional inverter manufactured by SMA (b) VRLA batteries placed at the back of laboratory

The battery pack is made up of 16 VRLA batteries manufactured by HOPPECKE. The VRLA batteries are configured in 4x4 strings as shown in Figure 3.6 where each battery is rated at $12V_{DC}$ and C10 rating of 111 Ah battery capacity as shown in Table 3.2 respectively. Each string is made up of four VRLA batteries connected in series to form 48 V. Four strings of the batteries provide a total capacity of 444 Ah. This type of VRLA battery features maintenance-free operation, faster charging, and no corrosive gas emission as compared to other refillable water-type acid batteries (Janine, 2014).

Table 3.2: Specification of VRLA battery

	Specification
Model	HOPPECKA Solar.Bloc
Capacity	111 Ah @ 10 h discharge rating
DC voltage	12.0 V
Type	Absorbent Glass Mat (AGM)
Weight	46.0 kg
Dimension (mm)	344x 170 x 275

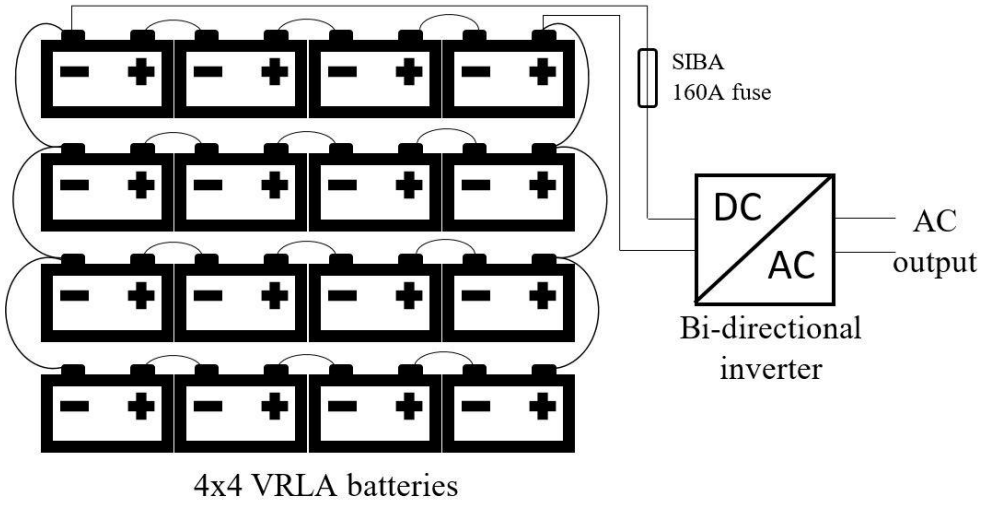

Figure 3.6: Wiring configuration of 4x4 VRLA batteries with bidirectional inverter

After setting up the hardware for the BESS system, a communication system is established between a supervisory computer and the BESS via TCP/IP network with the used of Speedwire Ethernet. Modbus protocol is used as the transmission modes to communicate with the bi-directional inverter. Figure 3.7 depicts the graphical codes written on the LabVIEW to retrieve necessary parameters such as the battery state-of-charge (SoC), temperature, current and voltage from the registers of the BESS. Besides, the “Pinv (W)” shown in the graphics programming is used as a variable to control the BESS output by

writing the desired active power into the respective register address. The development of the Modbus protocol was not part of the work in this dissertation, it has been developed by Mr. Alvey Hau, postgraduate student of UTAR (Hau et al., 2017).

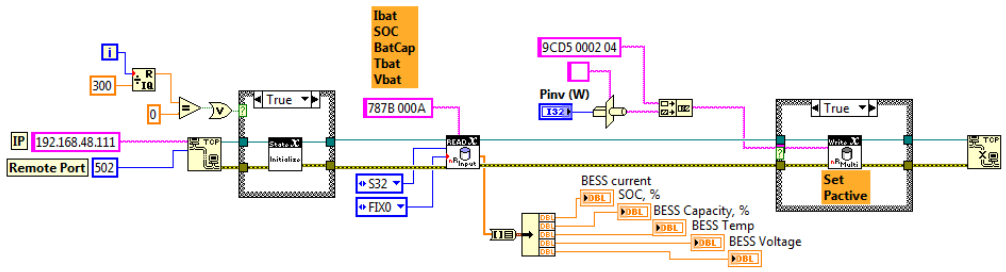

Figure 3.7: Block set model in LabVIEW to retrieve battery parameters

3.5.2. Data Acquisition System

A data acquisition system comprises of National Instrument's analogue-digital input modules. A voltage input module (NI-9225) and current input module (NI-9227) is used to measure the voltage, frequency, and power from PV, load, and BESS in the low voltage distribution network respectively. A Current Transformer (CT) with a rated turn ratio of 250/5A is utilised to convert the phase current to a lower rating current signal before entering NI-9227 current input module. The current module obtains the input from the CT output of 5A and computes the measured current in the LabVIEW by multiplying the current obtained with a coefficient of 50 to offset the step-down ratio from the three CT's. The details of the current calculation are illustrated in Eq. (3.1).

$$I_{PHASE} = I_{CT} \times CT\ Ratio \tag{3.1}$$

Where I_{PHASE} is the phase current

I_{CT} is the step down current output from CT to NI-9227 module

$CT\ Ratio$ is the winding ratio of the current transformer rated at 5/250

Figure 3.8 show configuration of NI-9225 and NI-9227 to measure voltage and current of the PV output respectively. Similar approach is used to measure the voltage and current for each node connecting BESS, PV and load as shown in Figure 3.9. In order to develop a graphical user interface (GUI) layout, LabVIEW™ Electrical Power Suite 2011 is used in addition to the basic program to analyse, compute and display the voltage, current, active and reactive power, and frequency for each node. Figure 3.10 shows the virtual instrument (VI) developed to read and display the required electrical parameters CompactDAQ device which houses voltage and current modules. In the VI, “for loop” is used to allow continuous measurement at 200 ms per cycle which generates 5 samples per second.

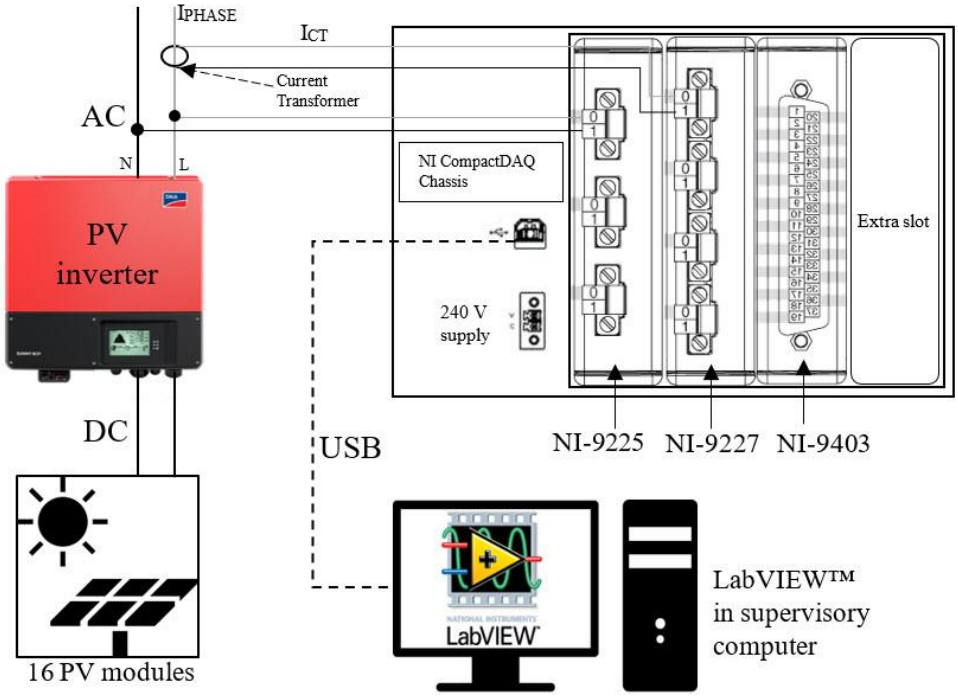

Figure 3.8: NI-9225 and NI-9227 voltage and current module wiring configuration

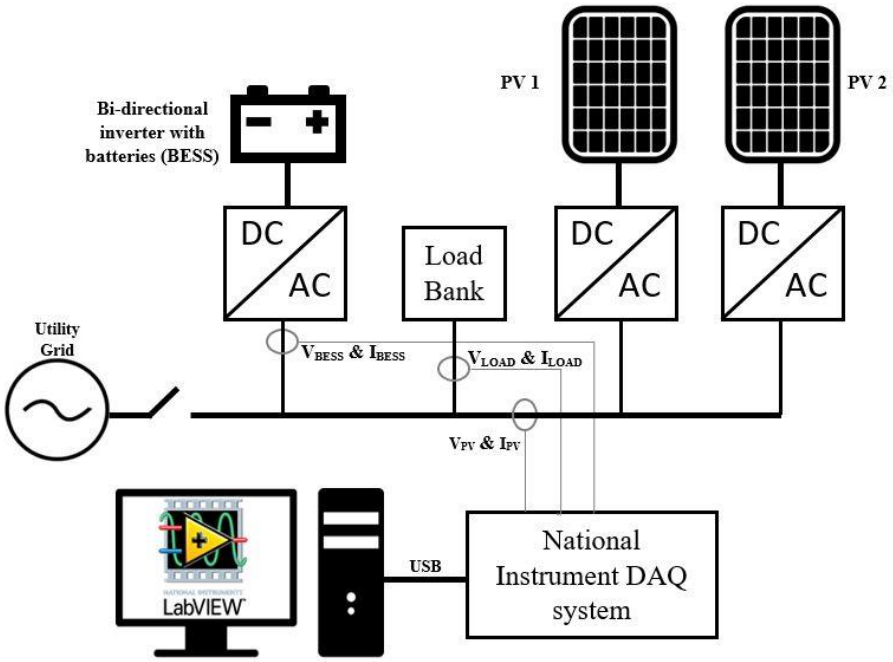

Figure 3.9: Measurement points for BESS, PV, and load consumption of the low voltage experimental network

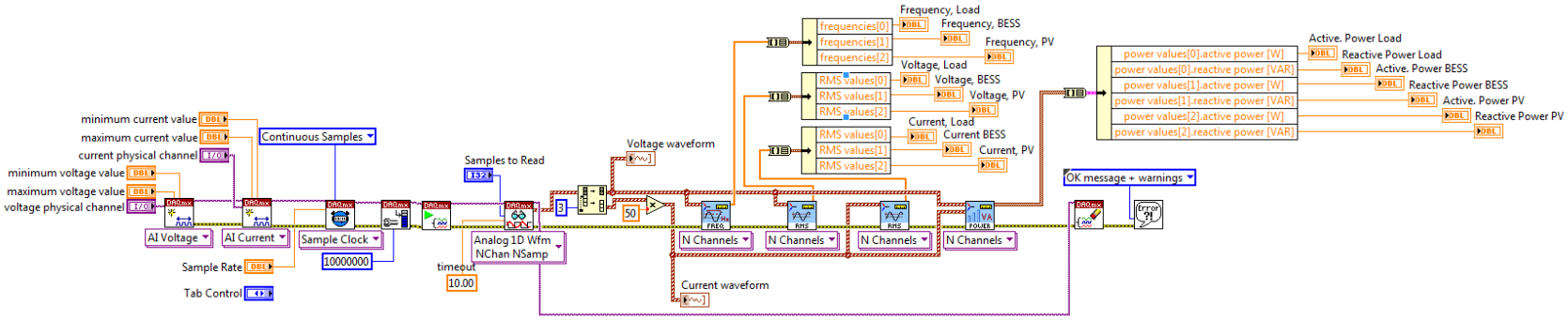

Figure 3.10: Graphical programming in LabVIEW for voltage, current, frequency, and power measurement for BESS, PV, and Load

3.6. Bi-directional Inverter Features

Droop control method has been widely applied in power electronic-based inverter to balance the power mismatch between the generation and demand in the islanded network, hence regulating the voltage and frequency of the islanded network. As mentioned in Chapter 2.9.2, a grid forming voltage source is required to provide voltage reference to other current source inverters in the event of grid outage. In this project, a BESS is integrated on the LV distribution network to regulate the voltage and frequency during islanding operation. The following section will describe the details on the features of the BESS.

3.6.1. Feature 1: Droop Control

In the conventional power system, droop control is adopted to vary the power output of the generator to regulate the network voltage and frequency. The same strategy, namely Selfsync™ is applied by the bi-directional inverter to vary its output according to a predefined droop characteristics curve to regulate the voltage and frequency during islanding operation (Engler, 2004).

Figure 3.11 shows the Selfsync™ strategy consists of four sections, namely power acquisition, decoupling, droop control and voltage reference blockset to produce a voltage reference, U_{ref}.

1. Power acquisition: To obtain instantaneous voltage and current from the output of the bi-directional inverter to compute active and reactive

power. The special filter consists of several proportional and integral elements to accurately calculate the complex notation of active and reactive power during steady-state operation. With the value of P and Q being computed by power acquisition, these values are then fed to a de-coupling network to decouple the active and reactive power (Engler, 2004).

2. Decoupling: To maintain the constant voltage and frequency under non-linear load condition, T_{mech} and T_{exc} decouple the active and reactive power respectively to achieve smoothing effect. De-coupled P and Q values are then sent to droop control system respectively for multiplication process as shown in the Figure 3.11.

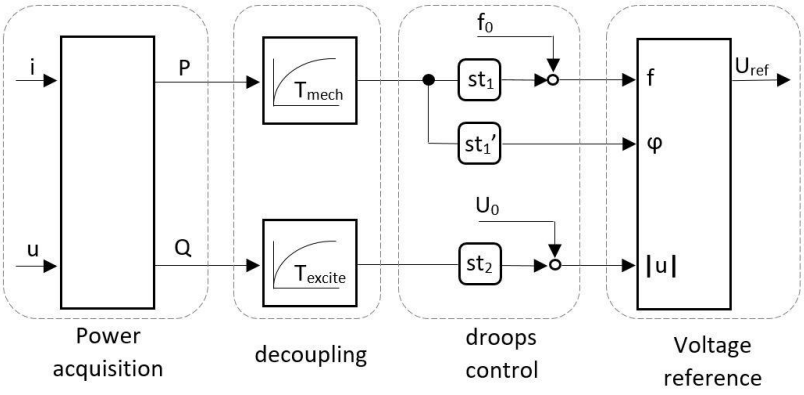

Figure 3.11: Selfsync™ control algorithm for voltage and frequency regulation (Engler, 2004)

3. Droop control: P and Q are multiplied with droop coefficient, st_1 and st_2 respectively which correspond to the droop characteristics curve as shown in Figure 3.12.

4. Voltage reference: The output from the multiplication proceeds to the addition stage where each output is added with prescribed frequency and voltage respectively. The output values of frequency and voltage addition represent the frequency reference and voltage reference in a form of amplitude respectively which is fed to the voltage reference block to generate voltage reference.

The frequency droop and voltage droop allow 1% and 4% change with respect to nominal value. When the network frequency decreases from the nominal value of f_0, the inverter will increase the inverter active power output corresponding to the droop curve as shown in Figure 3.12(a). Similarly, when the inverter senses voltage drops in the network, the reactive power output will be increased according to the droop curve as shown in Figure 3.12(b).

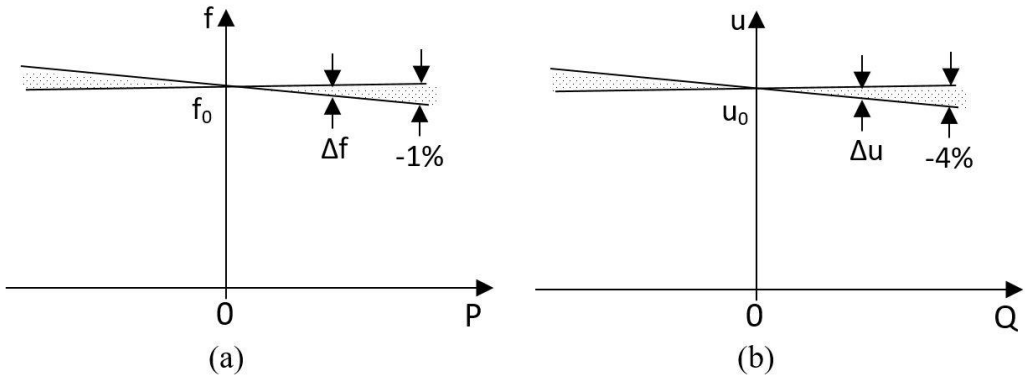

Figure 3.12: active power-frequency droop (b) reactive power-voltage droop control (Engler, 2004)

Referring to Figure 3.11, the voltage reference, U_{ref} is generated by using the equation (3.2).

$$U_{ref} = |u| \times \sin(2\pi ft) \tag{3.2}$$

The generated U_{ref} is a sinusoidal waveform in a function of time. This equation is only valid for flat frequency droop curve and the system will experience pendulum oscillations for a steeper frequency droop curve. To avoid large pendulum oscillation, st_1' is introduced by considering ϕ. Therefore, the time-lagged P value is multiplied by st_1' which produced phase angle, ϕ of the reference voltage, U_{ref}. As a result, U_{ref} is now being determined by f, |u|, and ϕ using the equation (3.3) which has damping effect to avoid power oscillations.

$$U_{ref} = |u| \times \sin(2\pi ft + \emptyset) \tag{3.3}$$

The reference voltage, U_{ref} is then compared with actual network voltage to generate an adjustment signal which is used to adjust the pulse width of the Pulse Width Modulation (PWM) to generate sinusoidal output. Thus, inverter embedded with Selfsync™ technology allows rapid change in output to regulate the voltage and frequency of the network without the need for communication devices.

3.6.2. Features 2: Battery Management System (BMS)

Battery Management System (BMS) is another feature comes with the bi-directional inverter to estimate the battery state of charge (SoC) in order to ensure the batteries operates safely within operating range to prolong its lifespan. The BMS utilises ampere-hour counting and voltage recalibration to estimate battery SoC to prevent overcharging or over-discharging of VRLA batteries (SMA, 2014). Ampere-hour counting method uses battery current integration (Coulomb counting) to estimates SoC. In the meantime, important parameters, such as temperature, charging current, battery voltage and time incorporated with self-learning process are used to further improve the accuracy for estimating SoC. Besides, SoC recalibration is used to further improve the SoC estimation by comparing the SoC obtained during no-load condition and the SoC obtained during ampere-hour counting. In case there is any dispute value during the comparison, the SoC estimation will be recalibrated to show a correct value. Besides, BMS is also capable of providing deep discharge protection to prevent potential damage to the battery from deep discharge. Figure 3.13 shows the working principle for BMS consists three phases as follows:

1. Constant Current Phase: A maximum permissible battery current applied to the charging current. When the battery SOC reaches 85%, the BMS switch constant current phase charging pattern to constant voltage phase.

2. Constant Voltage Phase: A high charging voltage is applied to the battery. As a result, battery current reduces exponentially to zero. When the required charging time has reached, BMS switches to float charge.

3. Float Charge: The battery is maintained at full charged state without overcharging

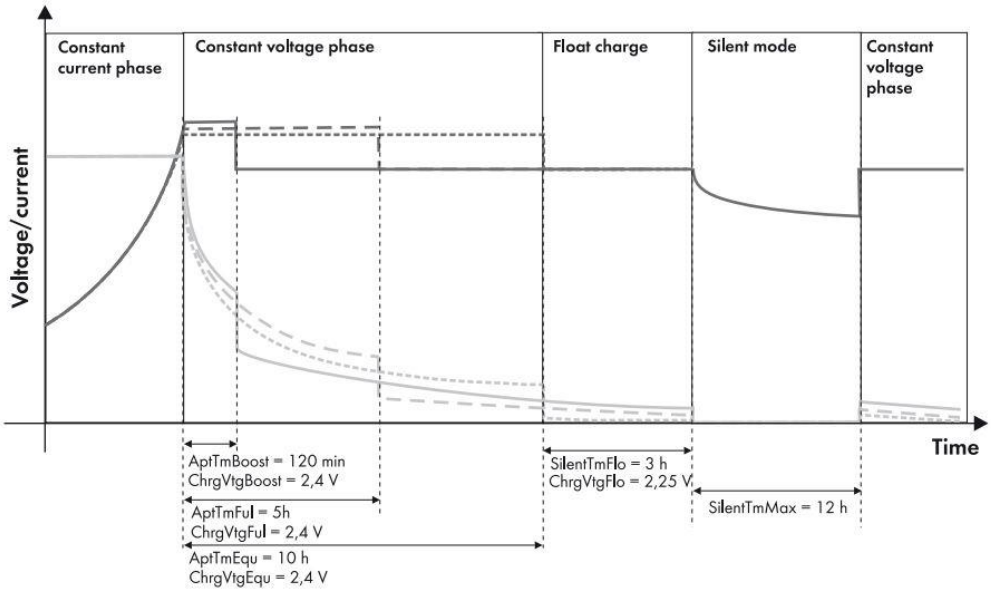

Figure 3.13: Charging phases of the battery coordinated by BMS (SMA, 2014)

3.7. Summary

In summary, a low voltage distribution network is setup and connected to the utility grid. A 6.0 kW bi-directional inverter with batteries, 2 x 3.6 kW_P PV system, 3.0 kW load emulator is integrated into the low voltage distribution network. The details on how each source is configured are elaborated and explained. The grounding of the distribution network is configured with TT

earthing system to complied with Malaysian standards. A data acquisition system is developed with LabVIEW graphical programming software to measure, record the electrical parameter of each source. The features of the bi-directional inverter are explained. With the proper setup of communication, data acquisition, and sources integrated into the low voltage distribution network, the feasibility study of conducting islanding operation of BESS with PV system with case studies are further elaborated in the next chapter.

CHAPTER 4

FEASIBILITY STUDIES ON CONTINUOUS OPERATION OF PV SYSTEMS WITH BESS DURING GRID OUTAGES

4.1. Introduction

The increasing growth of Renewable Energy Sources (RES) integrated on the distribution network has imposed changes on the traditional electrical grid system from unidirectional to bi-directional power flow. This change may cause voltage and frequency deviation, and proper measurement should be implied to regulate the voltage and frequency within the statutory limit in order to ensure safe operation of the electrical network. As discussed in the literature review, voltage and frequency are related to mismatches of active and reactive power. At present, diesel generator is used to regulate voltage and frequency in the islanded network. However, diesel that used to drive the generator releases GHG which is non-environmental friendly. Alternately, power electronic-based bi-directional inverter with batteries (BESS) can provide fast response in voltage and frequency regulation. Therefore, BESS is employed to provide voltage and frequency regulation within the islanded network. However, it is

worth noting that the frequency violation happens at the beginning of the grid outage due to maximum power mismatch between generation and demand. If frequency violation happens, PV system will be tripped off and available clean energy is not utilised. Thus, an innovative fuzzy control strategy is proposed to mitigate frequency violation at the beginning of grid outage. In this chapter, the study can divide into two major parts as follows:

Part 1: Feasibility study

Stage I : Islanding operation of PV system

Stage II : Islanding operation of PV system with BESS

Part 2: Fuzzy control strategy

Stage III : Increase operational window with fuzzy logic control – a fuzzy control algorithm is developed to mitigate the frequency violation during the transition period from grid-connected to islanded operation

Stage IV : Improved fuzzy logic control – Modification to the fuzzy membership function and rules to smoothen the output of the fuzzy logic control

Stage V : Controller comparison – Proposed fuzzy logic control is compared to Proportional-Integral (PI) controller to examine the strength of proposed controller.

Stage VI : Social aspect for load control strategy – Survey is conducted to analyse the social aspect of implementing load control in the residential area

4.2. Stage I: Operations of PV Systems during Grid-connected and Islanded Mode

Under the Malaysian Standard, MS 1837:2010 Installation of Grid-connected Solar Photovoltaic PV Systems, a grid-tied PV inverter is required to implement anti-islanding protection system in order to detect the occurrence of islanding and disconnect from the grid. The most commonly used anti-islanding method utilises passive detection which monitor the voltage and frequency. If the voltage and frequency fall outside the boundary known as Non-Detection Zone (NDZ), islanding is detected, and PV inverter will trip off by anti-islanding protection system.

In this section, a preliminary study is conducted to evaluate the performance of PV inverter when the grid is disconnected. To begin with this study, a 3.6 kW_P PV system is connected to the Low Voltage (LV) distribution network as shown in Figure 4.1. The configuration in Figure 4.1 shows the typical practice of a PV system installation in the residential area that complied with Malaysian Standard, MS 1837:2010 Installation of Grid-connected Solar Photovoltaic PV Systems.

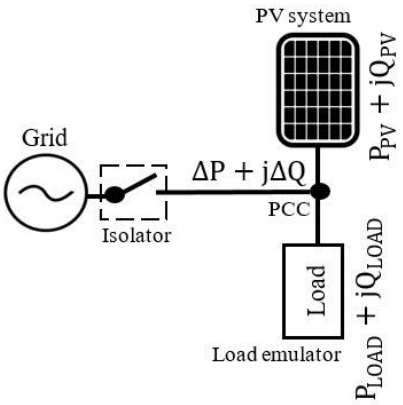

Figure 4.1: Simplified diagram of PV system configuration

The voltage and frequency within the islanded network in the event of grid outage is greatly depended on the active and reactive power mismatch, ΔP and ΔQ between generation and demand at the occurrence of islanding. The simplified diagram showing the power flow for each node on the LV distribution network and represented by equations as follows:

$$\Delta P = P_{LOAD} - P_{PV} \tag{4.1}$$

$$\Delta Q = Q_{LOAD} - Q_{PV} \tag{4.2}$$

Where; P_{PV} and P_{LOAD} are the active power of PV output and load respectively; Q_{PV} and Q_{LOAD} are the reactive power of the PV output and load respectively.

Figure 4.2 depicts the Non-Detection Zone (NDZ) for the PV inverter which indicates the boundary of over/under frequency and over/under voltage. According to Malaysia standards MS 1837, PV inverter shall only operate

during steady-state operation and cease to energise when the network voltage falls beyond +10/-6% of nominal voltage or frequency falls beyond ±1% of 50Hz. With these voltage and frequency disconnection criteria, it can be translated into the NDZ whereby the PV shall only operate within the grey region as shown in Figure 4.2.

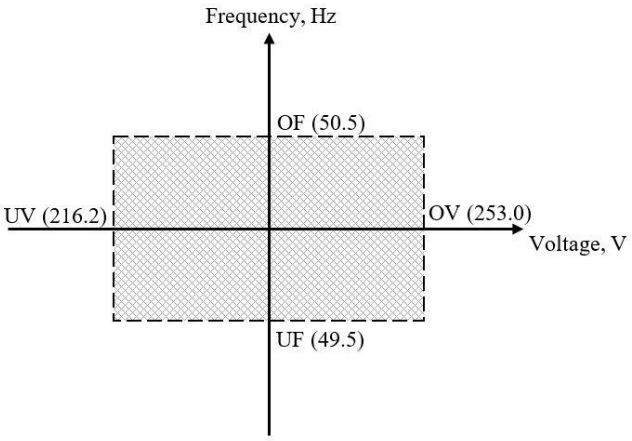

Figure 4.2: PV inverter shall only operate within the NDZ indicated by the grey region

Therefore, an experimental case study is conducted to investigate the ability of PV system in conducting islanding operation. Figure 4.3 shows the network topology for grid-connected and islanded operation of PV system. The network voltage and frequency are actively monitored and recorded. The isolator is functioned to disconnect partial of the network from the utility grid to form an islanded network for the PV system and load. When the system is islanded, ΔP and ΔQ create variation in voltage and frequency. If the value of ΔP and ΔQ is negligible, there are possibilities that the voltage and frequency would remain within NDZ. The power generated by PV system is closely

matched with the load consumption before the network is islanded to ensure the power mismatch between PV system (P_{PV}) and load (P_{LOAD}) is negligible.

In this stage, an experimental setup consists of a 2.0 kW load emulator connected to the PV system is developed as shown in Figure 4.3(a). Figure 4.3(b) shows the grid is disconnected by the isolator to form an islanded network. The voltage, frequency, active and reactive power at the PCC are regularly monitored.

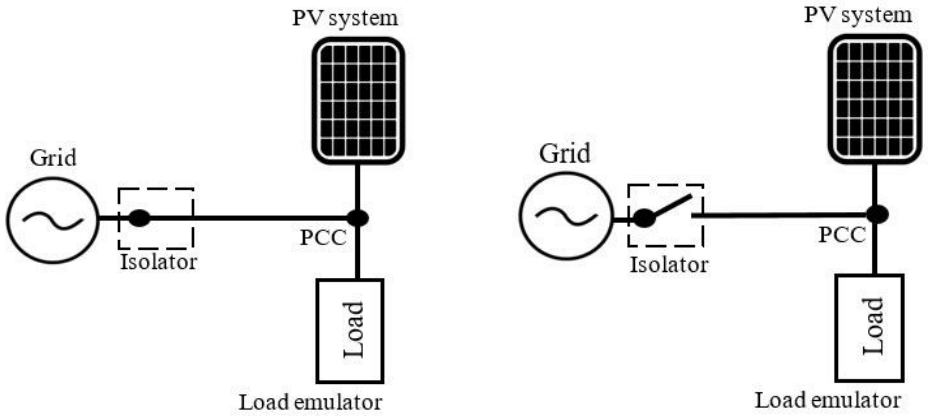

(a) (b)

Figure 4.3: Network topology for (a) grid-connected and (b) islanded operation of PV system

Figure 4.4 shows the active power consumed by the load (P_{LOAD}) and PV power output (P_{PV}) with respect to time during grid-connected mode to islanded mode at 5.8 seconds onwards respectively. It is shown that the PV system is disconnected even though the load is matched with the PV power output. Figure 4.5 shows the voltage and frequency of the network recorded at the PCC. Prior to islanding, the anti-islanding protection system is triggered,

and PV system ceases to energise at the start of islanding. This experiment shows that the PV system is unable to operate in the event of islanding due to anti-islanding protection features in the PV inverter despite negligible power mismatch, ΔP and ΔQ between PV power output and load consumption. Besides, it is also proven that PV system is unable to operate in the absence of grid reference because PV system is a current controlled source and at least one voltage source inverter has to provide a voltage reference to the working of the current control inverter.

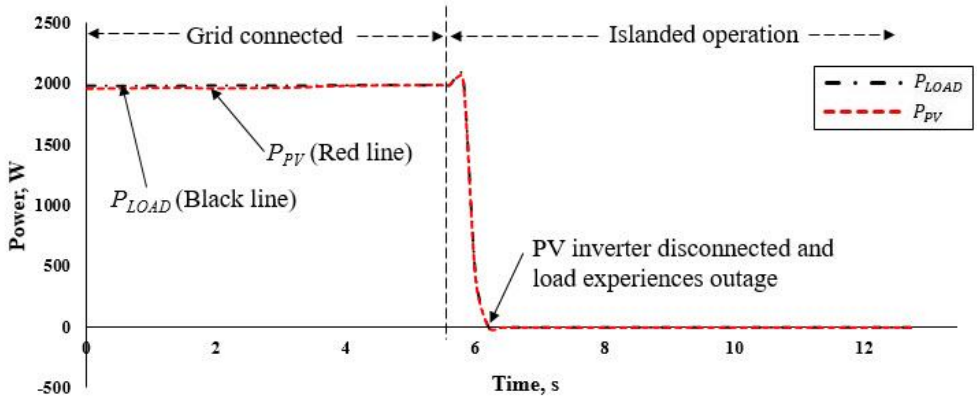

Figure 4.4: PV power output and load consumption during grid connected mode and islanded operation

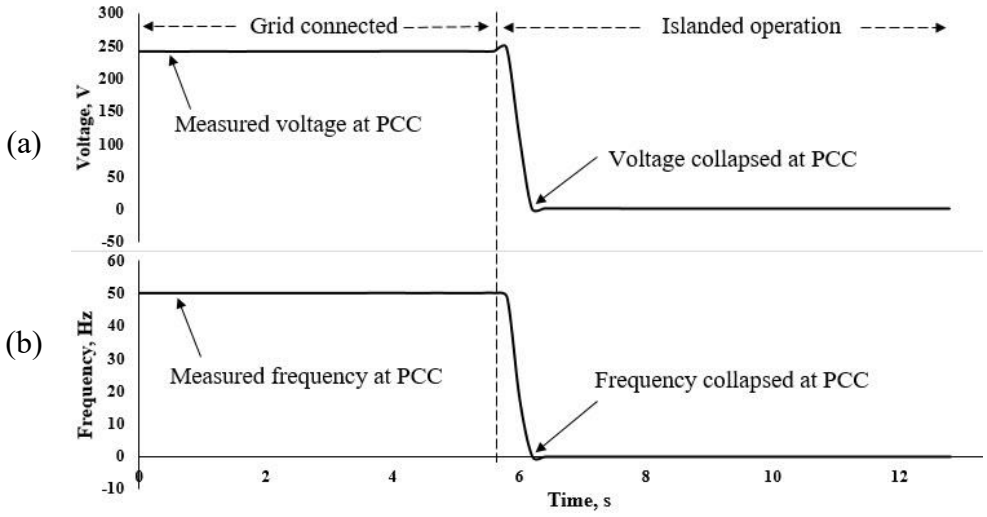

Figure 4.5: (a) Measured voltage and (b) frequency at the PCC during grid connected and islanded mode

4.3. Stage II: Operations of PV Systems during Islanded Mode with BESS

In the previous section, it is known that PV system will be trip off during grid outage because the PV system is unable to operate due to absence of grid reference. Therefore, a Battery-based Energy Storage System (BESS) acting as grid-forming unit is integrated into the LV distribution network. The BESS can be used to compensate the power mismatch between the load (P_{LOAD}) and PV power output (P_{PV}), hence regulating the voltage and frequency in the event of islanding. The following sections describe roles of BESS during grid-connected and islanded modes.

Grid-connected Operation:

Figure 4.6 shows the network topology consists of PV system, load and BESS during grid-connected operation. The relationship at node A and B can be represented by the equations as follows:

$$P_{GRID} = P_{LOAD} - P_{PV} - P_{BESS} = \Delta P - P_{BESS} \quad (4.3)$$

$$Q_{GRID} = Q_{LOAD} - Q_{PV} - Q_{BESS} = \Delta Q - Q_{BESS} \quad (4.4)$$

Where, P_{BESS} and Q_{BESS} are the BESS active and reactive power respectively; and P_{GRID} and Q_{GRID} are active and reactive power of export/import from the grid respectively.

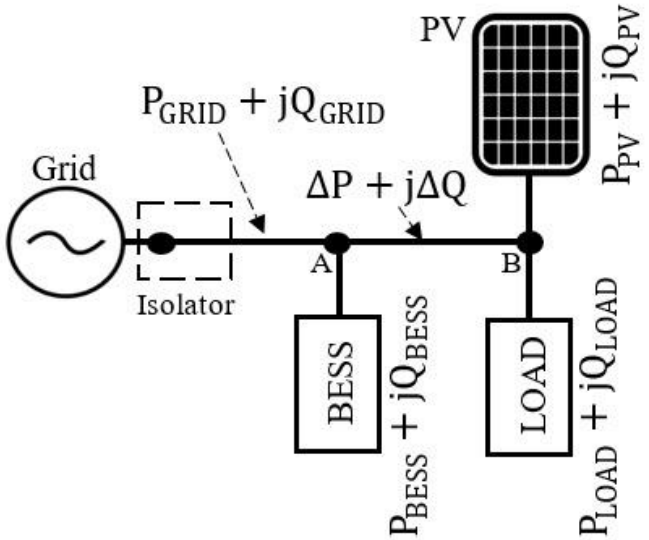

Figure 4.6: Experimental LV distribution network integrated with BESS during grid-connected operation

The active and reactive power mismatch between PV system and load are represented by ΔP and ΔQ respectively. The BESS power output, $P_{BESS} + jQ_{BESS}$ is required to match any power mismatch ($\Delta P + j\Delta Q$) between PV system (P_{PV}) and load (P_{LOAD}) during grid-connected operation. During the transition period between grid-connected and islanded mode, the BESS is required to maintain the power mismatch to be as small as possible in order to minimise any voltage and frequency fluctuations which would otherwise trip off the PV system at the beginning of the grid outages. This change in BESS power output from grid-connected to islanding operation can be represented by using the equation (4.5) and (4.6) respectively:

$$\Delta P_{BESS} = \Delta P - P_{BESS} \tag{4.5}$$

$$\Delta Q_{BESS} = \Delta Q - Q_{BESS} \tag{4.6}$$

As discussed in the chapter of 3.6.1, the BESS is equipped with droop control mechanism to regulate the voltage and frequency within the islanded network. Prior to islanding operation, the voltage and frequency change is indicated by equation (4.7) and (4.8) respectively.

$$\Delta f = K_f \times \Delta P_{BESS} \tag{4.7}$$

$$\Delta V = K_v \times \Delta Q_{BESS} \tag{4.8}$$

Where, K_f and K_v are coefficients of voltage and frequency change respectively

Islanded Operation:

After the system is islanded, the BESS is actively manipulating its power output, $P^*_{BESS} + Q^*_{BESS}$ to maintain the power balance in the islanded network to stabilise the voltage and frequency as shown in Figure 4.7. During the islanded mode, the BESS power output, $P^*_{BESS} + jQ^*_{BESS}$ is equivalent to the power mismatch between PV system and load, $\Delta P + j\Delta Q$ as shown in equation (4.9) and (4.10) as follows:

$$P^*_{BESS} = \Delta P \tag{4.9}$$

$$Q^*_{BESS} = \Delta Q \tag{4.10}$$

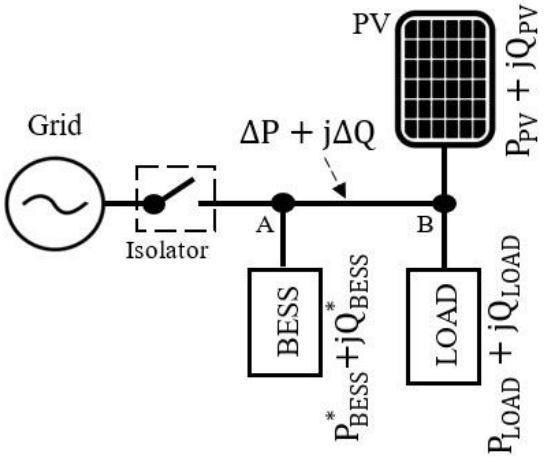

Figure 4.7: Simplified diagram for the network integrated with BESS during islanding operation

4.3.1. Case Study I: Experimental Study of BESS in Conducting Islanding Operation of PV Systems

The purpose of this case study is to investigate the voltage and frequency of the network during islanding operation of PV system with BESS. Figure 4.8(a) and (b) shows the network topology consists of two PV systems, load emulator and BESS are integrated into the experimental LV distribution network for grid-connected mode and islanded mode respectively.

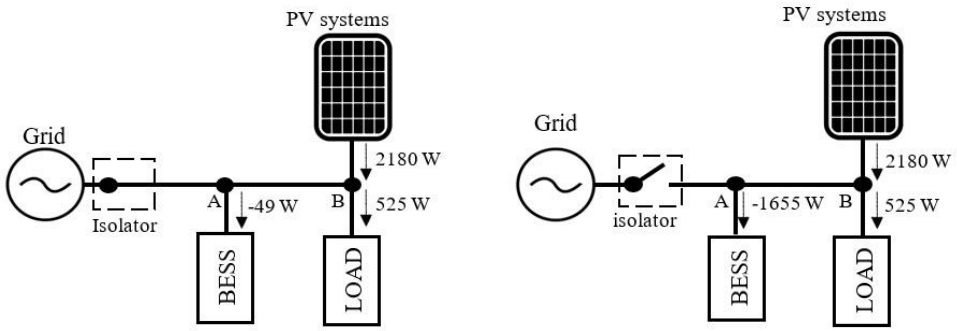

(a) (b)

Figure 4.8 Network configuration for experimental case study during (a) grid-connected and (b) islanded operation

The experiment begins with grid connected operation where the PV system is supplying 2180 W while load is consuming 525 W as shown in Figure 4.8. The calculated power mismatch between PV system and load, ΔP is recorded at -1655 W. Assuming the BESS is charging at -49 W during initial stage at 0 seconds. At 2.8 seconds, the experimental network has lost the grid connection. In the event of grid outage, the BESS is required to maintain the power balance within the islanded network by compensating the power

mismatch created between load (P_{LOAD}) and PV power output (P_{PV}). Hence the BESS charging power changes from -49 W to -1655 W. During the transition period, the BESS experienced a charging difference of -1606 W which is indicated as ΔP_{BESS}.

Figure 4.9 shows the power output from PV system, load, and BESS during grid-connected (from 0 to 2.8 seconds) and islanded mode (2.8 seconds onwards). Negative values in the graph indicating charging mode while positive indicating discharging mode in the BESS.

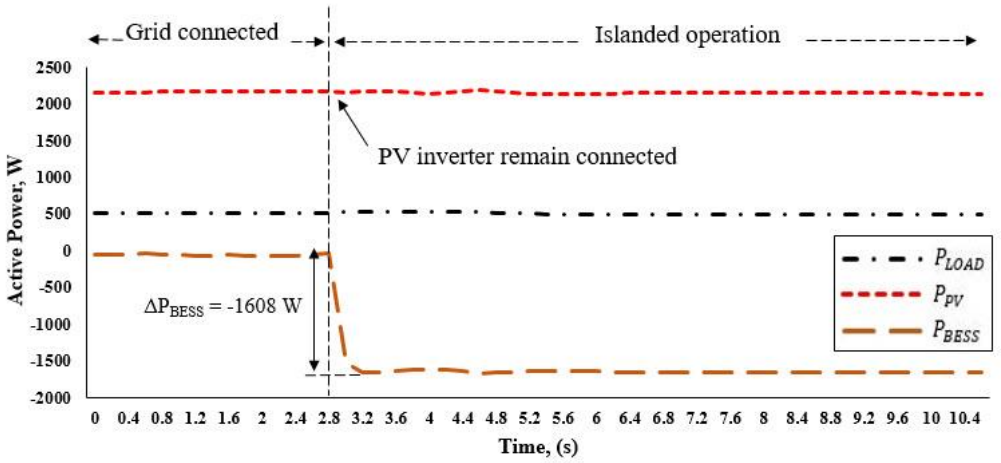

Figure 4.9: Active power output recorded for PV system, load, and BESS

Figure 4.10(a) and Figure 4.10(b) show the voltage and frequency excursion of the experimental LV distribution network during the transition from grid-connected and islanded operation. It is observed that there is a hike in voltage and frequency excursion during the starts of islanding at 2.8 seconds due to instantaneous power mismatch caused by supply changed from grid to BESS. After the BESS power output has reached a steady state value, the

voltage and frequency of the islanded network are stabilised. The red colour dotted line as indicated on the graph shows the over-voltage at 253 V and over-frequency limit at 50.5 Hz. This experimental case study has proven that the BESS can provide a voltage reference to the PV system, and in the same time maintaining the voltage and frequency within the statutory limits which allow the PV system to continue operates during islanding mode.

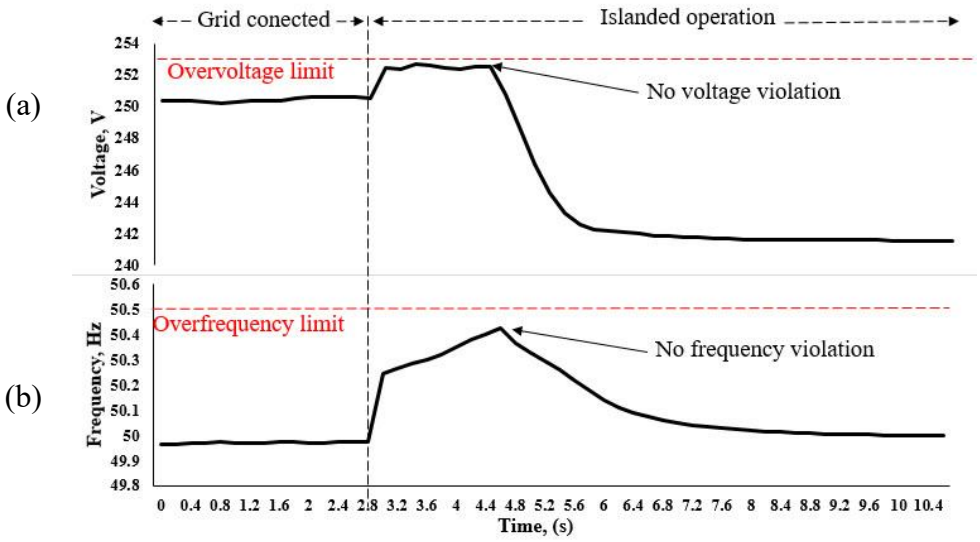

Figure 4.10: (a) Voltage and (b) frequency during grid-connected and islanded operation

4.3.2. Case Study II: Observation on Behaviour of System Under Greater Value of ΔP_{BESS}

Another experimental case study is conducted to observe the voltage and frequency excursion when a greater change in BESS power output, ΔP_{BESS} is occurred at the beginning of the grid outages as shown in Figure 4.11.

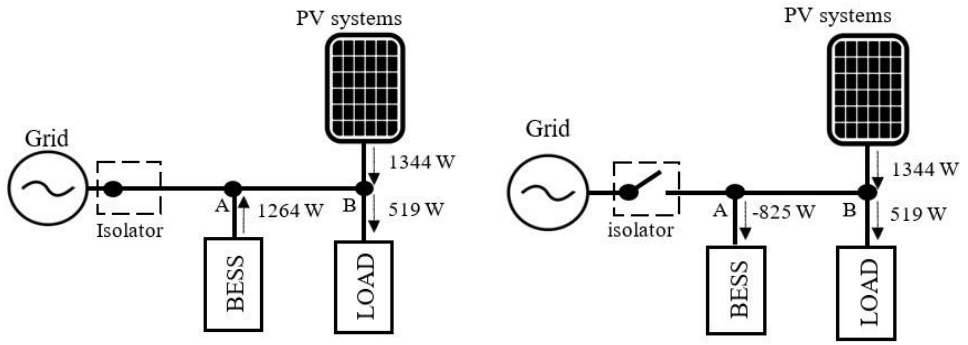

(a) (b)

Figure 4.11: Network configuration for experimental case study during (a) grid-connected and (b) islanded operation

Figure 4.12 shows the power output recorded for PV systems, load and BESS. The system is operating in grid-connected mode from 0 to 5.8 seconds and islanded mode after 5.8 seconds. Assuming the initial state of BESS is supplying 1264 W to the network, while PV system is generating 1344 W and load is consuming 519W. In the event of islanding, the BESS has to change its output from 1264 W to -825 W in order to achieve a power balance condition in the islanded network by compensating the power mismatch between PV system and load. This would result in change in BESS power output, ΔP_{BESS} of -2089

W. However, the PV system is disconnected at the starts of islanding as shown in Figure 4.12. After the PV system is disconnected, the BESS support the load by supplying adequate power. Consequently, the available clean energy generated by the PV system is not utilised.

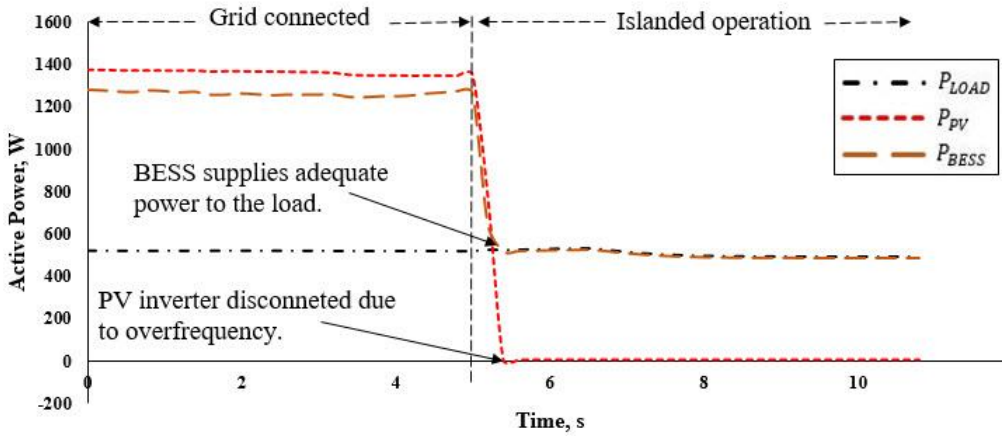

Figure 4.12: The PV is disconnected at 5.8 s prior to islanding occurrence

Figure 4.13(a) and Figure 4.13(b) shows the voltage and frequency of the LV distribution network during grid-connected and islanding operation. During the case study, it is observed that the voltage excursion of 249 V is well remained within the statutory limits. However, it is noticed that the frequency recorded at 50.58 Hz which is beyond the operating limits ±1% of 50 Hz, hence the PV system triggered the anti-islanding protection system and disconnected from the network due to frequency excursion greater than the statutory limit.

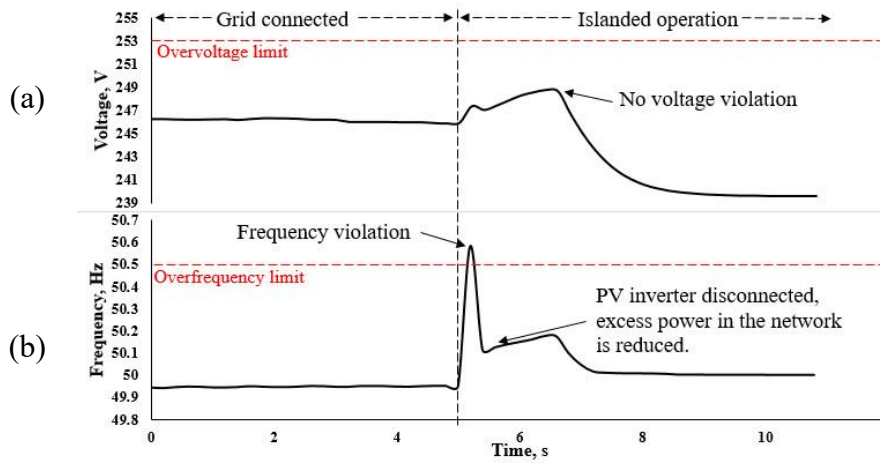

Figure 4.13: (a) voltage of the network maintained within statutory limit; (b) frequency violation at the starts of islanding which results in PV disconnection

Table 4.1 compares the parameters recorded for PV power output (P_{PV}), load consumption (P_{LOAD}), BESS power output (P_{BESS}), change in BESS power output (ΔP_{BESS}) and frequency excursion (f) in the case study I and case study II. It is observed that ΔP_{BESS} in case study II has a larger value as compared to case study I. The larger change in BESS power output during islanding occurrence results in a larger magnitude of frequency excursion. Consequently, the PV system is disconnected instantaneously by the anti-islanding protection. Thus, the case studies have proven that the BESS is not capable of maintaining the voltage and frequency within statutory limit for a larger change in BESS power output during the intercept of islanding.

Table 4.1: Comparison between the parameters recorded in case study I and case study II where frequency violation is highlighted in red for case study II

	Case Study I	Case Study II
P_{PV}, W	2180	1344
P_{LOAD}, W	525	519
P_{BESS}, W	-49	1264
ΔP_{BESS}, W	-1606	-2089
Frequency, Hz	50.42 (<1%)	50.58 (>1%)

4.3.3. Case Study III: Establish the Relationship Between the Magnitude of Frequency Excursion and ΔP_{BESS} Under Various Generation and Demand

It is observed from the previous case studies, the magnitude of frequency excursion varies with the change in BESS power output, ΔP_{BESS} at the starts of islanding. Thus, several sets of experiments are conducted to investigate the relationship between ΔP_{BESS} and the magnitude of frequency excursion. The experiments are repeated by switching from grid-connected mode to islanding mode. The value of ΔP_{BESS} for each set of the experiment can be varied by manipulating the P_{BESS} during grid-connected operation. Figure 4.14 shows the magnitude of frequency excursion with respective to ΔP_{BESS} at the beginning of the grid outages.

Figure 4.14 depicts the operating boundary of the BESS highlighted in grey. The trend of the blue dotted value gives an idea that the magnitude of frequency excursion is larger with a larger value of ΔP_{BESS}. It is observed that

the frequency would stay within the statutory limit of ±1% of 50Hz if the ΔP_{BESS} is maintained with the grey region, ±1.7 kW. If ΔP_{BESS} operate beyond the grey region, the system will experience frequency violation in the event of islanding which would trigger the PV system to disconnect. Thus, an innovative controller is required to ensure ΔP_{BESS} operates within the predefined operating range as shown by the grey region in Figure 4.14.

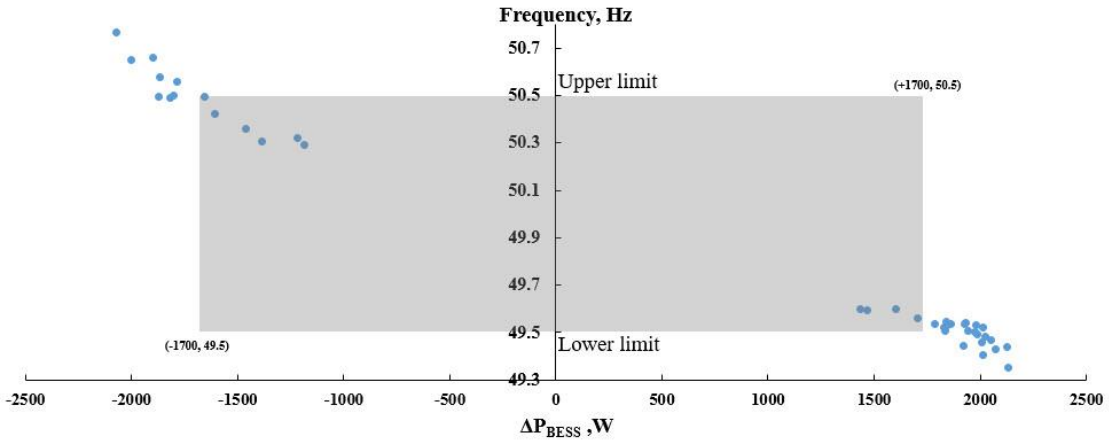

Figure 4.14: Correlation between ΔP_{BESS} and frequency deviation at the beginning of grid outages

4.4. Fuzzy Control

To avoid any frequency violation at the beginning of the grid outages, a novel fuzzy logic control (FLC) is developed using LabVIEW and implemented to manipulate the power output of BESS in order to ensure ΔP_{BESS} remained within the predefined operating range, ±1.7kW at all times. FLC is a system that utilising mathematical reasoning to analyse the inputs in terms of logical variable. Figure 4.15 shows the flow chart of the fuzzy logic control system consists of three stages, namely i) initialisation, ii) fuzzification and iii) defuzzification.

The algorithm begins with an initialisation on the BESS operating boundary, ΔP_{BESS} = ±1.7 kW. Setting the threshold value for ΔP_{BESS} is to limit power mismatch supplied by BESS during the transition from grid connected to islanding mode. In this section, the control strategy development by using fuzzy system to compute necessary corrective action based on two parameters: i) battery state of charge (SoC) and ii) power mismatch (ΔP) between load (P_{LOAD}) and PV system (P_{PV}), is explained in detail. As the battery is the most expensive equipment in the system, therefore, it is important to consider the SoC into the fuzzy system to ensure that the State of Health (SoH) of the battery is maintained properly. The battery SoC can be obtained from the BESS as the bi-directional inverter within the BESS is equipped with a battery management system (BMS) that is capable to estimate the SoC.

The algorithm is developed by using the fuzzy system designer toolbox in LabVIEW to define the fuzzy input memberships, fuzzy logic rules and fuzzy output membership function. The fuzzy system receives two inputs: i) battery SoC and ii) the power mismatch (ΔP) between the load (P_{LOAD}) and PV system (P_{PV}) to produce linguistic output via fuzzification. The linguistic output will be matched accordingly to the fuzzy logic rules to undergo defuzzification for generating the BESS power output (P_{BESS}). This process continues until ΔP_{BESS} is maintained within the predefined operating range. When ΔP_{BESS} is in range, the system will not experience voltage and frequency violation in the event of islanding. The flow chart of the fuzzy logic system is shown in Figure 4.15.

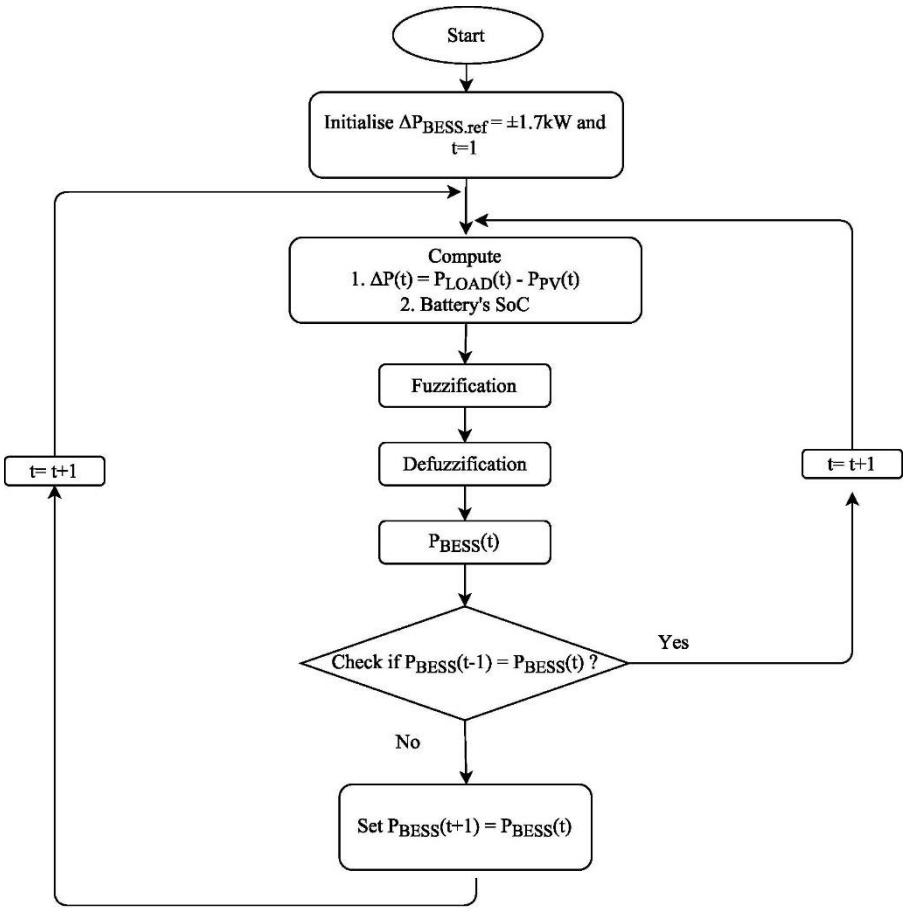

Figure 4.15: Flow chart of the proposed control strategy

Figure 4.16 depicts the proposed fuzzy control system with detailed block diagram. In the fuzzification process, the controller captures two input parameters, ΔP and SoC. The predefined fuzzy membership of ΔP is categorised into of four stages i) Very Negative (VN), ii) Negative (N), iii) Positive (P), and iv) Very Positive (VP) where very negative (VN) and negative (N) indicating the degree of excess power; and positive (P) and very positive (VP) indicating the degree of insufficient power within the system as shown in Figure 4.17. The fuzzy membership for SoC consists of three levels, i) Low (L), ii) Medium (M) and iii) High (H) as shown in Figure 4.18. During fuzzification, the input of ΔP to the fuzzy membership generates two conditions with their respective linguistic values. The input of SoC to the fuzzy membership generates two conditions of battery SoC with their respective fuzzy values. Hence, there are four linguistic outputs generated from the fuzzification.

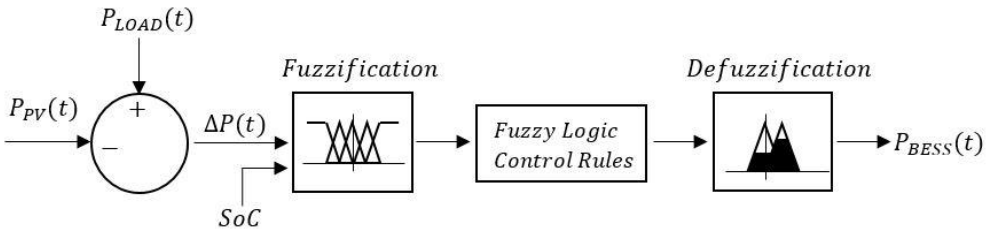

Figure 4.16: Proposed fuzzy control system

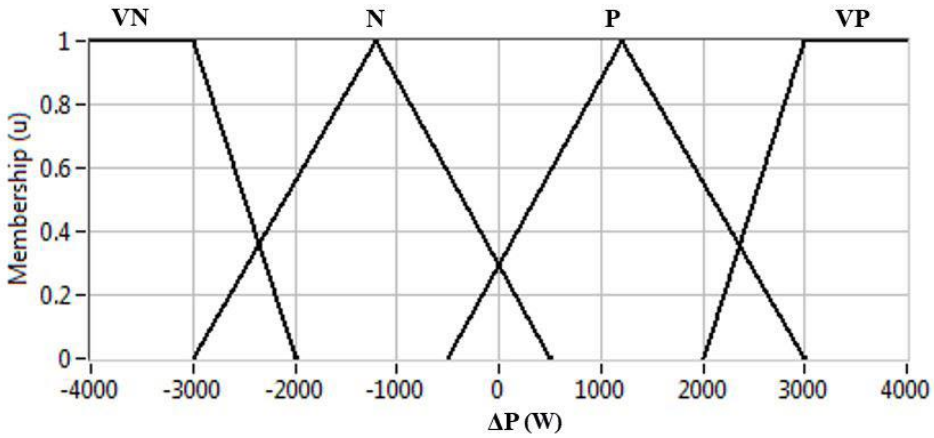

Figure 4.17: Pre-defined membership function of ΔP

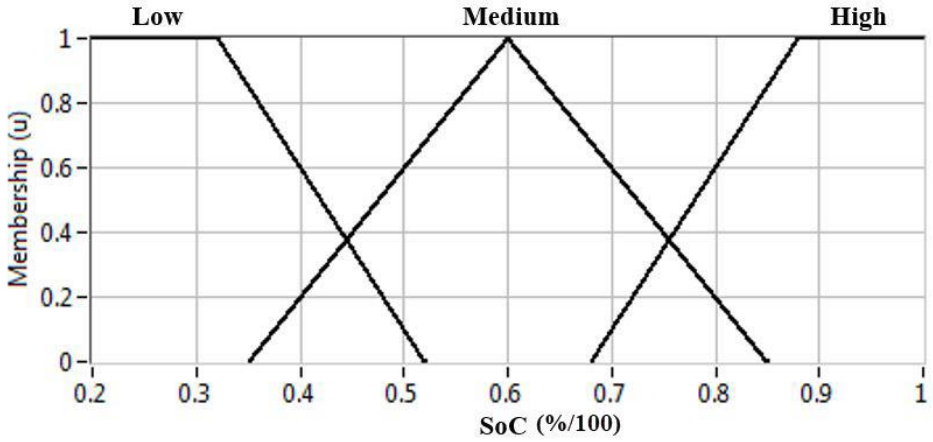

Figure 4.18: Pre-defined membership function of SoC

In the defuzzification stage, four linguistic outputs are mapped against each other in Table 4.2 to determine the type of instructions. There are five types of different instructions to be produced which can be categorised as i) High Charge (HC), ii) Charge (C), iii) Idle, iv) Discharge (D), and v) High Discharge (HD) as shown in Figure 4.19. The conditions and the values of the instructions are used to define the area enclosed under the fuzzy membership as required by Center of Area (CoA) defuzzification method, hence the value of the output, P_{BESS} is determined.

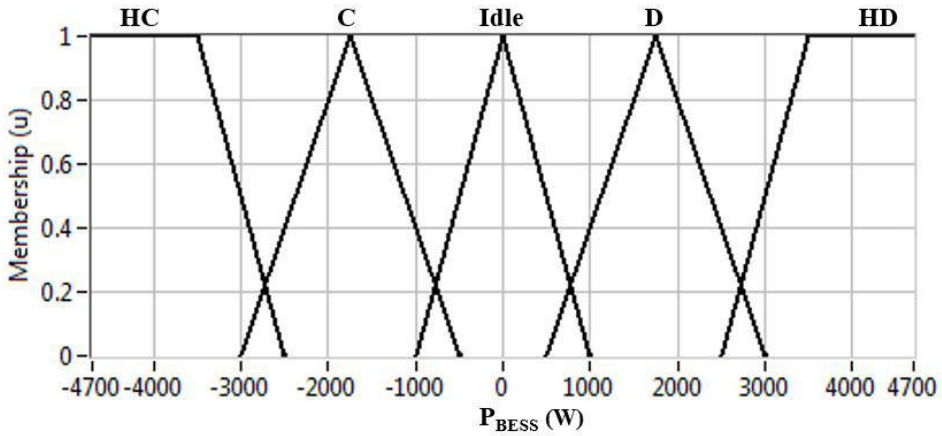

Figure 4.19: Output membership function of P_{BESS}

Table 4.2: Mapping table for generating the instructions

SoC	ΔP			
	Very Negative (VN)	Negative (N)	Positive (P)	Very Positive (VP)
Low (L)	High Charge (HC)	Charge (C)	Idle	Discharge (D)
Medium (M)	Charge (C)	Idle	Idle	Discharge (D)
High (H)	Charge (C)	Idle	Discharge (D)	High Discharge (HD)

A fuzzy system design toolbox available in LabVIEW is used to develop the fuzzy control system as shown in Figure 4.20. There are three control tabs as follows:

I. Tab 1 – Variable: It is used to define all the input and output membership functions in terms of different shapes and range. In this case, two input membership function are defined ΔP and SoC while one output variable P_{BESS} is defined.

II. Tab 2 – Fuzzy rules: All the possible combination for fuzzy rules are defined and translated in this tab.

III. Tab 3 – Test system: Before a fuzzy controller is implemented, a test system is functioned to verify the relationship between the inputs and output are correlated with each other.

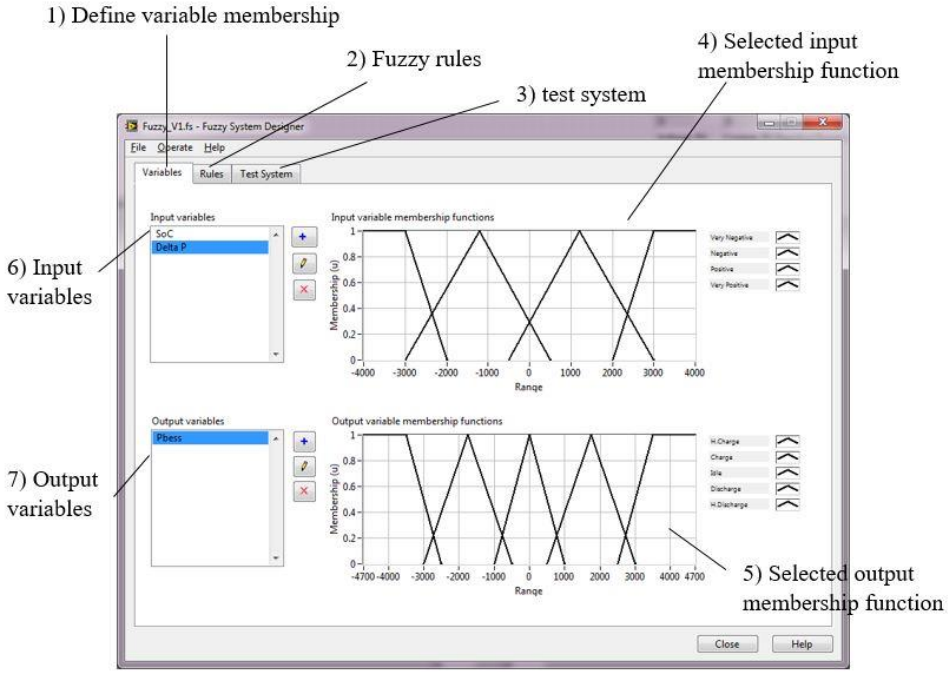

Figure 4.20: Fuzzy system designer toolbox available in LabVIEW to define the fuzzy logic controller

The definition for the fuzzy logic controller is saved as fuzzy system file with an extension of (.fs). This file will be loaded into the LabVIEW virtual instrument in order to generate the output of P_{BESS}. Figure 4.21 depicts a section of the programme where P_{BESS} is produced from the fuzzy system designer using two input membership function, ΔP and SoC into Multi Input Single

Output (MISO) fuzzy control block to generate the output of P_{BESS}. Figure 4.22 depicts the LabVIEW front panel for the grid parameters, BESS monitoring and the fuzzy control system.

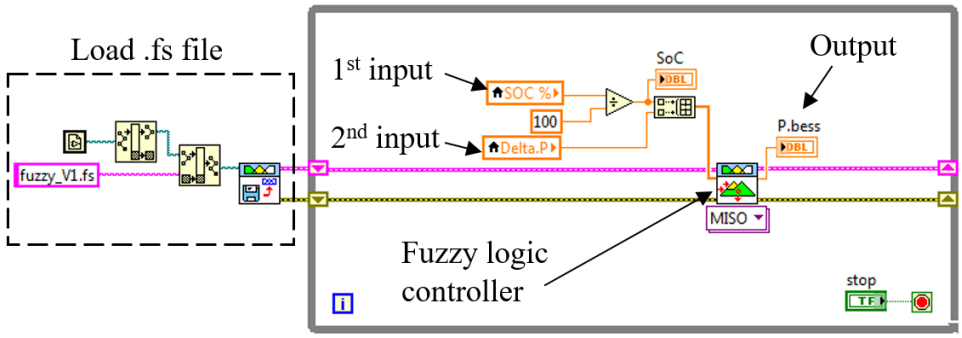

Figure 4.21: Graphical programming of fuzzy system designer in LabVIEW

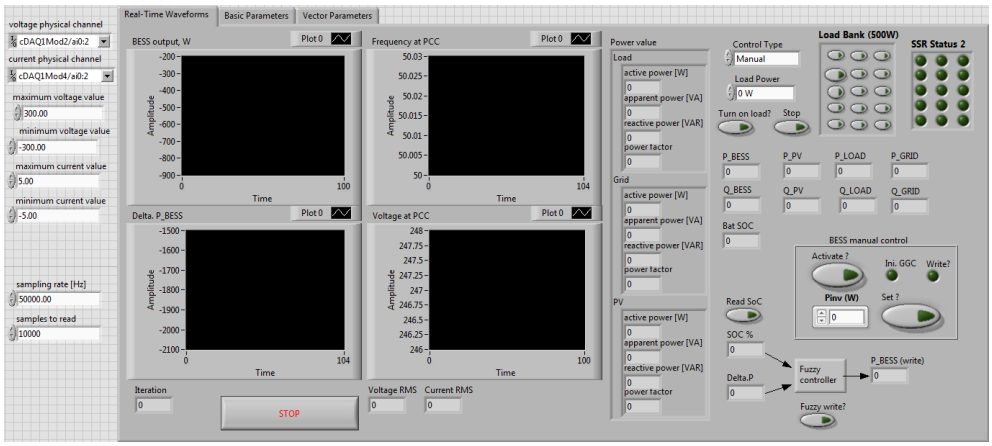

Figure 4.22: Graphical User Interface (GUI) for monitoring and controlling system developed using LabVIEW

4.5. Stage III: Operation of System

As mentioned in Chapter 4.3.3, in order to avoid the frequency violation at the start of islanding operation, ΔP_{BESS} must be as small as possible. The following case study is conducted to investigate the effectiveness of the fuzzy controlled strategy in ensuring ΔP_{BESS} remain within the predefined operating range.

4.5.1. Case Study IV: Performance of FLC Under High Intermittency of PV Output

The proposed fuzzy control algorithm is implemented using LabVIEW to manipulate the BESS power output. It is used to calculate necessary corrective action based on two input membership function, i) battery state of charge (SoC) and ii) power mismatch (ΔP) between load (P_{LOAD}) and PV system (P_{PV}), collected in real-time. In this case study, an experimental setup consists of two 3.6 kW_P PV system, 2.0 kW load, and BESS. Figure 4.23(a) shows the intermittent PV power output recorded throughout the case study. Figure 4.23(b) shows the instructions, P_{BESS} is produced by using FLC. It is noticed that within the first 300 seconds, the value for ΔP_{BESS} (indicated by the blue dotted line) is well maintained within the predefined operating range. However, from 400 seconds onwards, as the PV output is gradually increased, it is observed that the proposed fuzzy is unable to restore ΔP_{BESS} within the operating range and ΔP_{BESS} gradually increases beyond predefined operating limit. If islanding happens at this point of time, there will be frequency violation which will trigger the PV system to disconnect.

In this scenario, it is noticed that BESS can increase its charging power, P_{BESS} to a higher value in short term, so that ΔP_{BESS} can be restored within predefined operating range. In order to perform this, an improved version of the fuzzy controller is developed, and the details are discussed in the following section.

(a)

(b)

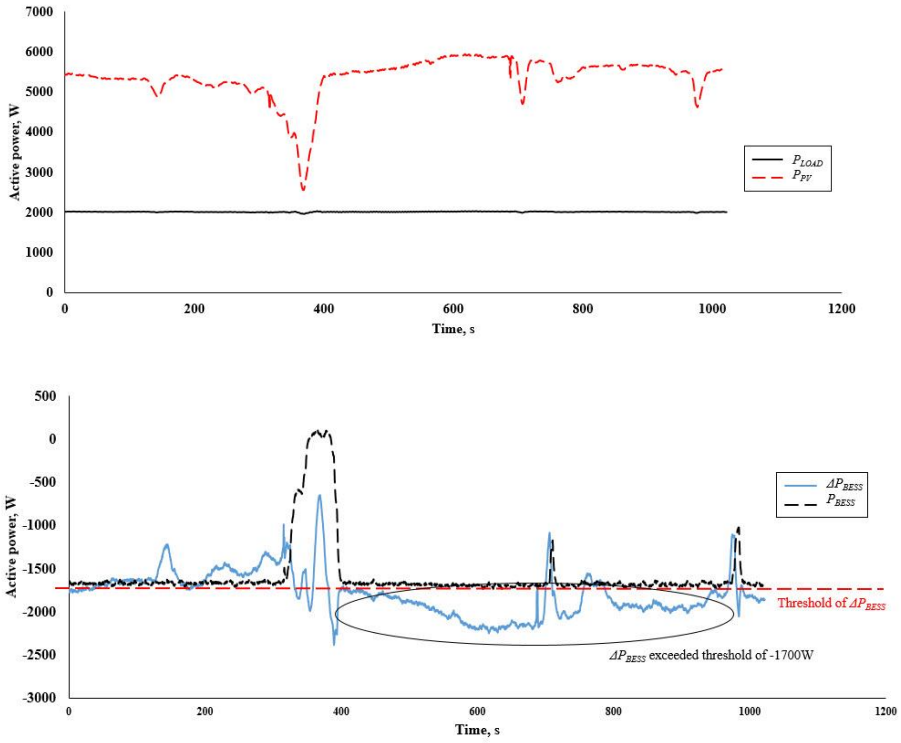

Figure 4.23: (a) Power output recorded from PV system and load at the PCC; (b) The BESS power output and instructions produced by using fuzzy controller to maintain ΔP_{BESS} within predefined operating limit

4.5.2. Improved Version of Fuzzy Logic Controller

The sensitivity of the controller can be improved by defining more states. Table 4.3 shows an improved version of the fuzzy membership rules. Additional states defining the input and output membership functions, ΔP and P_{BESS} are highlighted in grey. The improved fuzzy rules for ΔP is made up of 6 membership function, namely i) Extreme Very Negative (EVN), ii) Very Negative (VN), iii) Negative (N), iv) Positive (P), v) Very Positive (VP), vi) Extreme Very Positive (EVP). With the extension of ΔP, the output instructions are required to extend as well. Hence, the predefined fuzzy output instructions are enclosed in seven different windows, namely i) Extreme High Charge (EHC), ii) High Charge (HC), iii) Charge (C), iv) Idle, v) Discharge (D), vi) High Discharge (HD) and vii) Extreme High Discharge (EHD).

Table 4.3: Improved version of the mapping table for generating the instructions

	ΔP					
SoC	**Extreme Very Negative (EVN)**	**Very Negative (VN)**	**Negative (N)**	**Positive (P)**	**Very Positive (VP)**	**Extreme Very Positive (EVP)**
Low (L)	Extreme High Charge (EHC)	High Charge (HC)	Charge (C)	Idle	Discharge (D)	High Discharge (HD)
Medium (M)	High Charge (HC)	Charge (C)	Idle	Idle	Discharge (D)	High Discharge (HD)
High (H)	High Charge (HC)	Charge (C)	Idle	Discharge (D)	High Discharge (HD)	Extreme High Discharge (EHD)

With the addition of rules and instructions, membership function has to recalibrate. Figure 4.24 depicts the improved membership function of ΔP which is enclosed by 6 trapezium rules. Each of the membership function is tuned by using empirical method. The tuning process is done through by using the test system available in the fuzzy system designer toolbox as shown in Figure 4.20. The test system in the fuzzy system designer toolbox allowed user to verify the output by varying the inputs at different values. The fuzzy output served as an instruction to drive the BESS to ensure ΔP_{BESS} remained within predefined operating range. Hence, the membership function for ΔP and SoC are adjusted accordingly to ensure the output instruction is correct for all scenarios within the fuzzy rules. Besides, the membership function for SoC is remained at 3 types with a modified shape of membership function from triangle to trapezium as shown in Figure 4.25. The change in the membership function shape is necessary as the test system show that the power output of BESS, P_{BESS} is accurately produced to ensure ΔP_{BESS} remain within operating range. Figure 4.26 shows the fuzzy output membership function of P_{BESS} after tuned by empirical method and verified by the test system.

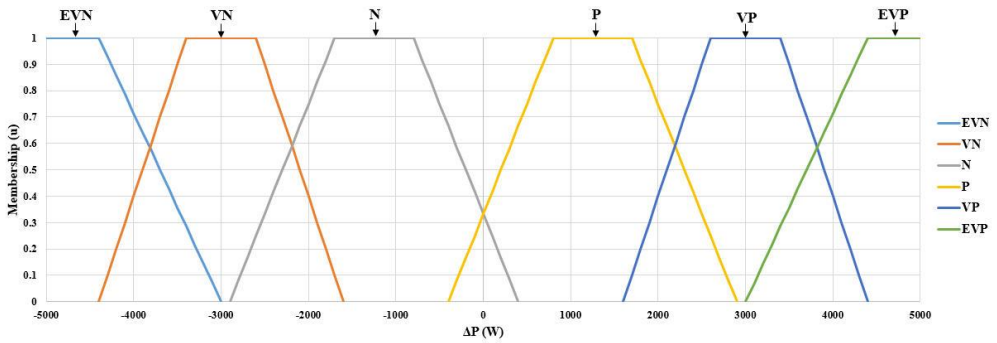

Figure 4.24: Improved membership function for ΔP

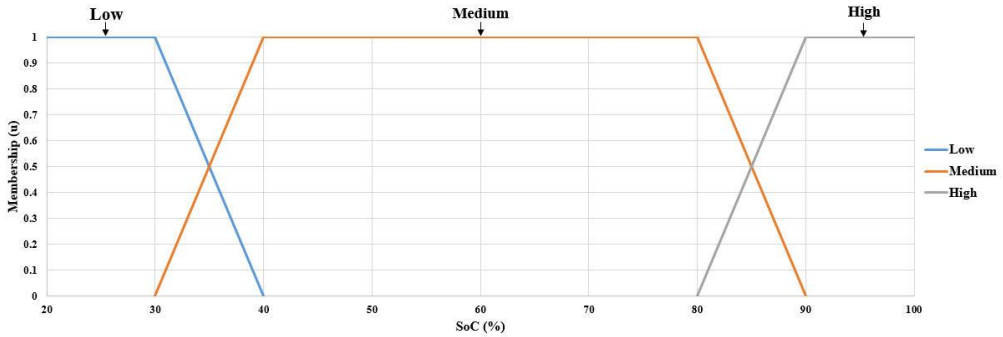

Figure 4.25: Recalibrated membership function for SoC

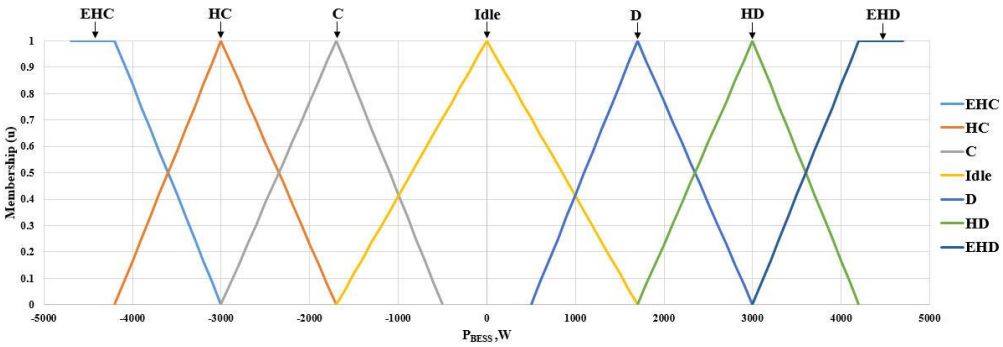

Figure 4.26: Extended membership function for P_{BESS}

4.6. Final stage: Experimental Validation of Improved Fuzzy Controlled Strategy

In this section, the improved version of the fuzzy controller is implemented into the BESS. Several case studies have been conducted in order to verify the effectiveness of the proposed control strategy for regulating ΔP_{BESS} within the predefined operating range.

4.6.1. Case Study V: ΔP_{BESS} Under Intermittent PV Power Output

Malaysia experiences cloudy condition whereby the solar irradiance is scattered throughout the year, hence, it is very common to have intermittent PV power output. The objective of this case study is to evaluate the performance of the proposed fuzzy controlled strategy to maintain ΔP_{BESS} within predefined operating range under variation of PV power output. Figure 4.27 depicts a graph showing the PV output (P_{PV}), load consumption (P_{LOAD}), BESS power output (P_{BESS}) and the change in BESS power output (ΔP_{BESS}). This experiment can be divided into two sections:

I. Section I: smooth PV power output
II. Section II: Fluctuating PV power output condition

In section I, it is observed that as the PV power output gradually increases, the fuzzy controller is capable to ensure ΔP_{BESS} always less than predefined operating range by instructing BESS to absorb more excess power

generated by the PV system. On the other hand, section II shows fluctuating in PV power output. It is observed that the proposed fuzzy control is capable to restore ΔP_{BESS} within operating range in the event of a sudden change in PV power output by sending the right instruction to the BESS. Besides, there is a peak of 61% overshoot with respect to the operating limit in the process of restoring ΔP_{BESS} as indicated with the dotted circle.

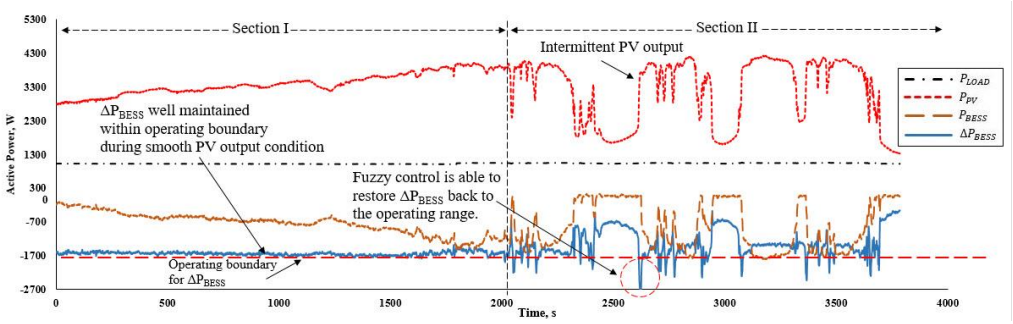

Figure 4.27: Performance of fuzzy controlled strategy under various weather conditions

To understand the reason behind this overshoot, several instructions from the fuzzy output and actual BESS output is compared. By considering the instruction sent to the BESS as P_{FUZZY} and the actual output of the BESS as P_{BESS}, Figure 4.28 depicts P_{FUZZY} and P_{BESS} plotted against time. Upon receiving the instruction from the fuzzy controller P_{FUZZY}, the BESS has to follow the instruction to change its power output, P_{BESS} to match the value of P_{FUZZY}. It is observed from the graph that the P_{BESS} is always lagged P_{FUZZY} throughout the time. The delay between P_{BESS} and P_{FUZZY} takes up to 4 seconds. This is due to the delay in communication between the supervisory computer with the BESS.

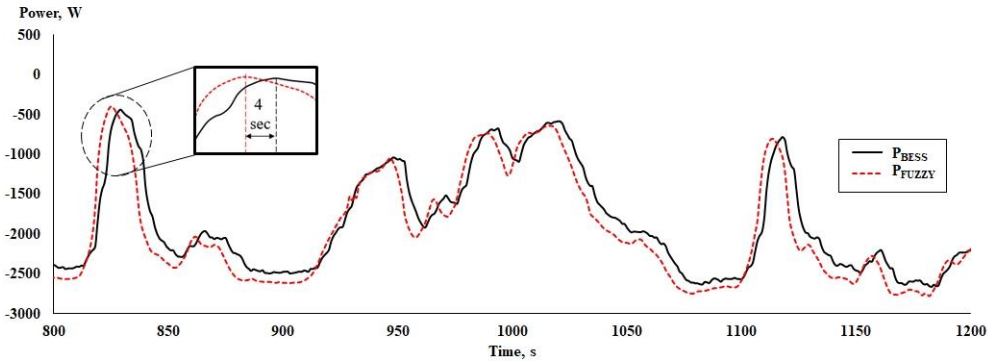

Figure 4.28: Graph of P_{BESS} and P_{FUZZY}; P_{BESS} lags P_{FUZZY} for a mere 4 seconds

On the other hand, the overshoot in ΔP_{BESS} can be solved by improving the delay of the communication system. Equation (4.11) and (4.12) shows the relationship between the exact instruction received by BESS after 4 seconds and the ideal value compute by fuzzy controller respectively.

With delay: $$P_{BESS}(t) = P_{FUZZY}(t-4) \quad (4.11)$$

Without delay: $$P_{BESS_{ideal}}(t) = P_{FUZZY}(t) \quad (4.12)$$

Where, t is time in second.

Thus, the equation for ΔP_{BESS} from equation (4.13) can be modified as equation (4.14) for an ideal scenario. The ΔP_{BESS} in an ideal scenario is indicated by ΔP_{BESS_ideal} and the equation for ΔP_{BESS_ideal} is considered by using P_{BESS_ideal} instead of P_{BESS}.

With delay $$\Delta P_{BESS} = P_{LOAD} - P_{PV} - P_{BESS} \quad (4.13)$$

Without delay $$\Delta P_{BESS\_ideal} = P_{LOAD} - P_{PV} - P_{BESS\_ideal} \quad (4.14)$$

Figure 4.29 illustrated a comparison between ΔP_{BESS} and ΔP_{BESS_ideal}. It is observed that ΔP_{BESS_ideal} in ideal scenario of ΔP_{BESS} is well maintained within the predefined operating range. This case study proves that the overshoot of ΔP_{BESS} can be solved by using a faster communication system.

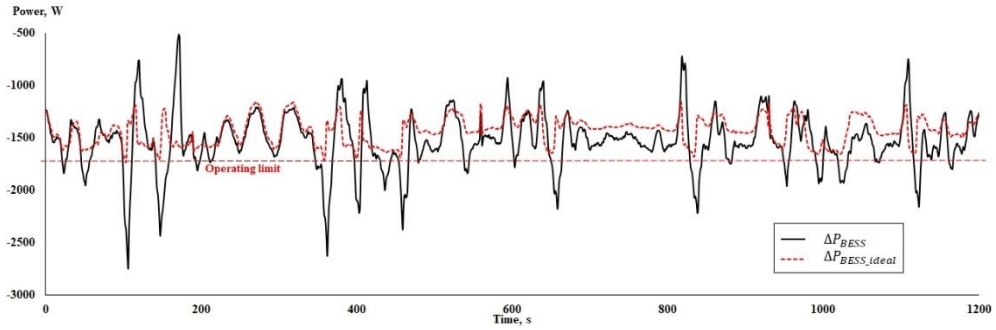

Figure 4.29: Comparison of ΔP_{BESS} and ΔP_{BESS_ideal}; ΔP_{BESS_ideal} is well maintain with the pre-defined operating range

4.6.2. Case Study VI: Continuous Operation of PV System after Grid Outages

This case study is conducted to investigate whether the PV system will continue to operate after the grid outage. In this section, the isolator will be opened randomly to island the network in order to verify the effectiveness of the proposed fuzzy controller.

Figure 4.30(a) depicts the PV power output (P_{PV}), load consumption (P_{LOAD}), BESS power output (P_{BESS}) and change in BESS power output (ΔP_{BESS}). The experiment starts with a constant load of 2.0 kW. The proposed fuzzy controlled strategy regulates the ΔP_{BESS} by manipulating the BESS power output under intermittency of PV power output. Figure 4.30(a) shows the system is islanded at 460 seconds, and the PV system is remained connected after the system is islanded. Figure 4.30(b) depicts the voltage and frequency of the network. It is observed that the voltage and frequency remained within the statutory of 230 V +10%/-6% and 50Hz ± 1% respectively. By ensuring the voltage and frequency remain within the statutory limit, anti-islanding protection of the PV inverter will not be triggered. This allows continuity supply from the PV in the event of islanding. Therefore, it is demonstrated that the proposed fuzzy controlled strategy can ensure continuity supply from the PV system in the event of islanding under intermittency of PV power output condition

(a)

(b)

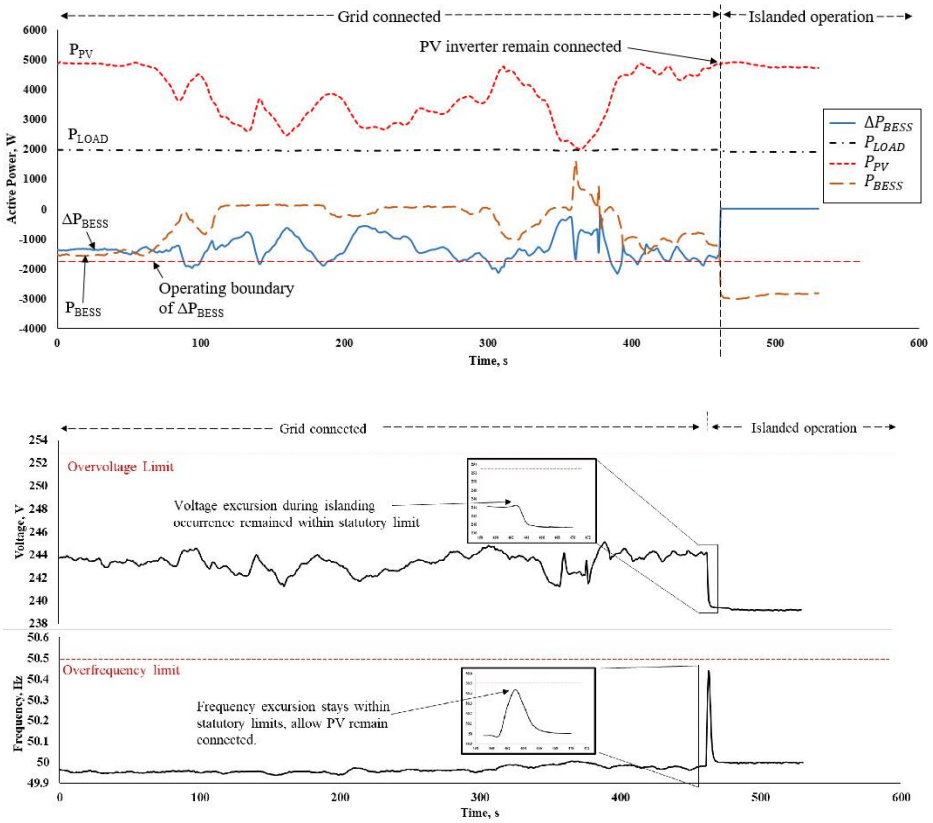

Figure 4.30: (a) PV power output, load consumed, BESS power output and power mismatch of BESS; (b) Voltage and frequency during grid-connected and islanded mode

4.6.3. Case Study VII: Performance of FLC Under Load Change Condition

In an actual environment, the power mismatch between generation and demand is not only affected by the intermittency of PV power output. However, varying in load consumption does contribute to the power mismatch between generation and demand. Therefore, this case study is conducted to investigate the effectiveness of the proposed fuzzy controlled strategy under load varying conditions. Figure 4.31 depicts the PV power output (P_{PV}), load consumption

(P_{LOAD}), BESS power output (P_{BESS}) and change in BESS power output (ΔP_{BESS}). In this experiment, the power consumption of the load changes periodically with a step size of 500 W. Figure 4.31 shows that the fuzzy controller will send a corrective action to the BESS with every step change for the load in order to restore ΔP_{BESS}. Therefore, it is shown that the proposed fuzzy controlled strategy is capable to maintain ΔP_{BESS} within predefined operation range under load change condition.

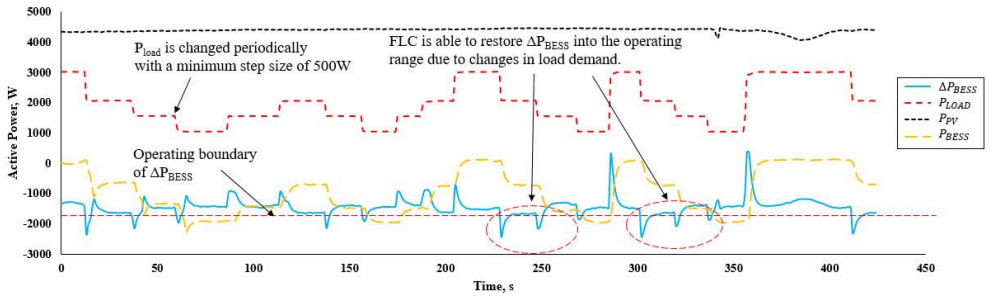

Figure 4.31: The proposed fuzzy controlled strategy can restore ΔP_{BESS} under sudden load change condition

4.7. Performance Comparison Between FLC and PI Controller

The objective of this case study is to compares the performance of the proposed fuzzy controller with a conventional PI controller. In this section, a comparison between the instructions compute by using fuzzy and PI controller is conducted under a same load change scenario. Figure 4.32 shows the PID controller developed using LabVIEW. The PID controller consists of PID control block and a plant block.

In order to construct the PI controller, a PID control block is used in the LabVIEW as illustrated in Figure 4.32. The purpose of the PID block is to compare the input of the instantaneous ΔP_{BESS} with a setpoint reference of -1650 W. The output from the PID block creates a corrective error based on the inputs difference which is fed to the next block named "plant". In the plant block, the error from PID block is added to an instantaneous value of P_{BESS} to compute a new instruction to be sent to the BESS for corrective action. In the meantime, plant measures the instantaneous value of ΔP_{BESS} to be sent to the PID block in the next cycle for further comparison. This process is repeated cyclically to ensure ΔP_{BESS} remains within the predefined operating range. The setting of the PID block is shown in Table 4.4. To create the PI controller, parameter of derivative time in the PID block is set to zero.

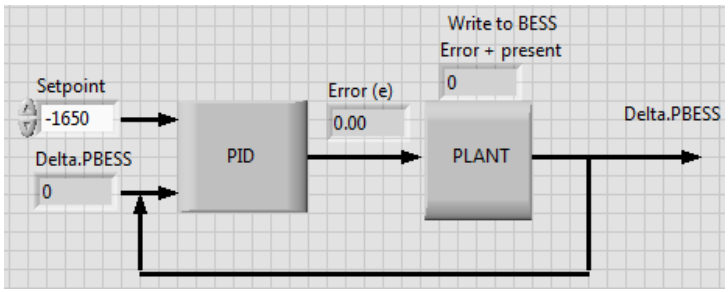

Figure 4.32: PI system in LabVIEW

Table 4.4: Parameter for PID block

Proportional gain, (K_C)	1.00
Integral time, (T_i, min)	1.00
Derivative time (K_D, min)	0.00

4.7.1. Performance of PI Controller

The comparison for PI controller in this case study is conducted under smooth PV output and varying load consumption. The experiment started with a 500 W load being switched from on to off, cyclically. Performance of the controller in restoring ΔP_{BESS} for each switching from on to off is mapped onto each other as shown in Figure 4.33. This experiment is repeated for 5 times, and the performance of the controller for each experiment are plotted in the same graph, namely PI 1 to PI 5. It is observed that among these curves, PI 3 has the shortest rise time in restoring ΔP_{BESS} back to the predefined operating range under load change condition as compared with PI 1, 2, 4 and 5.

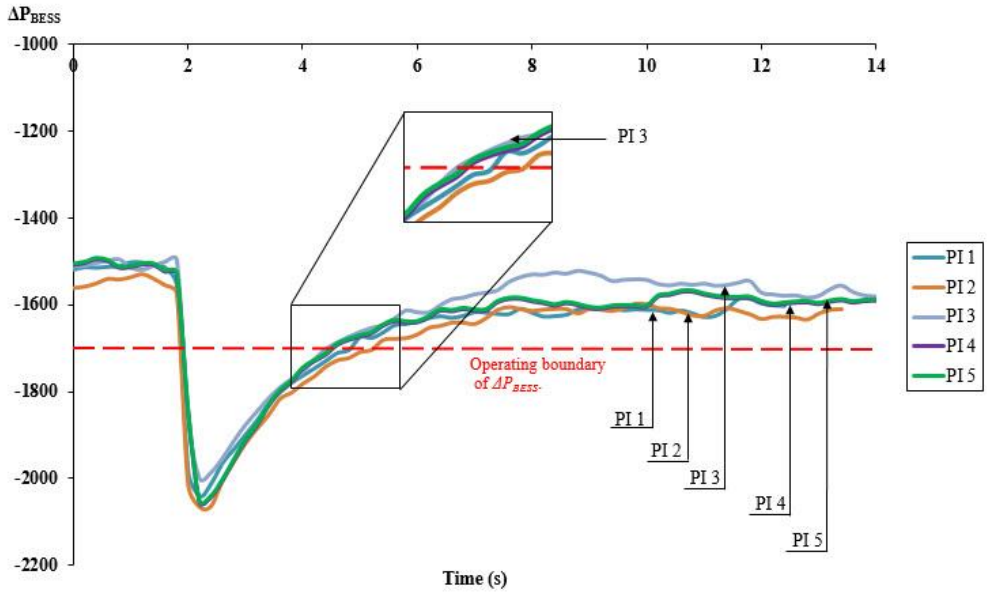

Figure 4.33: Each of load switching is mapped onto each other to compare the performance of individual PI controller

4.7.2. Performance of Proposed Fuzzy Controller

The case study in the previous section is conducted based on PI controller. To compare the performance of PI and fuzzy controller, this section of the case study is conducted to observe the performance of the proposed fuzzy controlled strategy under the same condition as undergoes by the PI controller in the previous section. Figure 4.34 shows the comparison of five sets fuzzy instructions computed under the same scenario with various load change condition and a smooth PV power output. It is observed that Fuzzy 3 have the shortest rise time in restoring ΔP_{BESS} back to the predefined operating range as compared with Fuzzy 1, 2, 4 and 5.

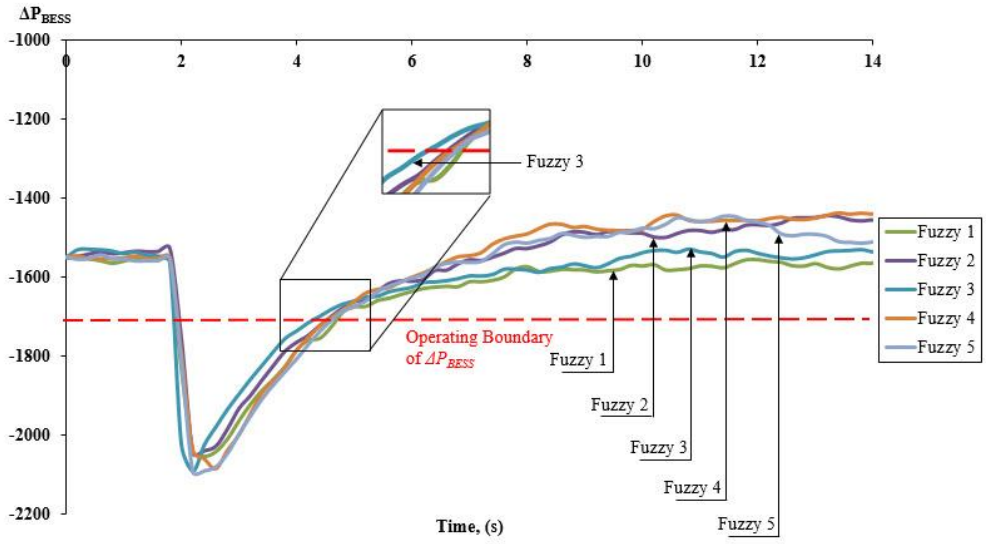

Figure 4.34: Comparison of each switching with fuzzy controller

4.7.3. Comparison Between Proposed Fuzzy with Conventional PI Controller

To compare the performance between PI and fuzzy controller, the fastest response from each experiment on fuzzy and PI is selected. In the previous case studies, it is observed that PI 3 and Fuzzy 3 have the best response to their respective category. Therefore, the performance of PI 3 and Fuzzy 3 can be compared by mapping on one another. Figure 4.35 shows the performance of Fuzzy 3 and PI 3 in restoring ΔP_{BESS} under load change condition with smooth PV output. As a reference to the graph, proposed fuzzy controlled strategy of Fuzzy 3 and PI 3 has a rise time of 2.2 sec and 3.0 sec respectively in restoring ΔP_{BESS} back to the predefined operating range as indicated by the dotted line. Shorter rise time indicates faster response time in restoring ΔP_{BESS}. Therefore, it is concluded that Fuzzy 3 perform better than PI 3 due to shorter rise time as shown in Figure 4.35.

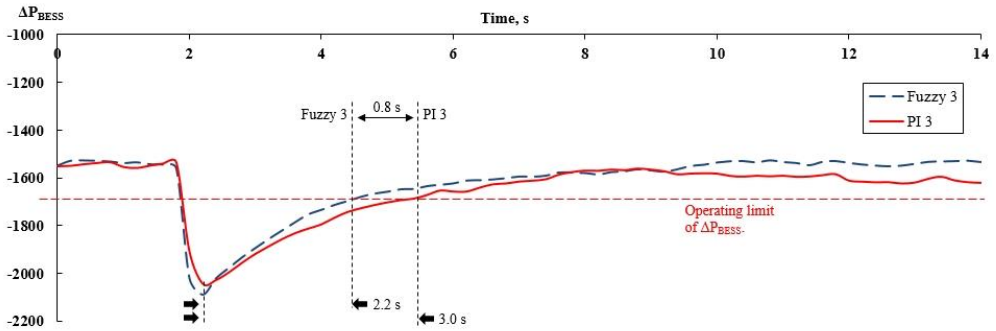

Figure 4.35: Proposed fuzzy controller performed 0.8 s faster than conventional PI controller in restoring ΔP_{BESS}

4.8. Summary

The islanding operation of PV system is proven to be not viable in the event of grid outage due to advancement in anti-islanding protection technology. The proposed bi-directional inverter with batteries (BESS) is integrated into the system as a grid forming unit is able to regulate the voltage and the frequency during islanding operation. Islanding operation of PV system with BESS integration is proven to be viable. In certain scenario, a large change in BESS power output in the event of islanding causes frequency violation which triggers the PV system to disconnect. Therefore, the relationship between ΔP_{BESS} with frequency excursion under various generation and demand is established. It is found that ΔP_{BESS} is required to be within a predefined operating range to ensure no frequency violation in the event of islanding. Thus, the fuzzy controlled strategy is proposed to maintain ΔP_{BESS} within a predefined operating range. Several experimental case studies have been conducted to evaluate the performance of fuzzy controlled strategy under various weather and load change conditions. It is observed that the fuzzy controlled strategy is proven to be able to mitigate frequency violation during islanding of PV which improve the reliability of the electricity supply. Also, the proposed fuzzy controlled strategy is proven to perform faster than the conventional PI controller.

CHAPTER 5

CONCLUSIONS AND FUTURE WORK

5.1. Conclusions

Solar outlook in Malaysia has been positive. This is because the country is geographically situated on the equator which has received tremendous amount of sunlight annually. In addition, the Malaysian government has taken initiative to promote the use of renewable energy by introducing various incentive programmes such as tax exemption, allowance and special tariff. Consequently, the growth of grid-connected renewable energy sources is expected to increase in the future. Nevertheless, the IEC 61727 standard has restricted the operation of PV systems during grid outage if the voltage and frequency of the network are detected to be out of specified ranges. This practice is established to avoid any equipment damages or risks due to the fact that the frequency and voltage of the islanded networks are not regulated within the required tolerances. Thus, an anti-islanding protection system is featured in PV inverter to detect islanding operation and disconnect the PV system during the grid outage. However,

shutting down PV system during grid outage causes wastage of available clean energy. To utilise the available clean energy and improve the reliability of the electricity supply, PV system has to remain energised during grid-outage. In order to achieve this, Battery-based Energy Storage System (BESS) is proposed in conjunction with the PV systems. The BESS can serve as a voltage source to the PV system during the grid outage and provide voltage and frequency regulation in the islanded network.

In this project, a Low Voltage (LV) experimental network consists of a 6 kW BESS, two 3.6 kWp PV systems and a 3 kW load emulator is developed. Multiple measuring devices are set up to measure and record the electrical parameters at the Point of Common Coupling (PCC) of each device. A communication system with the BESS and measuring device is established with the supervisory computer that is used to display the electrical parameters and to control the power flow of the BESS using LabVIEW.

Numerous case studies are conducted to investigate the feasibility of continues operation of PV systems with BESS during grid outages. In the preliminary study, it is observed that a standalone PV system failed to energise in the event of grid outage even though the generation and load consumption is closely matched. This has proven that PV system requires a voltage reference to initiate the operation. In this project, BESS is proposed to provide a voltage reference to the PV system during the grid outage, and provide voltage and frequency regulation by maintaining the power balance between the generation and demand in the islanded network. However, BESS without proper control

only allows PV system to remain connected during grid outage if the change in BESS power output (ΔP_{BESS}) is small.

There are scenarios where the PV system is disconnected in the event of the grid outage due to frequency violation stated in the Malaysian standard, MS 1837. The frequency violation is caused by a large amount of change in BESS power output, ΔP_{BESS} at the start of islanding. Therefore, a relationship between the magnitude of frequency excursion variation with ΔP_{BESS} under various levels of generation and demand is established. The operating range of the ΔP_{BESS} is used to ensure no frequency violation during the transition is established.

A proposed fuzzy control strategy is developed to regulate ΔP_{BESS} within the predefined operating range. Two inputs of SoC and ΔP is considered by the fuzzy control strategy to generate a control instruction for the BESS. The proposed fuzzy control strategy is tested under various weather conditions and load conditions. It is presented that the proposed control is able to regulate ΔP_{BESS} under intermittent PV power output with a slight overshoot. The overshoot is examined and found to be caused by the delay in communication between the supervisory computer and the BESS. The experimental case studies have proven that the proposed BESS driven by the proposed fuzzy control strategy is capable to regulate the voltage and frequency to be within the statutory limit during the starts of islanding operation. Hence, ensure the continuity supply of the PV system in the event of grid outage which further improves the reliability of the electricity supply and SAIDI indexes. Besides,

the proposed fuzzy controller is benchmarked with a conventional PI controller. The finding shows that fuzzy controller performed 0.8 seconds faster than the conventional PI controller.

In summary, the contribution of this research is outlined as followed:

1. A relationship between the magnitude of frequency excursion at the starts of islanding with various level of generation and demand is established which is not shown in other literature of the similar topic. The finding shows that greater mismatch of power would results in higher magnitude of frequency excursion during the starts of islanding.

2. An innovative fuzzy control strategy has been developed for the BESS. The controller has demonstrated its strength in ensure BESS operate within the predefined operating range.

3. The controller is tested under various weather and load condition. The voltage and frequency during the starts of islanding remain within statutory limit under the supervisory of the proposed control strategy. The controller has demonstrated the strength in improving reliability and quality of the electricity supply by ensuring PV system remain connected during islanding operation.

5.2. Future Work

Although the control strategy presented in this project has demonstrated its strength in improving the reliability of the electricity supply during islanding of PV system, there are still room for future improvement. For example, the experiment is conducted in a single-phase distribution system. In the future residential development, three-phase supplies are commonly adopted to cope with rising electricity demand. Therefore, the control strategy can be improved and implement on a three-phase network to meet the future trend of using three-phase in the residential area.

The fuzzy rules are made up of 6 by 3 matrices which consists of 6 stages for ΔP and 3 levels for SoC to produce 18 linguistic outputs. For future modification, the fuzzy rules can be expanded to smoothen the fuzzy output. For example, the SoC input can be further categorise into 5 levels instead of 3 which would result in 6 by 5 matrix and produces 30 linguistic outputs.

On the other hand, there is a delay for fetching the instruction from the supervisory computer to the BESS. Future work can consider accessing a lower level programming to control the BESS, hence reduce or minimise the delay time.

LIST OF PUBLICATIONS

Khaw, A.L.Y., Wong, J. and Lim, Y.S.., 2018. Fuzzy Controlled Energy Storage System for Improving Reliability of Electricity Supply During Islanding of Photovoltaic Systems. *International Transactions on Electrical Energy Systems*, 0(0), pp. 0 – 0. https://doi.org/10.1002/etep.2604

Khaw, A.L.Y., Lim, Y.S. and Wong, J., 2018. Feasibility of Continues Operation of Photovoltaic Systems with Energy Storage during Grid Outage. *International Journal of Electrical and Electronic Engineering & Telecommunications*, 7(1), pp. 1 – 6.

Khaw, A.L.Y., Wong, J. and Lim, Y.S., 2017. Review of droop-controlled bi-directional inverter in conducting islanded operation of photovoltaic systems. AIP Conference Proceedings, 1828(1), p.020028.

LIST OF REFERENCES

Abate-Stanford, T., 2015, *How gallium arsenide could outcompete silicon* [Online]. Available at: http://www.futurity.org/gallium-arsenide-solar-cells-885992/ [Accessed: 13 October 2017].

Agnoletto, E.J. et al., 2016. Fuzzy secondary controller applied to autonomous operated AC microgrid. *2016 European Control Conference (ECC)*. June 2016 pp. 1788–1793.

Agüero, J., 2015, *What Does the Future Hold for Utilities?* [Online]. Available at: http://www.tdworld.com/distribution/what-does-future-hold-utilities [Accessed: 1 September 2017].

Aguiar, C.R. et al., 2015. Frequency fuzzy anti-islanding for grid-connected and islanding operation in distributed generation systems. *IET Power Electronics*, 8(7), pp.1255–1262.

Alhamali, A., Farrag, M.E., Bevan, G. and Hepburn, D.M., 2016. Review of Energy Storage Systems in electric grid and their potential in distribution networks. *2016 Eighteenth International Middle East Power Systems Conference (MEPCON)*. December 2016 pp. 546–551.

Amcorp, 2013, *Malaysia's largest single site solar power plant, Amcorp Gemas 10.25MW Solar Power Plant powers up* [Online]. Available at: http://www.amcorpproperties.com/html/details.aspx?ID=6&PID=31&NID=90&Type=News [Accessed: 28 August 2017].

Andishgar, M.H., Gholipour, E. and Hooshmand, R., 2017. An overview of control approaches of inverter-based microgrids in islanding mode of operation. *Renewable and Sustainable Energy Reviews*, 80, pp.1043–1060.

Annuar A, 2010. *The Malaysian Distribution Code*, Suruhanjaya Tenaga.

Arulampalam, A., Mithulananthan, N., Bansal, R.C. and Saha, T.K., 2010. Micro-grid control of PV-Wind-Diesel hybrid system with islanded and grid connected operations. *2010 IEEE International Conference on Sustainable Energy Technologies (ICSET)*. December 2010 pp. 1–5.

Awer, 2011, *Power Consumption for Various Equipments at Home* [Online]. Available at: http://www.click.org.my/flash/pdf/howtouse.pdf [Accessed: 23 October 2017].

Azman, 2013. BRIEF OUTLOOK ON MALAYSIAN ELECTRICITY SUPPLY INDUSTRY, TNB & MALAYSIA NATIONAL COMMITTEE OF CIGRE (MNC-CIGRE). Available at: http://www.csee.net.cn/data/zt_aorc_cigre2013/ppt/ps4.pdf.

Balaguer, I.J. et al., 2011. Control for Grid-Connected and Intentional Islanding Operations of Distributed Power Generation. *IEEE Transactions on Industrial Electronics*, 58(1), pp.147–157.

Barker, P.P. and Mello, R.W.D., 2000. Determining the impact of distributed generation on power systems. I. Radial distribution systems. *2000 Power Engineering Society Summer Meeting (Cat. No.00CH37134)*. 2000 pp. 1645–1656 vol. 3.

Bayrak, G. and Kabalci, E., 2016. Implementation of a new remote islanding detection method for wind–solar hybrid power plants. *Renewable and Sustainable Energy Reviews*, 58, pp.1–15.

Best, R.J., Morrow, D.J., McGowan, D.J. and Crossley, P.A., 2007. Synchronous Islanded Operation of a Diesel Generator. *IEEE Transactions on Power Systems*, 22(4), pp.2170–2176.

Bitaraf, H., Sheikholeslamzadeh, M., Ranjbar, A.M. and Mozafari, B., 2012. Neuro-fuzzy islanding detection in distributed generation. *IEEE PES Innovative Smart Grid Technologies*. May 2012 pp. 1–5.

Brabandere, K.D. et al., 2007. A Voltage and Frequency Droop Control Method for Parallel Inverters. *IEEE Transactions on Power Electronics*, 22(4), pp.1107–1115.

Cengiz, M.S., Mami and Mehmet Salih, 2015, *Price-Efficiency Relationship for Photovoltaic Systems on a Global Basis* [Online]. Available at: https://www.hindawi.com/journals/ijp/2015/256101/ [Accessed: 25 July 2017].

Cha, S.T., Wu, Q., Zhao, H. and Wang, C., 2014. Frequency Control for Island Operation of Bornholm Power System. *Energy Procedia*, 61, pp.1389–1393.

Choudhury, S., Choudhury, A., Panda, D. and Rout, P.K., 2016. Optimal control of islanded microgrid with adaptive fuzzy logic PI controller using HBCC under various voltage load variation. *2016 International Conference on Circuit, Power and Computing Technologies (ICCPCT)*. March 2016 pp. 1–8.

Chowdhury, S.P., Chowdhury, S., Ten, C.F. and Crossley, P.A., 2008. Islanding operation of distributed generators in active distribution networks. *2008 43rd International Universities Power Engineering Conference*. September 2008 pp. 1–5.

Chua, K.H., Lim, Y.S. and Morris, S., 2017. A novel fuzzy control algorithm for reducing the peak demands using energy storage system. *Energy*, 122(Supplement C), pp.265–273.

Dempsey, M., 2017, *Island Life: Operating Your Microgrid in Island Mode* [Online]. Available at: https://www.districtenergy.org/viewdocument/island-life-operating-your-microgr [Accessed: 26 December 2017].

Divshali, P.H., Alimardani, A., Hosseinian, S.H. and Abedi, M., 2012. Decentralized Cooperative Control Strategy of Microsources for Stabilizing Autonomous VSC-Based Microgrids. *IEEE Transactions on Power Systems*, 27(4), pp.1949–1959.

Energy Commission, 2015a, *Electricity Statistics - Electricity Supply Interruption per 1,000 Consumers* [Online]. Available at: http://meih.st.gov.my/statistics?p_auth=i2POSmdC&p_p_id=Eng_Statistic_WAR_STOASPublicPortlet&p_p_lifecycle=1&p_p_state=maximized&p_p_mode=view&_Eng_Statistic_WAR_STOASPublicPortlet_execution=e1s1&_Eng_Statistic_WAR_STOASPublicPortlet__eventId=ViewStatisticELC9&categoryId=10&flowId=73 [Accessed: 1 September 2017].

Energy Commission, 2015b, *Electricity Statistics - Electricity Supply Interruption per 1,000 Consumers. Sabah* [Online]. Available at: http://meih.st.gov.my/statistics?p_auth=i2POSmdC&p_p_id=Eng_Statistic_WAR_STOASPublicPortlet&p_p_lifecycle=1&p_p_state=maximized&p_p_mode=view&_Eng_Statistic_WAR_STOASPublicPortlet_execution=e1s1&_Eng_Statistic_WAR_STOASPublicPortlet__eventId=ViewStatisticELC9&categoryId=10&flowId=96 [Accessed: 1 September 2017].

Energy Commission, 2015c, *Statistics - Malaysia Energy Information Hub* [Online]. Available at: http://meih.st.gov.my/statistics [Accessed: 23 August 2017].

Engler, A., 2004. *Device for equal-rated parallel operation of single-or three-phase voltage sources*, US6693809 B2

Esmaeilian, A. and Kezunovic, M., 2017. Prevention of Power Grid Blackouts Using Intentional Islanding Scheme. *IEEE Transactions on Industry Applications*, 53(1), pp.622–629.

Falahati, S., Taher, S.A. and Shahidehpour, M., 2016. Grid frequency control with electric vehicles by using of an optimized fuzzy controller. *Applied Energy*, 178(Supplement C), pp.918–928.

Fuangfoo, P., Lee, W.J. and Kuo, M.T., 2007. Impact Study on Intentional Islanding of Distributed Generation Connected to a Radial Subtransmission System in Thailand's Electric Power System. *IEEE Transactions on Industry Applications*, 43(6), pp.1491–1498.

Giampaolo, B., Barater, D., Tarisciotti, L. and Zanchetta, P., 2014. High-dynamic single-phase Hilbert-based PLL for improved phase-jump ride-through in grid-connected inverters. *2014 IEEE Energy Conversion Congress and Exposition (ECCE)*. September 2014 pp. 4932–4939.

Green Building Index, 2013, *Green Building Index* [Online]. Available at: http://new.greenbuildingindex.org/how/system [Accessed: 25 August 2017].

Green, M.A. et al., 2017. Solar cell efficiency tables (version 50). *Progress in Photovoltaics: Research and Applications*, 25(7), pp.668–676.

Greenpowerco, 2016. Solar PV prices. *The Green Power Company | Solar Power Systems*. Available at: http://greenpowerco.com.au/solar-pv-prices-the-swanson-effect/ [Accessed: 28 August 2017].

Guerrero, J.M. et al., 2009. Control Strategy for Flexible Microgrid Based on Parallel Line-Interactive UPS Systems. *IEEE Transactions on Industrial Electronics*, 56(3), pp.726–736.

Guerrero, J.M. et al., 2011. Hierarchical Control of Droop-Controlled AC and DC Microgrids #x2014;A General Approach Toward Standardization. *IEEE Transactions on Industrial Electronics*, 58(1), pp.158–172.

Guerrero, J.M., Chandorkar, M., Lee, T.L. and Loh, P.C., 2013. Advanced Control Architectures for Intelligent Microgrids - Part I: Decentralized and Hierarchical Control. *IEEE Transactions on Industrial Electronics*, 60(4), pp.1254–1262.

Hanif, M., Basu, M. and Gaughan, K., 2011. A discussion of anti-islanding protection schemes incorporated in a inverter based DG. *2011 10th International Conference on Environment and Electrical Engineering*. May 2011 pp. 1–5.

Hashemi, F., Mohammadi, M. and Kargarian, A., 2017. Islanding detection method for microgrid based on extracted features from differential transient rate of change of frequency. *Transmission Distribution IET Generation*, 11(4), pp.891–904.

Hau, L.C., Lim, Y.S. and Chua, K.H., 2017. Active Control Strategy of Energy Storage System for Reducing Maximum Demand Charges under Limited Storage Capacity. *Journal of Energy Engineering*, 143(4), p.04017010.

Hayes, G.J. and Clemens, B.M., 2015. Laser liftoff of gallium arsenide thin films. *MRS Communications*, 5(1), pp.1–5.

Heidari, A. et al., 2016. On Exploring Potential Reliability Gains Under Islanding Operation of Distributed Generation. *IEEE Transactions on Smart Grid*, 7(5), pp.2166–2174.

Huang, X., Jin, X., Ma, T. and Tong, Y., 2011. A voltage and frequency droop control method for microsources. *2011 International Conference on Electrical Machines and Systems*. August 2011 pp. 1–5.

IEC, 2004, *IEC 61727:2004 | IEC Webstore | invertor, smart city, LVDC* [Online]. Available at: http://www.ecn.nl/docs/library/report/2004/c04032.pdf [Accessed: 30 August 2017].

IEEE Std, 2012. IEEE Guide for Electric Power Distribution Reliability Indices - Redline. *IEEE Std 1366-2012 (Revision of IEEE Std 1366-2003) - Redline*, pp.1–92.

IEEE Std, 1992. IEEE Recommended Practice for Grounding of Industrial and Commercial Power Systems. *IEEE Std 142-1991*, pp.1–240.

IEEE Std, 2003. IEEE Standard for Interconnecting Distributed Resources with Electric Power Systems. *IEEE Std 1547-2003*, pp.1–28.

IEEE Std, 2014. IEEE Standard for Interconnecting Distributed Resources with Electric Power Systems - Amendment 1. *IEEE Std 1547a-2014 (Amendment to IEEE Std 1547-2003)*, pp.1–16.

Isa, A.I.M., Mohamad, H. and Yasin, Z.M., 2015. Evaluation on non-detection zone of passive islanding detection techniques for synchronous distributed generation. *2015 IEEE Symposium on Computer Applications Industrial Electronics (ISCAIE)*. April 2015 pp. 100–104.

Jamroen, C., Namproom, P. and Dechanupaprittha, S., 2016. TS-Fuzzy Based Adaptive PEVs Charging Control for Smart Grid Frequency Stabilization Under Islanding Condition. *Procedia Computer Science*, 86, pp.124–127.

Janine, 2014. Flooded vs. Sealed Rechargeable Batteries. *Sure Power, Inc*. Available at: http://www.sure-power.com/2014/01/flooded-vs-sealed-rechargeable-batteries/ [Accessed: 8 December 2017].

Jeong, J.-W., Kim, D.-H. and Lee, B.-K., 2013. Development tendency of sliding mode frequency shift type anti-islanding of Japanese companies. *2013 International Conference on Electrical Machines and Systems (ICEMS)*. October 2013 pp. 409–413.

Kermani, M., 2016. Transient voltage and frequency stability of an isolated microgrid based on energy storage systems. *2016 IEEE 16th International Conference on Environment and Electrical Engineering (EEEIC)*. June 2016 pp. 1–5.

Khamis, A., Shareef, H., Bizkevelci, E. and Khatib, T., 2013. A review of islanding detection techniques for renewable distributed generation systems. *Renewable and Sustainable Energy Reviews*, 28, pp.483–493.

Ku Ahmad, K.N.E., Selvaraj, J. and Rahim, N.A., 2013. A review of the islanding detection methods in grid-connected PV inverters. *Renewable and Sustainable Energy Reviews*, 21, pp.756–766.

Kumar, M., Kumar, P., Yadav, A. and Pal, N., 2016. Fuzzy gain scheduled intelligent frequency control in an AC microgrid. *2016 3rd International Conference on Recent Advances in Information Technology (RAIT)*. March 2016 IEEE, Chandad, India, pp. 237–242.

Laghari, J.A. et al., 2015. An islanding detection strategy for distribution network connected with hybrid DG resources. *Renewable and Sustainable Energy Reviews*, 45, pp.662–676.

Laour, M., Mahrane, A., Akel, F. and Bendib, D., 2014. Implementation of Active Anti-Islanding Methods Protection Devices for Grid Connected Photovoltaic Systems. *International Journal of Electrical Energy*, pp.89–93.

Lebrón, C. and Andrade, F., 2016. An intelligent battery management system based on fuzzy controller for home microgrid working in grid-connected and island mode. *2016 IEEE ANDESCON*. October 2016 pp. 1–4.

Lee, S.H., Son, G. and Park, J.W., 2013. Power Management and Control for Grid-Connected DGs With Intentional Islanding Operation of Inverter. *IEEE Transactions on Power Systems*, 28(2), pp.1235–1244.

Li, C. et al., 2014. A review of islanding detection methods for microgrid. *Renewable and Sustainable Energy Reviews*, 35, pp.211–220.

Lidula, N.W.A. and Rajapakse, A.D., 2011. Microgrids research: A review of experimental microgrids and test systems. *Renewable and Sustainable Energy Reviews*, 15(1), pp.186–202.

Liu, F. et al., 2010. Improved SMS islanding detection method for grid-connected converters. *IET Renewable Power Generation*, 4(1), pp.36–42.

Mahat, P., Chen, Z. and Bak-Jensen, B., 2008. Review of islanding detection methods for distributed generation. *2008 Third International Conference on Electric Utility Deregulation and Restructuring and Power Technologies*. April 2008 pp. 2743–2748.

Mahat, P., Chen, Z. and Bak-Jensen, B., 2011. Review on islanding operation of distribution system with distributed generation. *2011 IEEE Power and Energy Society General Meeting*. July 2011 pp. 1–8.

Malaysia Standard, 2013, *INSTALLATION OF GRID-CONNECTED PHOTOVOLTAIC (PV) SYSTEM* [Online]. Available at: http://www.msonline.gov.my/catalog.php [Accessed: 30 August 2017].

Malaysian Government, 2011. *Renewable Energy Act 2011*,

Manaffam, S., Talebi, M., Jain, A.K. and Behal, A., 2017. Intelligent Pinning Based Cooperative Secondary Control of Distributed Generators for Microgrid in Islanding Operation Mode. *IEEE Transactions on Power Systems*, PP(99), pp.1–1.

Mohamad, H., Mokhlis, H., Bakar, A.H.A. and Ping, H.W., 2011. A review on islanding operation and control for distribution network connected with small hydro power plant. *Renewable and Sustainable Energy Reviews*, 15(8), pp.3952–3962.

Mohammadpour, B., Pahlevaninezhad, M., Kaviri, S.M. and Jain, P., 2016. A New Slip Mode Frequency Shift Islanding Detection Method for single phase grid connected inverters. *2016 IEEE 7th International Symposium on Power Electronics for Distributed Generation Systems (PEDG)*. June 2016 pp. 1–7.

Moradi, M.H., Eskandari, M. and Hosseinian, S.M., 2016. Cooperative control strategy of energy storage systems and micro sources for stabilizing microgrids in different operation modes. *International Journal of Electrical Power & Energy Systems*, 78, pp.390–400.

Neves, R.V.A. et al., 2016. Fuzzy secondary controller for autonomous stand-alone and grid-connected AC microgrid. *IECON 2016 - 42nd Annual Conference of the IEEE Industrial Electronics Society*. October 2016 pp. 7028–7033.

NREL, 2014, *Grid Standards and Codes | Grid Modernization | NREL* [Online]. Available at: https://www.nrel.gov/grid/standards-codes.html [Accessed: 30 August 2017].

Oureilidis, K.O. and Demoulias, C.S., 2016. A decentralized impedance-based adaptive droop method for power loss reduction in a converter-dominated islanded microgrid. *Sustainable Energy, Grids and Networks*, 5, pp.39–49.

Planas, E. et al., 2013. General aspects, hierarchical controls and droop methods in microgrids: A review. *Renewable and Sustainable Energy Reviews*, 17, pp.147–159.

Prime Minister's Department, 2001. Eighth Malaysia Plan 2001-2005. Available at: http://www.epu.gov.my/en/rmk/eighth-malaysia-plan-2001-2005 [Accessed: 24 August 2017].

Prime Minister's Department, 2017. Eleventh Malaysia Plan, 2016-2020. Available at: http://www.epu.gov.my/en/rmk/eleventh-malaysia-plan-2016-2020.

Prime Minister's Department, 2006. Ninth Malaysia Plan, 2006 - 2010. Available at: http://www.epu.gov.my/en/rmk/ninth-malaysia-plan-2006-2010 [Accessed: 24 August 2017].

Prime Minister's Department, 2016. Tenth Malaysia Plan (10th MP). Available at: http://www.epu.gov.my/en/rmk/tenth-malaysia-plan-10th-mp [Accessed: 24 August 2017].

Qamar, H., Qamar, H. and Vaccaro, A., 2017. Design of fuzzy logic controllers for decentralized voltage regulation in grid connected photovoltaic systems. *2017 IEEE International Conference on Fuzzy Systems (FUZZ-IEEE)*. July 2017 pp. 1–6.

Quirós-Tortós, J. et al., 2015. Constrained spectral clustering-based methodology for intentional controlled islanding of large-scale power systems. *Transmission Distribution IET Generation*, 9(1), pp.31–42.

Reis, M.V.G. et al., 2015. Active frequency drift with positive feedback anti-islanding method for a single phase two-stage grid-tied photovoltaic system. *2015 IEEE 13th Brazilian Power Electronics Conference and 1st Southern Power Electronics Conference (COBEP/SPEC)*. November 2015 pp. 1–6.

Ryan, C., 2017, *Edra plans to develop 50MW solar project in Malaysia* [Online]. Available at: https://www.pv-tech.org/news/edra-plans-to-develop-50mw-solar-project-in-malaysia [Accessed: 4 January 2018].

Samantaray, S.R., El-Arroudi, K., Joos, G. and Kamwa, I., 2010. A Fuzzy Rule-Based Approach for Islanding Detection in Distributed Generation. *IEEE Transactions on Power Delivery*, 25(3), pp.1427–1433.

SEDA, 2017a, *Operational Plants* [Online]. Available at: http://www.seda.gov.my/?omaneg=00010100000001010101000100001000000000000000000&s=539 [Accessed: 17 August 2017].

SEDA, 2011a, *Overview of Seda* [Online]. Available at: http://www.seda.gov.my/?omaneg=00010100000001010101000100001000000000000000000&s=2 [Accessed: 29 August 2017].

SEDA, 2011b, *Overview of the FiT System in Malaysia* [Online]. Available at: http://www.seda.gov.my/?omaneg=00010100000001010101000100001000000000000000000&s=6 [Accessed: 29 August 2017].

SEDA, 2011c, *Renewable Energy Act 2011* [Online]. Available at: http://seda.gov.my/go-home.php?omaneg=000101000000010101010001000010000000000000000000000&s=146 [Accessed: 25 July 2017].

SEDA, 2013a. SEDA MALAYSIA EXPLAINS THE 1% SURCHARGE FROM TNB BILLS IS FOR FUNDING FEED-IN TARIFF. Available at: https://www.google.com/url?sa=t&rct=j&q=&esrc=s&source=web&cd=3&ved=0ahUKEwiMq--X4_vVAhXEpI8KHe-MAosQFgg2MAI&url=https%3A%2F%2Fefit.seda.gov.my%2F%3Fomaneg%3D000101000000010101010001000010000000010100001000110%26id%3D1430&usg=AFQjCNHv1ZW1U15_yDK1oB94lKozp1_M1g [Accessed: 29 August 2017].

SEDA, 2017b, *SEDA PORTAL* [Online]. Available at: http://www.seda.gov.my/?omaneg=00010100000001010101000100001000000000000000000&s=161 [Accessed: 25 August 2017].

SEDA, 2013b, *Surcharge on Electricity Bills for Renewable Energy Fund Revised from 1.0% to 1.6%* [Online]. Available at: http://seda.gov.my/?omaneg=000101000000010101010001000010000000000000000000&s=3198 [Accessed: 29 August 2017].

SEDA, 2011d, *Sustainable Energy Development Authority Act 2011* [Online]. Available at: http://www.seda.gov.my/?omaneg=00010100000001010101000100000100000000000000000000&s=147 [Accessed: 29 August 2017].

Shafiee, Q., Nasirian, V., et al., 2014. Team-oriented adaptive droop control for autonomous AC microgrids. *IECON 2014 - 40th Annual Conference of the IEEE Industrial Electronics Society*. October 2014 pp. 1861–1867.

Shafiee, Q., Guerrero, J.M. and Vasquez, J.C., 2014. Distributed Secondary Control for Islanded Microgrids - A Novel Approach. *IEEE Transactions on Power Electronics*, 29(2), pp.1018–1031.

Shayeghi, H., Sobhani, B., Shahryari, E. and Akbarimajd, A., 2016. Optimal neuro-fuzzy based islanding detection method for Distributed Generation. *Neurocomputing*, 177, pp.478–488.

Singam, B. and Hui, L.Y., 2006. Assessing SMS and PJD Schemes of Anti-Islanding with Varying Quality Factor. *2006 IEEE International Power and Energy Conference*. November 2006 pp. 196–201.

SMA, 2014, *Technical Information - Battery Management of the Sunny Island* [Online]. Available at: http://files.sma.de/dl/7910/SI_Batteriemanagement-TI-en-21.pdf [Accessed: 25 September 2017].

Solar Frontier, 2017. Solar Frontier's CIS Thin-Film Submodule Achieves Highest Efficiency World Record of 19.2%. Available at: http://www.solar-frontier.com/eng/news/2017/0227_press.html [Accessed: 13 October 2017].

Solarvis, E., 2017. Advantages and disadvantages of Solar Photovoltaic | Solar Energy News. Available at: https://www.solarvis.energy/advantages-and-disadvantages-of-solar-photovoltaic/ [Accessed: 28 August 2017].

Suruhanjaya Tenaga, 2015. Energy Malaysia. *Suruhanjaya Tenaga*, 6, p.19.

Suruhanjaya Tenaga, 2017, *Peninsular Malaysia Electricity Supply Outlook 2017* [Online]. Available at: http://www.st.gov.my/index.php/en/all-publications/item/765-peninsular-malaysia-electricity-supply-industry-outlook-2017 [Accessed: 23 August 2017].

Tantimaporn, T., Srikacha, P., Loahacharoensombat, K. and Waraphok, P., 2010. Islanding operation of mini-hydro generation in real distribution network. *Proceedings of the International Conference on Energy and Sustainable Development: Issues and Strategies (ESD 2010)*. June 2010 pp. 1–6.

Tayab, U.B., Roslan, M.A.B., Hwai, L.J. and Kashif, M., 2017. A review of droop control techniques for microgrid. *Renewable and Sustainable Energy Reviews*, 76, pp.717–727.

Tedde, M. and Smedley, K., 2014. Anti-Islanding for Three-Phase One-Cycle Control Grid Tied Inverter. *IEEE Transactions on Power Electronics*, 29(7), pp.3330–3345.

Tenti, P., Caldognetto, T., Costabeber, A. and Mattavelli, P., 2013. Microgrids operation based on master-slave cooperative control. *IECON 2013 - 39th Annual Conference of the IEEE Industrial Electronics Society*. November 2013 IEEE, Vienna, Austria, pp. 7623–7628.

Teo, T.T., Logenthiran, T., Woo, W.L. and Abidi, K., 2016. Fuzzy logic control of energy storage system in microgrid operation. *2016 IEEE Innovative Smart Grid Technologies - Asia (ISGT-Asia)*. November 2016 pp. 65–70.

Thompson, 2016. Advancements in Synchronizing Systems for Microgrids and Grid Restoration. 3 July 2016 Edinburgh, United Kingdom.

TNB, 2016, *Technical Guideline for Connection of Indirect Solar PV Power Generation for Net Energy Metering* [Online]. Available at: http://www.seda.gov.my/?omaneg=00010100000001010101000100001000000000000000000000&s=5704 [Accessed: 14 April 2017].

US EPA, O., 2015, *Overview of Greenhouse Gases* [Online]. Available at: https://www.epa.gov/ghgemissions/overview-greenhouse-gases [Accessed: 25 July 2017].

Usman, M., Khan, M.T., Rana, A.S. and Ali, S., 2017. Techno-economic analysis of hybrid solar-diesel-grid connected power generation system. *Journal of Electrical Systems and Information Technology*. Available at: http://www.sciencedirect.com/science/article/pii/S2314717217300405 [Accessed: 2 January 2018].

Ustun, T.S., Ozansoy, C. and Zayegh, A., 2011. Recent developments in microgrids and example cases around the world—A review. *Renewable and Sustainable Energy Reviews*, 15(8), pp.4030–4041.

Vandoorn, T.L., De Kooning, J.D.M., Meersman, B. and Vandevelde, L., 2013. Review of primary control strategies for islanded microgrids with power-electronic interfaces. *Renewable and Sustainable Energy Reviews*, 19, pp.613–628.

Vasquez, J.C., Mastromauro, R.A., Guerrero, J.M. and Liserre, M., 2009. Voltage Support Provided by a Droop-Controlled Multifunctional Inverter. *IEEE Transactions on Industrial Electronics*, 56(11), pp.4510–4519.

Velasco, D., Trujillo, C.L., Garcerá, G. and Figueres, E., 2010. Review of anti-islanding techniques in distributed generators. *Renewable and Sustainable Energy Reviews*, 14(6), pp.1608–1614.

Wang, S. et al., 2016. An improved active frequency drift anti-islanding detection method. *2016 IEEE 11th Conference on Industrial Electronics and Applications (ICIEA)*. June 2016 pp. 2170–2473.

Wang, W. et al., 2007. A Power Line Signaling Based Scheme for Anti-Islanding Protection of Distributed Generators mdash;Part II: Field Test Results. *IEEE Transactions on Power Delivery*, 22(3), pp.1767–1772.

Wen, B. et al., 2016. Impedance-Based Analysis of Active Frequency Drift Islanding Detection for Grid-Tied Inverter System. *IEEE Transactions on Industry Applications*, 52(1), pp.332–341.

William, E., Scott, M. and Jakov, V., 2017. Microgrid Islanding and Grid Restoration With Off-the-Shelf Utility Protection Equipment. 20 July 2017 IEEE, Torronto, Canada.

Wong, J., Lim, Y.S., Tang, J.H. and Morris, E., 2014. Grid-connected photovoltaic system in Malaysia: A review on voltage issues. *Renewable and Sustainable Energy Reviews*, 29, pp.535–545.

Xu, W. et al., 2007. A Power Line Signaling Based Technique for Anti-islanding Protection of Distributed Generators: Part I: Scheme and Analysis. *2007 IEEE Power Engineering Society General Meeting*. June 2007 pp. 1–1.

Xu, X., Bishop, M., Oikarinen, D.G. and Hao, C., 2016. Application and modeling of battery energy storage in power systems. *CSEE Journal of Power and Energy Systems*, 2(3), pp.82–90.

Yang, S.Y. et al., 2006. Study on the Control Strategy for Parallel Operation of Inverters Based on Adaptive Droop Method. *2006 1ST IEEE Conference on Industrial Electronics and Applications*. May 2006 pp. 1–5.

Ye, Z. et al., 2003. Evaluation of anti-islanding schemes based on nondetection zone concept. *Power Electronics Specialist Conference, 2003. PESC '03. 2003 IEEE 34th Annual*. June 2003 pp. 1735–1741 vol.4.

Yoshikawa, K. et al., 2017. Silicon heterojunction solar cell with interdigitated back contacts for a photoconversion efficiency over 26%. *Nature Energy*, 2(5), p.nenergy201732.

Yusof R, 2015. *The Malaysian Grid Code*, Suruhanjaya Tenaga.

Zamora, R. and Srivastava, A.K., 2010. Controls for microgrids with storage: Review, challenges, and research needs. *Renewable and Sustainable Energy Reviews*, 14(7), pp.2009–2018.

Zhang, G. et al., 2014. A novel control strategy for parallel-connected converters in low voltage microgrid. *2014 IEEE Conference and Expo Transportation Electrification Asia-Pacific (ITEC Asia-Pacific)*. August 2014 pp. 1–6.

Zhao, H., Hong, M., Lin, W. and Loparo, K.A., 2017. Voltage and Frequency Regulation of Microgrid With Battery Energy Storage Systems. *IEEE Transactions on Smart Grid*, PP(99), pp.1–1.

Zhao, H., Yang, Q. and Zeng, H., 2017. Multi-loop virtual synchronous generator control of inverter-based DGs under microgrid dynamics. *Transmission Distribution IET Generation*, 11(3), pp.795–803.

Zhu, X. et al., 2009. Analysis of the Non-detection Zone with Passive Islanding Detection Methods for Current Control DG System. *2009 Twenty-Fourth Annual IEEE Applied Power Electronics Conference and Exposition*. February 2009 pp. 358–363.

LIST OF APPENDICES

Proposed fuzzy controlled strategy as a single control is not sufficient to mitigate frequency violation at the occurrence of islanding operation in all scenario. There are scenarios whereby secondary control is needed to support the fuzzy controlled strategy. For example, a scenario whereby the SoC of the battery is critically low and there is a shortage in electricity generation. In this scenario, load shedding on non-critical load is required to protect the battery from deep discharge which would potentially damage the battery prematurely. A load control can be implemented in this scenario to perform load shedding on non-critical load. Therefore, this section presents the social aspect of implementing load shedding in the residential area via survey study by using a load control.

A survey study is conducted for the purpose of investigating the feedback from the respondent towards implementing load control. One hundred respondents are selected from Universiti Tunku Abdul Rahman for this study. The research was conducted by using face-to-face interview and self-rated questionnaires. A face-to-face interview is conducted with the respective respondent to ensure the risk of missing data can be reduced during the data collection process in the present survey study. Due to time-consuming of face-to-face interview and limited time on research schedule, the number of respondent in this survey is limited to 100. The inclusion criteria for the respondent is as follows: working adult, defined as an individual who has been 23 years old or above, able to read in English and willing to participate in this

study. This study is approved by Universiti Tunku Abdul Rahman Scientific and Ethical Review Committee (Reference number: U/SERC/73/2016). Only consenting respondents were included in the study. The study was conducted from November to December 2016 using random sampling method.

The sociodemographic profiles of the 100 respondents showed that they were primarily from the age group of 35 to 44 years old, followed by 25 to 34 years old category as shown in APPENDIX A. Out of the total number of the respondents, 56% of the respondent is male as shown in APPENDIX B. In addition, the results also showed that most respondents lived in a terraced house which is more than a single story as shown in APPENDIX C. Most of the houses have a total number of occupants of 3, followed by 4 as shown in APPENDIX D. Majority of respondents of 63% have 2 working adults in their respectively household as shown in APPENDIX E. Besides, it is found that 30% of the respondent have monthly electricity bill in between RM 101 to RM 200. Followed by 26% of which have lower electricity bill in between RM 51 to RM 100 as shown in APPENDIX F.

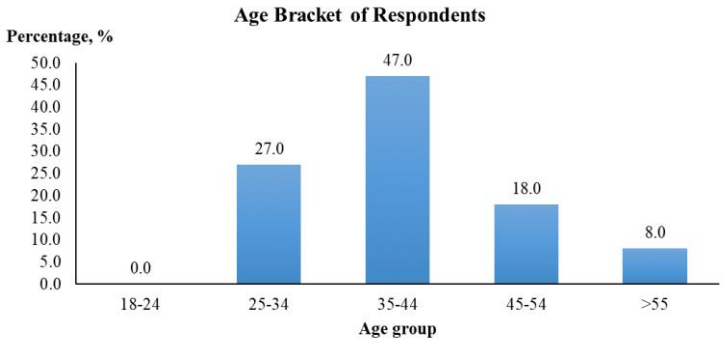

APPENDIX A: Age bracket of respondents

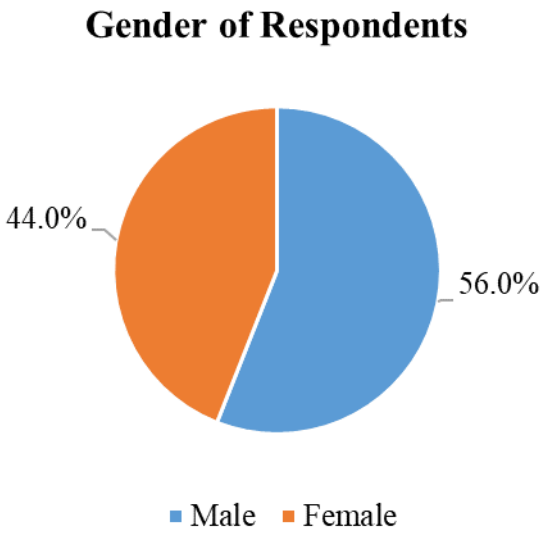

APPENDIX B: Gender of respondents

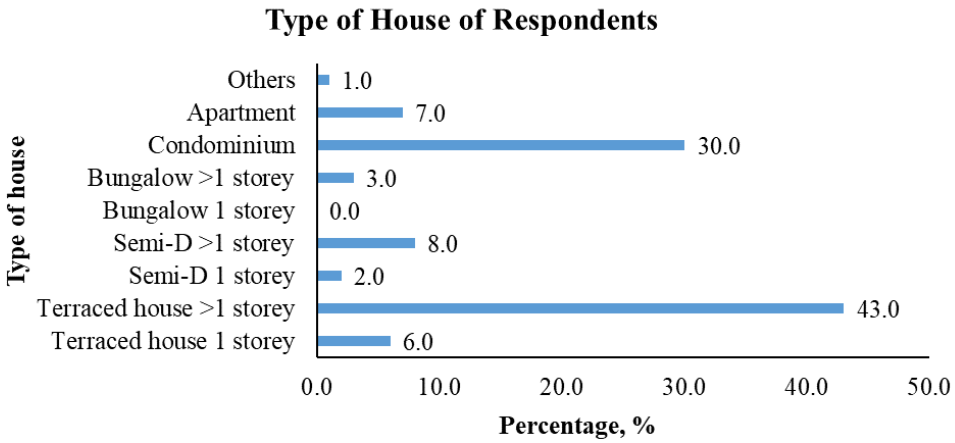

APPENDIX C: Type of house of respondents

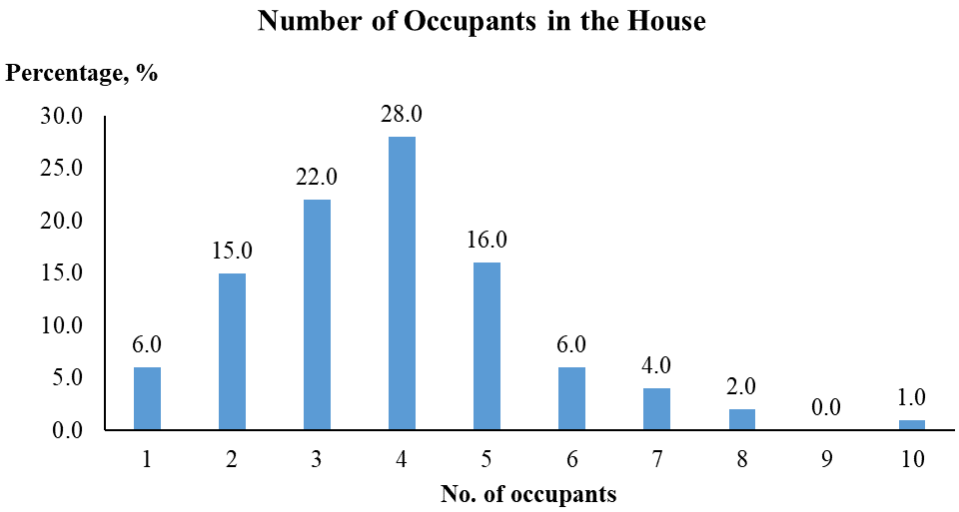

APPENDIX D: Number of occupants in the house

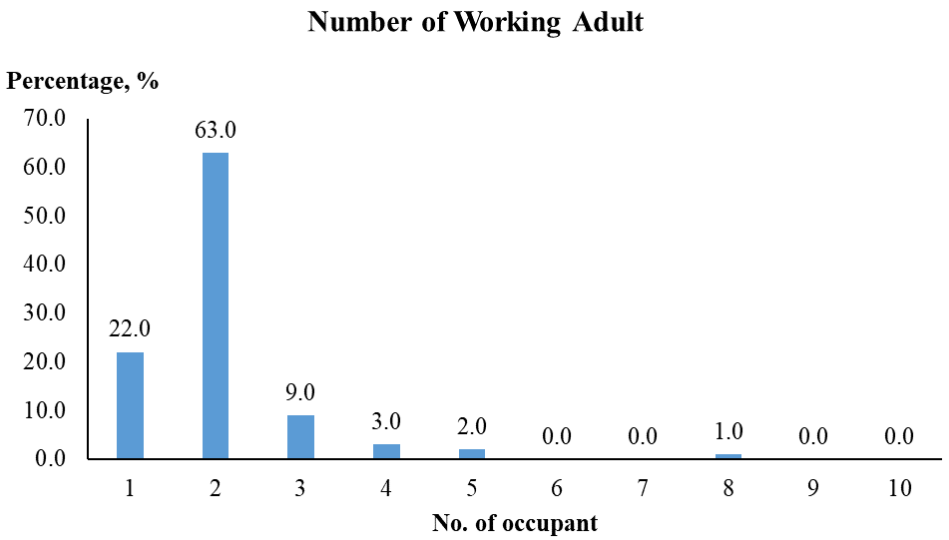

APPENDIX E: Number of working adult

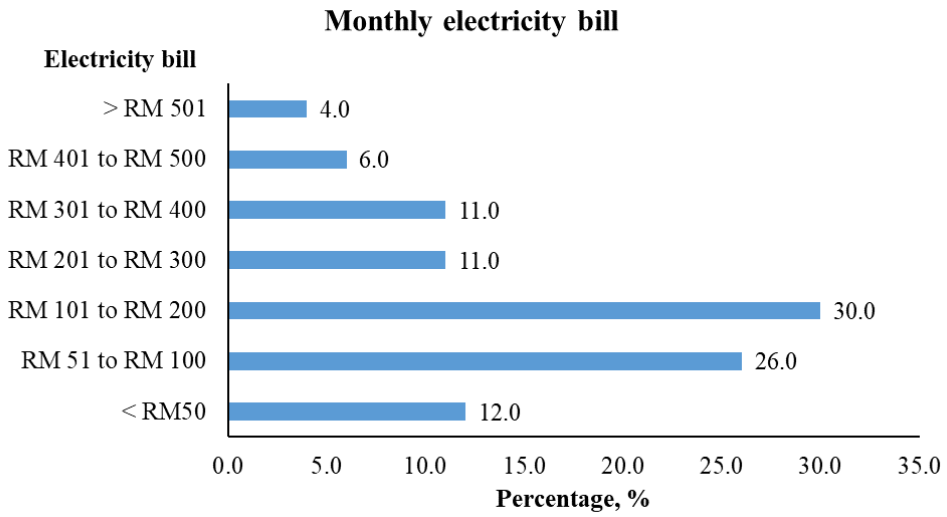

APPENDIX F: Monthly electricity bill

It was found that 82% respondents were most likely to be interested in implementing load control if cash incentive is given by the authorities as shown in APPENDIX G. The remaining 18% of the total respondents show no interest to the implementation of load control. These respondents have a common comment on the freedom to use electricity. Nevertheless, all respondents are required to respond to the priorities in implementing load control.

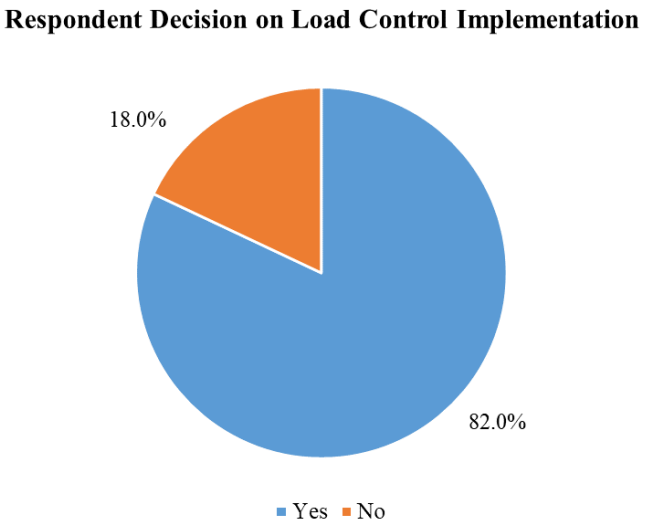

APPENDIX G: 82% of respondents agreed to load control implementation if incentive were given

APPENDIX H depicts the response for the types of controllable household appliances. It is found that 86% of the respondent allowed washing machine to be controllable. Followed by rechargeable devices. The air-conditioning unit as one of the top 3 controllable load stood at 71%. The graph is arranged in decreasing manner from top priority to low priority. The lowest priority for the controllable load is lighting, fridge and fan. As explained by the respondents, lighting and fan are the minimum consumption required by household to achieve minimum comfort. To consider the amount of power which is controllable in a household, top 5 choices of electrical appliances is chosen. APPENDIX I depicts the highest and lowest power rating of each electrical appliances. Rechargeable devices are excluded in this consideration as the type of rechargeable devices various among household. It is shown that the amount of controllable power for each household varies from 5,920 W to 11,450 W.

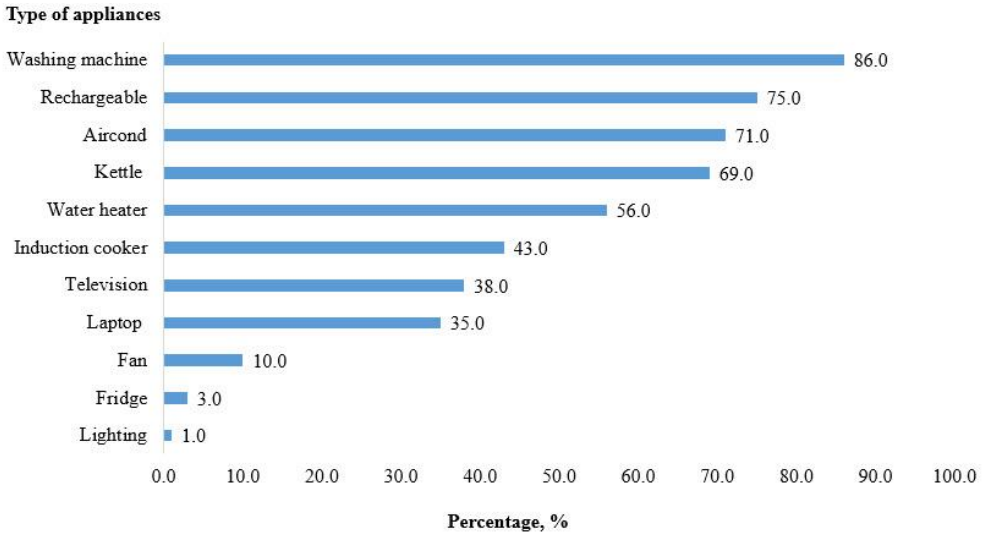

APPENDIX H: Washing machine as the top priority in implementing load control

APPENDIX I: Electrical appliances rating with highest rating and lowest rating, obtained from (Awer, 2011)

	Power consumption range, W	
Electrical appliances	**Lowest**	**Highest**
Washing machine	850	1800
Air conditioning	670	2750
Kettle	1800	2400
Water heater	2600	4500
Total	5920	11,450